Chapter 5
Switching Dynamical Systems

In this chapter, dynamics of switching dynamical systems will be presented. A switching system of multiple subsystems with transport laws at switching points will be discussed. The existence and stability of switching dynamical systems will be discussed through equi-measuring functions. The G-function of the equi-measuring functions will be introduced. The local increasing and decreasing of switching systems to equi-measuring functions will be presented. The global increasing and decreasing of the switching systems to equi-measuring functions will be discussed. Based on the global and local properties of the switching dynamical systems to the equi-measuring function, the stability of switching systems can be discussed. To demonstrate flow regularity and complexity of switching systems, the impulsive system is as a special switching system to present, and the quasi-periodic flows and chaotic diffusion of impulsive systems will be presented. A frame work for periodic flows in switching systems will be presented. The periodic flows and stability for linear switching systems will be discussed. This framework can be applied to nonlinear switching systems. The further results on stability and bifurcation of periodic flows in nonlinear switching systems can be discussed.

5.1 Continuous Subsystems

On an open domain $\Omega_i \subset \mathscr{R}^n$, there is a C^{r_i}-continuous system ($r_i > 1$) in the time interval $t \in [t_{k-1}, t_k]$

$$\dot{\mathbf{x}}^{(i)} = \mathbf{F}^{(i)}(\mathbf{x}^{(i)}, t, \mathbf{p}^{(i)}) \in \mathscr{R}^n, \mathbf{x}^{(i)} = (\mathbf{x}_1^{(i)}, \mathbf{x}_2^{(i)}, \cdots, \mathbf{x}_n^{(i)})^{\mathrm{T}} \in \Omega_i. \tag{5.1}$$

The time is t and $\dot{\mathbf{x}}^{(i)} = d\mathbf{x}^{(i)}/dt$. $\mathbf{p}^{(i)} = (p_1^{(i)}, p_2^{(i)}, \cdots, p_{m_i}^{(i)})^{\mathrm{T}} \in \mathscr{R}^{m_i}$ is a parameter vector. On the domain $\Omega_i \subset \mathscr{R}^n$, the vector field $\mathbf{F}^{(i)}(\mathbf{x}^{(i)}, t, \mathbf{p}^{(i)})$ with the parameter vector $\mathbf{p}^{(i)}$ is C^{r_i}-continuous in $\mathbf{x}^{(i)}$ for time interval $t \in [t_{k-1}, t_k]$. With an initial condition $\mathbf{x}^{(i)}(t_{k-1}) = \mathbf{x}_{k-1}^{(i)}$, the dynamical system in Eq. (5.1) possesses a continuous flow as

A. C. J. Luo, *Regularity and Complexity in Dynamical Systems*,
DOI: 10.1007/978-1-4614-1524-4_5, © Springer Science+Business Media, LLC 2012

$$\mathbf{x}^{(i)}(t) = \mathbf{\Phi}^{(i)}(\mathbf{x}_{k-1}^{(i)}, t, \mathbf{p}^{(i)}) \text{ with } \mathbf{x}_{k-1}^{(i)} = \mathbf{\Phi}^{(i)}(\mathbf{x}_{k-1}^{(i)}, t_{k-1}, \mathbf{p}^{(i)}). \tag{5.2}$$

To investigate the switching system consisting of many subsystems, the following assumptions of the ith subsystem should be held.
(A5.1)

$$\left.\begin{array}{l} \mathbf{F}^{(i)}(\mathbf{x}^{(i)}, t, \mathbf{p}^{(i)}) \in C^{r_i}, \\ \mathbf{\Phi}^{(i)}(\mathbf{x}_k^{(i)}, t, \mathbf{p}^{(i)}) \in C^{r_i+1} \end{array}\right\} \text{ on } \Omega_i \text{ for } t \in [t_{k-1}, t_k], \tag{5.3}$$

(A5.2)

$$\left.\begin{array}{l} ||\mathbf{F}^{(i)}|| \le K_1^{(i)}(\text{const}), \\ ||\mathbf{\Phi}^{(i)}|| \le K_2^{(i)}(\text{const}) \end{array}\right\} \text{ on } \Omega_i \text{ for } t \in [t_{k-1}, t_k], \tag{5.4}$$

(A5.3)

$$\mathbf{x}^{(i)} = \mathbf{\Phi}^{(i)}(t) \notin \partial\Omega_{ij} \quad \text{for } t \in [t_{k-1}, t_k]. \tag{5.5}$$

(A5.4) The switching of any two subsystems possesses the time-continuity.

From the foregoing assumptions, the subsystem possesses a finite solution in the finite time interval as a candidate to be selected for the resultant switching system. From Assumption (A5.3), any flow in the ith subsystem for $t \in (t_{k-1}, t_k)$ will not arrive to the boundary of the domains before the flow switches to the next subsystem. If the flow of the ith subsystem for $t \in (t_{k-1}, t_k)$ reaches the domain boundary of the systems, it will be discussed in discontinuous switching systems. Suppose the vector $\mathbf{x} \in \mathscr{R}^n$ can be decomposed into two vectors $\mathbf{x}_{n_1} \in \mathscr{R}^{n_1}$ and $\mathbf{x}_{n_2} \in \mathscr{R}^{n_2}$, where $n = n_1 + n_2$ and $\mathbf{x} = (\mathbf{x}_{n_1}, \mathbf{x}_{n_2})^{\mathrm{T}}$. From such concepts, such a finite and bounded solution in phase space is sketched for the time interval $t \in [t_{k-1}, t_k]$ in Fig. 5.1a, and the corresponding time-history of the dynamical flow is presented in Fig. 5.1b.

5.2 Switching Systems

To investigate the switching system, a set of dynamical systems in finite time intervals will be introduced first. From such a set of dynamical systems, the dynamical subsystems in a resultant switching system can be selected.

Definition 5.1 From dynamical systems in Eq. (5.1), a set of dynamical systems on the open domain Ω_i in the time interval $t \in [t_{k-1}, t_k]$ for $i = 1, 2, \cdots, m$ is defined as

$$\mathfrak{S}_{\mho} \equiv \{ S_i \,|\, i = 1, 2, \cdots, m \}, \tag{5.6}$$

where

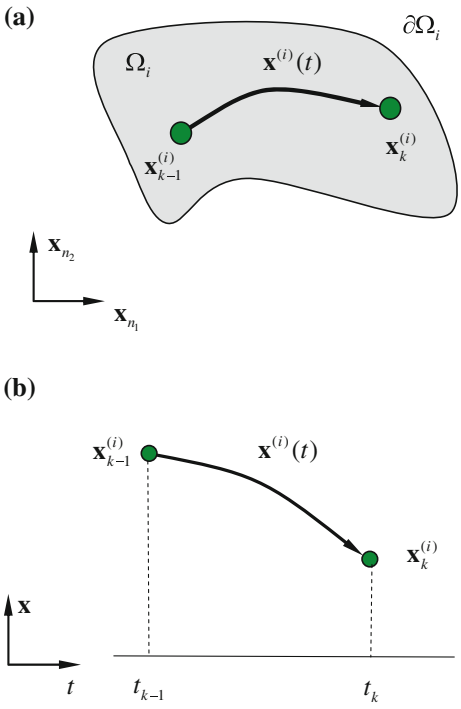

Fig. 5.1 **a** A flow in phase space and **b** a flow in the time-history

$$S_i \equiv \left\{ \dot{\mathbf{x}}^{(i)} = \mathbf{F}^{(i)}(\mathbf{x}^{(i)}, t, \mathbf{p}^{(i)}) \in \mathscr{R}^n \,\middle|\, \begin{array}{l} \mathbf{x}^{(i)} \in \Omega_i \subset \mathscr{R}^n, \mathbf{p}^{(i)} \in \mathscr{R}^{m_i}; \\ \mathbf{x}^{(i)}(t_{k-1}) = \mathbf{x}^{(i)}_{k-1}; t \in [t_{k-1}, t_k]; \\ k \in \mathbb{N} \end{array} \right\}. \quad (5.7)$$

To discuss the switchability of two subsystems at time t_k, the existence and uniqueness of solutions of the two systems are very important. From Assumptions (A5.1–A5.3), the subsystem possesses a finite solution in the finite time interval and such a solution will not reach the corresponding domain boundary. From the set of subsystems, the corresponding set of solutions for such subsystems can be defined as follows.

Definition 5.2 For the ith dynamical subsystems in Eq. (5.1), with an initial condition $\mathbf{x}^{(i)}_{k-1} \in \Omega_i$ for $k \in \mathbb{N}$, there is a unique solution $\mathbf{x}^{(i)}(t) = \mathbf{\Phi}^{(i)}(\mathbf{x}^{(i)}_{k-1}, t, \mathbf{p}^{(i)})$. For all $i = 1, 2, \cdots, m$, a set of solutions for the ith subsystem in Eq. (5.1) on the open domain D_i in the time interval $t \in [t_{k-1}, t_k]$ is defined as

$$\mathbb{S} = \left\{ \Theta^{(i)} \,|i = 1, 2, \cdots, m \right\}, \quad (5.8)$$

where

$$\Theta^{(i)} \equiv \left\{ \mathbf{x}^{(i)}(t) \,\middle|\, \begin{array}{l} \mathbf{x}^{(i)}(t) = \mathbf{\Phi}^{(i)}(\mathbf{x}^{(i)}_{k-1}, t, \mathbf{p}^{(i)}) \\ t \in [t_{k-1}, t_k], k \in \mathbb{N} \end{array} \right\}. \quad (5.9)$$

To discuss the switching of two subsystems for time t_k, the overlapping of domains of vector fields should be discussed. For different time intervals, two open domains Ω_i and Ω_j can be overlapped or separated, (i.e., $\Omega_i \cap \Omega_j \neq \varnothing$ or $\Omega_i \cap \Omega_j = \varnothing$). However, in discontinuous dynamical systems, the open domains for subsystems should be $\Omega_i \cap \Omega_j = \varnothing$ (also see, Luo 2006). In other words, the domains for the discontinuous systems cannot be overlapped. If the two domains of the ith and jth subsystems in Eq. (5.1) can be overlapped partially or fully (i.e., $\Omega_i \subseteq \Omega_j$ or $\Omega_i \supseteq \Omega_j$), there are two kinds of switching in the overlapping zone of the two domains. The two switching include (i) the continuous switching and (ii) C^0-discontinuous switching. However, for either the two separated domains or the switching points in the non-overlapping zone, only the C^0-discontinuous switching. Because the time intervals for two systems are different, the domains for the two systems can be overlapped. In other words, on the same domain, many different dynamical systems can be defined. Thus, there is a relation for the ith and jth switchable subsystems

$$\Omega_i \subseteq \Omega_j \quad \text{or} \quad \Omega_i \supseteq \Omega_j. \tag{5.10}$$

From the foregoing relation, different systems can be defined on the *full* or *partial*, same domain for different time intervals. To extend such a concept for two subsystems, the domain for the resultant switching system of many subsystems can be defined. Before doing so, as in Luo (2005, 2006, 2008a), the inaccessible and accessible domains in phase space will be defined for discontinuous dynamical systems in phase space.

Definition 5.3 On a domain $\Omega_0 \subset \mathscr{R}^n$ in phase space, if no dynamical system is defined, the domain Ω_0 is called an inaccessible domain.

Definition 5.4 On a domain $\Omega_i \subset \mathscr{R}^n$ in phase space, if the ith-subsystem is defined, the domain Ω_i is called an accessible domain.

Definition 5.5 In the neighborhood of a point $\mathbf{x}_p$, if there is a set of domains Ω_{l_i} ($l_i \in \{1, 2, \cdots, m\}$, $i = 1, 2, \cdots, m_1$) for subsystems and an inaccessible domain Ω_0 in phase space, there is the union of the domains as

$$\mho = \cup_{i=1}^{m_1} \Omega_{l_i} \cup \Omega_0 \text{ and } \Omega_{l_i} \subseteq \mho \tag{5.11}$$

for the subsystems to switch. Such a union is called the resultant domain in the neighborhood of a point $\mathbf{x}_p$ for the switching system of subsystems.

To investigate the responses of the switching system in the resultant domain D in the neighborhood of a point $\mathbf{x}_p$, the switchability of any two systems should be discussed. The concept of the switching from a subsystem to another subsystem is presented.

Definition 5.6 Consider two subsystems $S_i, S_j \in \mathfrak{S}_D$ on the domains Ω_i and Ω_j.

(i) For $\mathbf{x}_k^{(i)}, \mathbf{x}_k^{(j)} \in \Omega_i \cap \Omega_j \neq \varnothing$ at $t = t_k$, if

$$\left.\begin{array}{l} \dfrac{d^s \mathbf{x}_k^{(i)}}{dt^s} = \dfrac{d^s \mathbf{x}_k^{(j)}}{dt^s} \text{ for } s = 0, 1, 2, \cdots, r; \\ \dfrac{d^{r+1} \mathbf{x}_k^{(i)}}{dt^{r+1}} \neq \dfrac{d^{r+1} \mathbf{x}_k^{(j)}}{dt^{r+1}}, \end{array}\right\} \tag{5.12}$$

then the switching of the two subsystems S_i and S_j at time t_k is called a C^r-continuous switching,

(ii) For $\mathbf{x}_k^{(i)} \in \Omega_i$ and $\mathbf{x}_k^{(j)} \in \Omega_j$ at $t = t_k$, if $\mathbf{x}_k^{(i)} \neq \mathbf{x}_k^{(j)}$ and there is an transport law

$$\mathbf{g}^{(ij)}(\mathbf{x}_k^{(i)}, \mathbf{x}_k^{(j)}, \mathbf{p}_{ij}) = \mathbf{0} \tag{5.13}$$

then the switching of the two subsystems S_i and S_j at time t_k is called the C^0-discontinuous switching.

To illustrate the aforementioned concept for the switching of the two subsystems, the switching of the ith and jth subsystems are sketched in Fig. 5.2. A flow from the ith subsystem switching to the jth-subsystem at time t_k is presented. The domain of the ith subsystem is filled with gray color. The flow is depicted by the curves with arrows. The switching points are labeled by circular symbols. The hatched areas are the overlapped domains. In Fig. 5.2a, the two subsystems at time t_k are switched with at least $\mathbf{x}_k^{(i)} = \mathbf{x}_k^{(j)}$. In Fig. 5.2b, the domains of the ith and ith subsystems are separated at time t_k. To complete the switching of the ith and jth subsystems at point t_k, the transport law (i.e., $\mathbf{g}^{(ij)}(\mathbf{x}_k^{(i)}, \mathbf{x}_k^{(j)}, t_k) = 0$) should be used. The transport law is presented with a dashed line with an arrow.

Definition 5.7 For a flow $\mathbf{x}^{(i)} \in \mho$, two positive constants with $0 \leq C_1 < C_2$ exist. If the following relation holds

$$C_1 \leq ||\mathbf{x} - \mathbf{x}_p|| \leq C_2 \tag{5.14}$$

where $||\bullet||$ is a norm, the domain $\mho$ is called the finite domain in the vicinity of point $\mathbf{x}_p$.

From the resultant domain $\mho$ and the switchability conditions between any two subsystems, a resultant switching system can be defined.

Definition 5.8 A switching system on the domain $\mho = \cup_{i=1}^{m_1} \Omega_{l_i} \cup \Omega_0$ is defined as

$$\begin{array}{l} \dot{\mathbf{x}}^{(\alpha_k)} = \mathbf{F}^{(\alpha_k)}(\mathbf{x}^{(\alpha_k)}, t, \mathbf{p}^{(\alpha_k)}) \text{ for } t \in [t_{k-1}, t_k] \\ \alpha_k \in \{l_1, l_2, \cdots, l_{m_1}\} \subseteq \{1, 2, \cdots, m\}, k = 1, 2, \cdots \end{array} \tag{5.15}$$

with an given initial condition $\mathbf{x}^{(\alpha_1)} = \mathbf{x}_0^{(\alpha_1)}$ and the corresponding transport laws at time t_k

$$\mathbf{g}^{(\alpha_k \alpha_{k+1})}(\mathbf{x}_k^{(\alpha_k)}, \mathbf{x}_k^{(\alpha_{k+1})}, \mathbf{p}_{\alpha_k \alpha_{k+1}}) = \mathbf{0} \text{ for } k = 1, 2, \cdots. \tag{5.16}$$

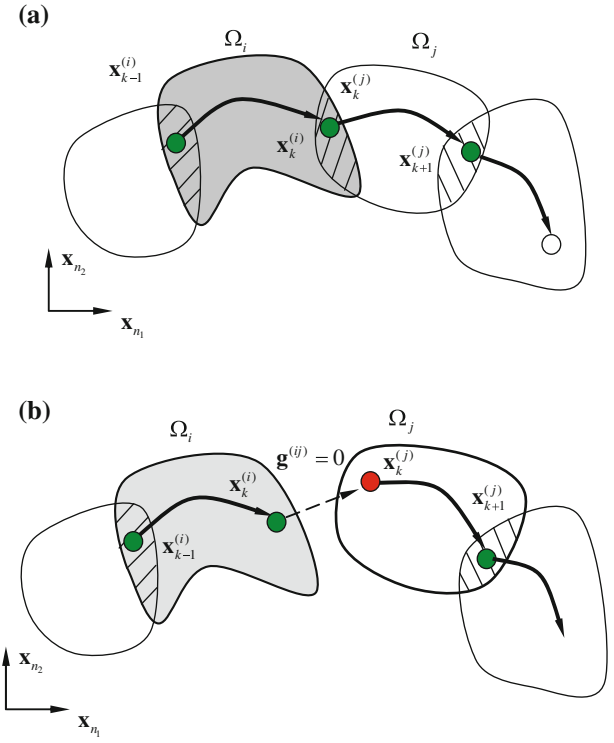

Fig. 5.2 The dynamical system switching: **a** continuous switching, and **b** C^0-discontinuous switching with transport laws $P_0^{(ij)}$ in phase space

At a switching point at time t_k, if the C^r-continuous switching of any the switching system exists, then Eq. (5.16) is expressed by

$$\frac{d^\beta \mathbf{g}^{(\alpha_k \alpha_{k+1})}}{dt^\beta} \equiv \frac{d^\beta \mathbf{x}_k^{(\alpha_{k+1})}}{dt^\beta} - \frac{d^\beta \mathbf{x}_k^{(\alpha_k)}}{dt^\beta} = \mathbf{0} \text{ for } k \in \mathbb{N}, \beta = 0, 1, 2, \cdots, r. \quad (5.17)$$

For $\beta = 0$, one obtains $\mathbf{g}^{(\alpha_k \alpha_{k+1})} \equiv \mathbf{x}_k^{(\alpha_{k+1})} - \mathbf{x}_k^{(\alpha_k)} = \mathbf{0}$. Therefore, no matter how the system is switching, the transport law as a general expression is adopted from now on. Consider a resultant switching system on the domain $\mho = \cup_{i=0}^{m_1} \Omega_{l_i}$ for $l_i \in \{0, 1, 2, \cdots, m\}$ in the vicinity of point $\mathbf{p}_k$ to be formed by

$$\begin{aligned} &S \equiv \cdots \oplus S_{\alpha_k} \oplus \cdots \oplus S_{\alpha_2} \oplus S_{\alpha_1} \\ &\text{for } S_{\alpha_k} \in \mathfrak{S}_D, \alpha_k \in \{l_1, l_2, \cdots, l_{m_1}\} \subseteq \{1, 2, \cdots, m\}, k = 1, 2, \cdots \\ &t \in \cup_{k=1}^{\infty} [t_k, t_{k-1}] \end{aligned} \quad (5.18)$$

with the corresponding switching conditions given by the transport law.

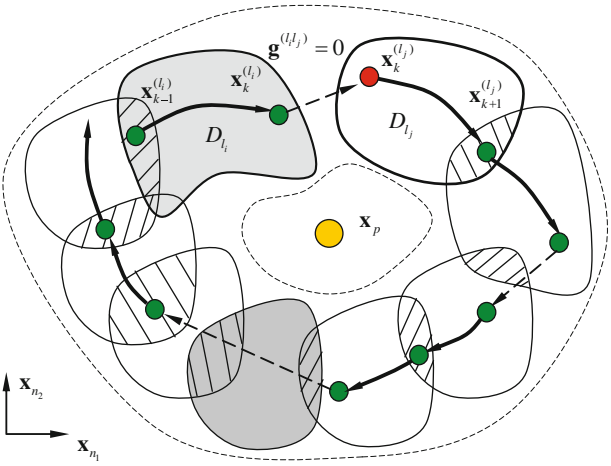

Fig. 5.3 A flow and switching of a switching system on the resultant domain in neighborhood of point $\mathbf{x}_p$

$$\left.\begin{array}{l} \mathbf{x} = \mathbf{x}_0^{(\alpha_1)} \in \Omega_{\alpha_1} \text{ at } t = t_0 \\ \mathbf{g}^{(\alpha_k \alpha_{k+1})}(\mathbf{x}_k^{(\alpha_k)}, \mathbf{x}_k^{(\alpha_{k+1})}, \mathbf{p}_{\alpha_k \alpha_{k+1}}) = \mathbf{0} \text{ at } t = t_k, \\ \text{for } \ k = 1, 2, \cdots . \end{array}\right\} \tag{5.19}$$

From the set of the solutions in Eq. (5.9) for subsystems, the solution of the switching system is given by

$$\left.\begin{array}{l} \mathbf{x}^{(\alpha_k)} = \mathbf{\Phi}^{(\alpha_k)}(\mathbf{x}_{k-1}^{(\alpha_k)}, t, \mathbf{p}^{(\alpha_k)}) \in \Omega_{\alpha_k} \text{ for } t \in [t_{k-1}, t_k] \\ \mathbf{g}^{(\alpha_k \alpha_{k+1})}(\mathbf{x}_k^{(\alpha_k)}, \mathbf{x}_k^{(\alpha_{k+1})}, \mathbf{p}_{\alpha_k \alpha_{k+1}}) = \mathbf{0}, \\ \alpha_k \in \{l_1, l_2, \cdots, l_{m_1}\} \subseteq \{1, 2, \cdots, m\}, k = 1, 2, \cdots . \end{array}\right\} \tag{5.20}$$

Note that symbol "$\oplus$" means the switching action of two subsystems. To explain the two system switching, on the domain $\mho = \cup_{i=1}^{m_1} \Omega_{l_i} \cup \Omega_0$ a switching dynamical system given by Eq. (5.18) with the switching and initial conditions are sketched in Fig. 5.3. The short-dashed curves are the boundary of the domain D in the neighborhood of point $\mathbf{x}_p$, and the accessible domains are given by closed solid curves. The thick solid curves with arrows are flows. The circular symbols represent the switching points and the dashed lines with arrows are the transport laws for the two systems.

Definition 5.9 For a switching system in Eqs. (5.18) and (5.19), if there is a switching pattern of the subsystems as

$$\begin{array}{l} S \equiv \cdots \oplus S^{(j)} \oplus \cdots \oplus S^{(2)} \oplus S^{(1)} \ \text{ with } \ t \in \cup_{j=1} \cup_{i=1}^{m_1} [t_{i-1}^{(j)}, t_i^{(j)}] \\ \text{where } S^{(j)} \equiv S_{\alpha_{m_1}} \oplus \cdots \oplus S_{\alpha_2} \oplus S_{\alpha_1} \ \text{ for } \ t \in \cup_{i=1}^{m_1} [t_{i-1}^{(j)}, t_i^{(j)}] \\ t_0^{(1)} = t_0 \ \text{ for } \ j = 1, 2, \cdots ; \end{array} \tag{5.21}$$

then, the switching system S is called *a repeated, switching system of subsystems*. For each repeating pattern of the subsystem, if

$$t_{m_1}^{(j)} - t_0^{(j)} = T = const \quad \text{for} \quad j = 1, 2, \cdots, \tag{5.22}$$

then, the switching system S in Eq. (5.21) is called *a repeated, switching system with the equi-time interval* (or, an equi-time, repeated, switching system).

Definition 5.10 Under the switching conditions in Eq. (5.19), a switching system of subsystems on the domain $\mho = \cup_{i=1}^{m_1} \Omega_{l_i} \cup \Omega_0$ for $l_i \in \{1, 2, \cdots, m\}$ in the vicinity of point $\mathbf{x}_p$ is defined by

$$S \equiv S_{\alpha_{m_1}} \oplus \cdots \oplus S_{\alpha_2} \oplus S_{\alpha_1} \quad \text{with} \quad t \in \cup_{i=1}^{m_1} [t_{i-1}, t_i]. \tag{5.23}$$

If the flow of the switching system satisfies the following condition

$$\mathbf{x}_{m_1}^{(\alpha_{m_1})} = \mathbf{x}_0^{(\alpha_1)} \text{ and } t_{m_1} - t_0 \equiv T = const \tag{5.24}$$

then, the switching system S in Eq. (5.23) possesses *a periodic flow on* the domain $\mho$ in the vicinity of point $\mathbf{x}_p$.

Definition 5.11 With the switching conditions in Eq. (5.19), for a switching system S in Eq. (5.23), if there is a new switching system as

$$\begin{aligned} S' &\equiv S \oplus S = \underbrace{S_{\alpha_{m_1}} \oplus \cdots \oplus S_{\alpha_2} \oplus S_{\alpha_1}}_{S} \oplus \underbrace{S_{\alpha_{m_1}} \oplus \cdots \oplus S_{\alpha_2} \oplus S_{\alpha_1}}_{S} \\ &\text{for } t \in \cup_{i=1}^{2m_1} [t_{i-1}, t_i] \end{aligned} \tag{5.25}$$

with the conditions

$$\mathbf{x}_{2m_1}^{(\alpha_{m_1})} = \mathbf{x}_0^{(\alpha_1)} \quad \text{and} \quad t_{2m_1} - t_0 \equiv 2T = const \tag{5.26}$$

then, the new switching system S' is called a *period-doubling* system of the switching system S. The corresponding flow is called the *period-doubling* flow of the switching system S.

Definition 5.12 From the switching system S in Eq. (5.23), if there is a new switching system as

$$\begin{aligned} S' &\equiv \underbrace{S \oplus \cdots \oplus S}_{l} \\ &= \underbrace{\underbrace{S_{\alpha_{m_1}} \oplus \cdots \oplus S_{\alpha_2} \oplus S_{\alpha_1}}_{S} \oplus \cdots \oplus \underbrace{S_{\alpha_{m_1}} \oplus \cdots \oplus S_{\alpha_2} \oplus S_{\alpha_1}}_{S}}_{l} \\ &\text{with} \quad t \in \cup_{i=1}^{l \times m_1} [t_{i-1}, t_i] \end{aligned} \tag{5.27}$$

with the conditions

$$\mathbf{x}_{l\times m_1}^{(\alpha_{m_1})} = \mathbf{x}_0^{(\alpha_1)} \text{ and } t_{l\times m_1} - t_0 \equiv l \times T = const \tag{5.28}$$

then, the new switching system S' is called a period-l system of the switching system S. The corresponding flow is called the period-l flow of the switching system S. If $l \to \infty$, the new switching system S' is called a *chaotic* system of the switching system S, and the corresponding flow is called the *chaotic* flow of the switching system S.

5.3 Measuring Functions and Stability

To investigate the stability of the switching systems consisting of many subsystems on the domain in the vicinity of point $\mathbf{x}_p$, a measuring function should be introduced through the relative position vector to point $\mathbf{x}_p$. The relative position vector is given by

$$\mathbf{r} = \mathbf{x} - \mathbf{x}_p. \tag{5.29}$$

From the relative position vector, a distance function of two points $\mathbf{x}_p$ and $\mathbf{x}$ can be defined. Further, using such a distance function, the measuring function can be introduced herein. If $\mathbf{x}_p = \mathbf{0}$, such a position vector is called the absolute position vector.

Definition 5.13 For a given point $\mathbf{x}_p$, consider a flow $\mathbf{x} \in \mho(\mathbf{x}_p)$ in the switching system of Eq. (5.23). A relative distance function for the flow $\mathbf{x}$ to the fixed point $\mathbf{x}_p$ is defined by

$$d(\mathbf{x}, \mathbf{x}_p) = ||\mathbf{x} - \mathbf{x}_p||. \tag{5.30}$$

If $d(\mathbf{x}, \mathbf{x}_p) = C = const$, there is a surface given by

$$||\mathbf{x} - \mathbf{x}_p|| = C \tag{5.31}$$

which is called *the equi-distance surface* of point $\mathbf{x}_p$. Further, if there is a monotonically increasing or decreasing function of the relative distance $d(\mathbf{x}, \mathbf{x}_p)$,

$$E = V(\mathbf{x}, \mathbf{x}_p) \equiv f(d(\mathbf{x}, \mathbf{x}_p)) \tag{5.32}$$

with the following property

$$V(\mathbf{x}, \mathbf{x}_p) = f(d(\mathbf{x}, \mathbf{x}_p)) = \min \text{ (or max) if } d(\mathbf{x}, \mathbf{x}_p) = 0. \tag{5.33}$$

Such a monotonic function $V(\mathbf{x}, \mathbf{x}_p)$ is called a generalized measuring function of switching system in neighborhood of the point $\mathbf{x}_p$. If $E = C = \text{const}$, there is a surface given by

$$V(\mathbf{x}, \mathbf{x}_p) = C \tag{5.34}$$

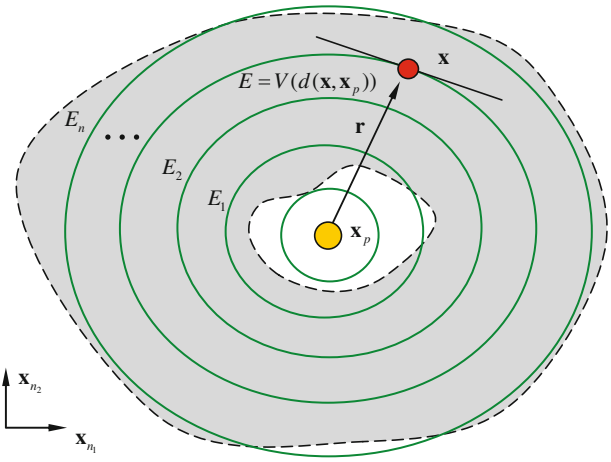

Fig. 5.4 A relative position vector from $\mathbf{x}_p$ to $\mathbf{x}$ and a measuring function with $n_1 + n_2 = n$

which is called the *equi-measuring function* surface.

Consider a distance function $d(\mathbf{x}, \mathbf{x}_p) \equiv [(\mathbf{x} - \mathbf{x}_p) \cdot (\mathbf{x} - \mathbf{x}_p)]^{1/2}$ as an example. From the foregoing definition, consider two monotonically increasing, metric functions to the relative distance to the point $\mathbf{x}_p$ as

$$\begin{aligned} V &= d(\mathbf{x}, \mathbf{x}_p) + C = [(\mathbf{x} - \mathbf{x}_p) \cdot (\mathbf{x} - \mathbf{x}_p)]^{1/2} + C \quad \text{or} \\ V &= (d(\mathbf{x}, \mathbf{x}_p))^2 + C = (\mathbf{x} - \mathbf{x}_p) \cdot (\mathbf{x} - \mathbf{x}_p) + C \end{aligned} \tag{5.35}$$

where C is an arbitrarily selected constant. Without losing generality, one can choose $C=0$. Similarly, the monotonically decreasing functions can be expressed. Such a selection of the monotonic, measuring functions is dependent on the convenience and efficiency in applications. From the foregoing discussion, the relative distance is a simple measuring function. From Eq. (5.14), the maximum and minimum relative distances in $\mho(\mathbf{x}_p)$ are C_1 and C_2, respectively. The minimum and maximum values of the monotonically increasing metric functions for domain $\mathbf{x} \in \mho(\mathbf{x}_p)$ are $E_{\min} = V(C_1)$ and $E_{\max} = V(C_2)$ from Eq. (5.32). For the two simple metric function in Eq. (5.33), one obtains the minimum and maximum values ($E_{\min} = C_1 + C$ and $E_{\max} = C_2 + C$) or ($E_{\min} = C_1^2 + C$ and $E_{\max} = C_2^2 + C$).

To explain the concept of the measuring function, consider a domain $\mho(\mathbf{x})$ in phase space for a subsystem in the vicinity of the given point $\mathbf{x}_p$ with big circular symbol, as shown in Fig. 5.4. Suppose a point $\mathbf{x}$ with a small circular symbol is the solution of the subsystem. The relative location vector to the given point $\mathbf{x}_p$ is expressed by a vector $\mathbf{r} = \mathbf{x} - \mathbf{x}_p$ and the corresponding relative distance is expressed by $d(\mathbf{x}, \mathbf{x}_p)$. Such a point $\mathbf{x}$ is on the equi-measuring function surface of $E = V(d(\mathbf{x}, \mathbf{x}_p))$. For different values of $E = E_i$ $(i = 1, 2, \cdots)$, a set of the equi-measuring function surfaces will fill the entire domain of $\mho(\mathbf{x})$, which are depicted by the green curves in Fig. 5.4. Based on the equi-measuring function surface, there is a dynamical system.

Definition 5.14 For any *equi-measuring function* surface in Eq. (5.34), there is a dynamical system as

$$\dot{\mathbf{x}}^m = \mathbf{f}^m(\mathbf{x}^m) \tag{5.36}$$

with the initial condition $(\mathbf{x}_0^m, t_0)$ and the equi-measuring function surface can be expressed by

$$V(\mathbf{x}^m, \mathbf{x}_p) = V(\mathbf{x}_0^m, \mathbf{x}_p) = E. \tag{5.37}$$

The dynamical system given in Eq. (5.36) is invariant in sense of the measuring function in Eq. (5.34). The subscript or superscript "m" represents the follow on the "equi-measuring function surface". This system can be designed from the practical applications. To measure the dynamical behaviors of any subsystems to the equi-measuring function surface, from Luo (2008a, b), the following functions are introduced.

Definition 5.15 Consider a flow $\mathbf{x}^{(i)}$ of the ith dynamical subsystem with a vector field $\mathbf{F}^{(i)}(\mathbf{x}^{(i)}, t, \mathbf{p}^{(i)})$ in Eq. (5.1). At time t, if the flow $\mathbf{x}^{(i)}$ arrives to the *equi-measuring function* surface with the corresponding constant $(E = C)$ in Eq. (5.33), the kth-order, G-functions at the constant measuring function level are defined as

$$\begin{aligned} G_m^{(k)}(\mathbf{x}^{(i)}, \mathbf{x}_p, t) &= (k+1)! \lim_{\varepsilon \to 0} \frac{1}{\varepsilon^{k+1}} \left\{ [\mathbf{n}(\mathbf{x}^m, \mathbf{x}_p, t+\varepsilon)]^{\mathrm{T}} \cdot \mathbf{x}^{(i)}(t+\varepsilon) \right. \\ &\quad \left. - [\mathbf{n}(\mathbf{x}^m, \mathbf{x}_p, t)]^{\mathrm{T}} \cdot \mathbf{x}^{(i)}(t) - \sum_{q=1}^{k} \frac{1}{q!} G_m^{(q-1)}(\mathbf{x}^{(i)}, \mathbf{x}_p, t)\varepsilon^q \right\} \\ &= \textstyle\sum_{r=1}^{k+1} C_{k+1}^r D^{(k+1-r)}[\mathbf{n}(\mathbf{x}^m, \mathbf{x}_p, t)]^{\mathrm{T}} \cdot [D^{(r-1)}\mathbf{F}^{(i)}(\mathbf{x}^{(i)}, t, \mathbf{p}^{(i)}) \\ &\quad - D^{(r-1)}\mathbf{f}^m(\mathbf{x}^m, \mathbf{x}_p)]\big|_{\mathbf{x}^m = \mathbf{x}^{(i)}} \end{aligned} \tag{5.38}$$

for $k = 0, 1, 2, \cdots$. The normal vector of the equi-measuring function surface is

$$\mathbf{n}(\mathbf{x}^m, \mathbf{x}_p, t) = \frac{\partial V(\mathbf{x}^m, \mathbf{x}_p)}{\partial \mathbf{x}^m} = \left(\frac{\partial V}{\partial x_1^m}, \frac{\partial V}{\partial x_2^m}, \cdots, \frac{\partial V}{\partial x_n^m}\right)^{\mathrm{T}} \tag{5.39}$$

where the total differential operator is given by

$$\begin{aligned} &D = \dot{\mathbf{x}} \frac{\partial}{\partial \mathbf{x}} + \frac{\partial}{\partial t}, \\ &D^{(r)}(\cdot) = D \circ D^{(r-1)}(\cdot) = D(D^{(r-1)}(\cdot)), \\ &\text{and} \quad D^{(0)} = 1 \end{aligned} \tag{5.40}$$

with

$$C_{k+1}^r = \frac{(k+1)!}{r!(k+1-r)!} \quad \text{and} \quad r! = 1 \times 2 \times 3 \cdots \times r. \tag{5.41}$$

From Eq. (5.34), the following relation holds

$$0 = \dot{\mathbf{x}} \cdot \frac{\partial V}{\partial \mathbf{x}} = \mathbf{n}(\mathbf{x}^m, \mathbf{x}_p) \cdot \mathbf{f}^m(\mathbf{x}^m, \mathbf{x}_p). \tag{5.42}$$

For a zero-order G-function ($k = 0$), one obtains

$$\begin{aligned} G_m^{(0)}(\mathbf{x}^{(i)}, \mathbf{x}_p, t) &= [\mathbf{n}(\mathbf{x}^m, \mathbf{x}_p)]^{\mathrm{T}} \cdot [\mathbf{F}^{(i)}(\mathbf{x}^{(i)}, t, \mathbf{p}^{(i)}) - \mathbf{f}^m(\mathbf{x}^m, \mathbf{x}_p)]\Big|_{\mathbf{x}^m = \mathbf{x}^{(i)}} \\ &= [\mathbf{n}(\mathbf{x}^{(i)}, \mathbf{x}_p)]^{\mathrm{T}} \cdot \mathbf{F}^{(i)}(\mathbf{x}^{(i)}, t, \mathbf{p}^{(i)}). \end{aligned} \tag{5.43}$$

The zero-order G-function is the dot product of the vector field $\mathbf{F}^{(i)}(\mathbf{x}^{(i)}, t, \mathbf{p}^{(i)})$ and normal vector $\mathbf{n}(\mathbf{x}^m, \mathbf{x}_p)$ for the ith subsystem. Consider an instantaneous value of the equi-measuring function at time t. In other words, letting $\mathbf{x}^m = \mathbf{x}^i$, equation (5.37) is

$$E^{(i)}(t) = V(\mathbf{x}^{(i)}, \mathbf{x}_p). \tag{5.44}$$

The corresponding time change ratio of the measuring function is

$$\begin{aligned} \frac{dE^{(i)}(t)}{dt} &= \frac{\partial V(\mathbf{x}^{(i)}, \mathbf{x}_p)}{\partial \mathbf{x}^{(i)}} \cdot \dot{\mathbf{x}}^{(i)} \\ &= [\mathbf{n}(\mathbf{x}^{(i)}, \mathbf{x}_p)]^{\mathrm{T}} \cdot \mathbf{F}^{(i)}(\mathbf{x}^{(i)}, t, \mathbf{p}^{(i)}) \\ &= G_m^{(0)}(\mathbf{x}^{(i)}, \mathbf{x}_p, t). \end{aligned} \tag{5.45}$$

From the foregoing equation, the change of the equi-measuring function for the ith dynamical subsystem for time $t \in [t_k, t_{k+1}]$ can be defined from Luo (2008a, b).

Definition 5.16 For a flow $\mathbf{x}^{(i)}$ of the ith dynamical subsystem with a vector field $\mathbf{F}^{(i)}(\mathbf{x}^{(i)}, t, \mathbf{p}^{(i)})$ in Eq. (5.1), consider the equi-measuring function $V(\mathbf{x}^{(i)}, \mathbf{x}_p)$ in Eq. (5.32) to be monotonically increased to a metric function $d(\mathbf{x}, \mathbf{x}_p)$ in Eq. (5.30). The total change of the equi-measuring function for the time interval $[t_k, t]$ is defined as

$$\begin{aligned} L^{(i)}(\mathbf{x}_p, t_k, t) &= \int_{t_k}^{t} \frac{dE^{(i)}(t)}{dt} = \int_{t_k}^{t} G_m^{(0)}(\mathbf{x}^{(i)}, \mathbf{x}_p, t)dt \\ &= \int_{t_k}^{t} [\mathbf{n}(\mathbf{x}^{(i)}, \mathbf{x}_p)]^{\mathrm{T}} \cdot \mathbf{F}^{(i)}(\mathbf{x}^{(i)}, t, \mathbf{p}^{(i)})dt \\ &= V(\mathbf{x}^{(i)}(t), \mathbf{x}_p) - V(\mathbf{x}_k^{(i)}, \mathbf{x}_p) \end{aligned} \tag{5.46}$$

where $\mathbf{x}_k^{(i)} = \mathbf{x}^{(i)}(t_k)$. For a given $t = t_{k+1} > t_k$, the increment of the equi-measuring function to the ith subsystem in Eq. (5.1) for $t \in [t_k, t_{k+1}]$ is

$$\begin{aligned} L^{(i)}(\mathbf{x}_p, t_k, t_{k+1}) &= \int_{t_k}^{t_{k+1}} G_m^{(0)}(\mathbf{x}^{(i)}, \mathbf{x}_p, t)dt \\ &= \int_{t_k}^{t_{k+1}} [\mathbf{n}(\mathbf{x}^{(i)}, \mathbf{x}_p)]^{\mathrm{T}} \cdot \mathbf{F}^{(i)}(\mathbf{x}^{(i)}, t, \mathbf{p}^{(i)})dt \\ &= V(\mathbf{x}_{k+1}^{(i)}, \mathbf{x}_p) - V(\mathbf{x}_k^{(i)}, \mathbf{x}_p). \end{aligned} \tag{5.47}$$

From Eq. (5.47), it is observed that the equi-measuring function quantity is used to measure changes of the *i*th subsystem. Thus such a function can be used to investigate the stability of dynamical systems. Before the stability theory of the switching system is discussed, the following concepts are defined first.

Definition 5.17 For the *i*th dynamical subsystem in Eq. (5.1), consider the equi-measuring function $V(\mathbf{x}^{(i)}, \mathbf{x}_p)$ in Eq. (5.32) to be monotonically increased to a metric function $d(\mathbf{x}, \mathbf{x}_p)$ in Eq. (5.30). A flow $\mathbf{x}^{(i)}(t)$ at $\mathbf{x}_k^{(i)}$ for $t = t_k$ in the domain $\Omega_i \subset \mathscr{R}^n$ is:

(i) locally decreasing to the equi-measuring function surface in $\Omega_i \subset \mathscr{R}^n$ if

$$\left.\begin{aligned} V(\mathbf{x}_k^{(i)}, \mathbf{x}_p, t_k) - V(\mathbf{x}_{k-\varepsilon}^{(i)}, \mathbf{x}_p, t_{k-\varepsilon}) < 0, \\ V(\mathbf{x}_{k+\varepsilon}^{(i)}, \mathbf{x}_p, t_{k+\varepsilon}) - V(\mathbf{x}_k^{(i)}, \mathbf{x}_p, t_k) < 0; \end{aligned}\right\} \tag{5.48}$$

(ii) locally increasing to the equi-measuring function surface in $\Omega_i \subset \mathscr{R}^n$ if

$$\left.\begin{aligned} V(\mathbf{x}_k^{(i)}, \mathbf{x}_p, t_k) - V(\mathbf{x}_{k-\varepsilon}^{(i)}, \mathbf{x}_p, t_{k-\varepsilon}) > 0, \\ V(\mathbf{x}_{k+\varepsilon}^{(i)}, \mathbf{x}_p, t_{k+\varepsilon}) - V(\mathbf{x}_k^{(i)}, \mathbf{x}_p, t_k) > 0; \end{aligned}\right\} \tag{5.49}$$

(iii) locally tangential to the equi-measuring function surface in $\Omega_i \subset \mathscr{R}^n$ if

$$\begin{aligned} \text{either} \quad & \left.\begin{aligned} V(\mathbf{x}_k^{(i)}, \mathbf{x}_p, t_k) - V(\mathbf{x}_{k-\varepsilon}^{(i)}, \mathbf{x}_p, t_{k-\varepsilon}) < 0, \\ V(\mathbf{x}_{k+\varepsilon}^{(i)}, \mathbf{x}_p, t_{k+\varepsilon}) - V(\mathbf{x}_k^{(i)}, \mathbf{x}_p, t_k) > 0; \end{aligned}\right\} \\ \text{or} \quad & \left.\begin{aligned} V(\mathbf{x}_k^{(i)}, \mathbf{x}_p, t_k) - V(\mathbf{x}_{k-\varepsilon}^{(i)}, \mathbf{x}_p, t_{k-\varepsilon}) > 0, \\ V(\mathbf{x}_{k+\varepsilon}^{(i)}, \mathbf{x}_p, t_{k+\varepsilon}) - V(\mathbf{x}_k^{(i)}, \mathbf{x}_p, t_k) < 0. \end{aligned}\right\} \end{aligned} \tag{5.50}$$

From the previous definitions, the locally increasing and decreasing of a flow $\mathbf{x}^{(i)}(t)$ at $\mathbf{x}_k$ to the measuring function surface can be described in Fig. 5.5 in the vicinity of the point $\mathbf{x}_p$. A flow $\mathbf{x}^{(i)}(t)$ at $\mathbf{x}_k^{(i)}$, locally tangential to the equi-measuring function surface, can be similarly sketched.

Theorem 5.1 *For the ith dynamical subsystem in Eq. (5.1), consider the equi-measuring function* $V(\mathbf{x}^{(i)}, \mathbf{x}_p)$ *in Eq. (5.32) to be monotonically increased to a metric function* $d(\mathbf{x}, \mathbf{x}_p)$ *in Eq. (5.30). A flow* $\mathbf{x}^{(i)}(t)$ *at* $\mathbf{x}_k^{(i)}$ *for* $t = t_k$ *in the domain* $\Omega_i \subset \mathscr{R}^n$ is:

(i) *locally decreasing to the equi-measuring function surface in* $\Omega_i \subset \mathscr{R}^n$ *if and only if*

$$G_m^{(0)}(\mathbf{x}_k^{(i)}, \mathbf{x}_p, t) = [\mathbf{n}(\mathbf{x}_k^{(i)}, \mathbf{x}_p)]^{\mathrm{T}} \cdot \mathbf{F}^{(i)}(\mathbf{x}_k^{(i)}, t_k, \mathbf{p}^{(i)}) < 0; \tag{5.51}$$

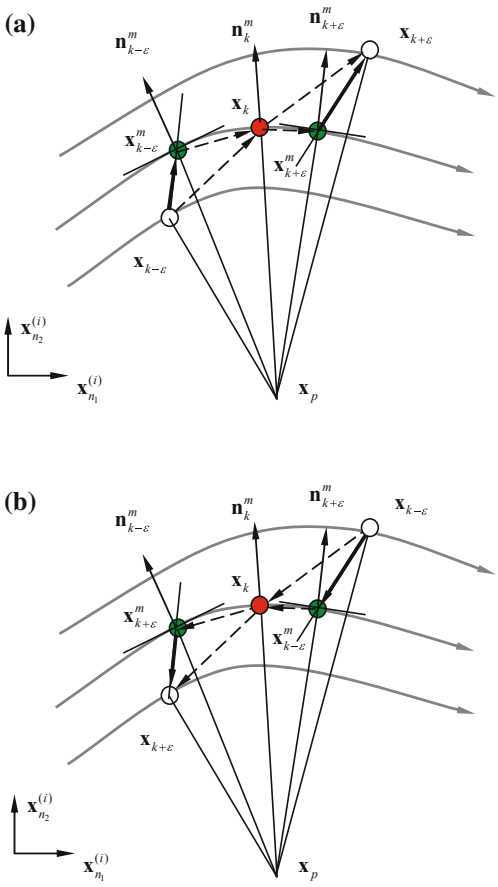

Fig. 5.5 **a** A locally increasing flow, and **b** a locally decreasing flow to a measuring function with $n_1 + n_2 = n$

(ii) *locally increasing to the equi-measuring function surface in* $\Omega_i \subset \mathscr{R}^n$ *if and only if*

$$G^{(0)}_m(\mathbf{x}^{(i)}_k, \mathbf{x}_p, t) = [\mathbf{n}(\mathbf{x}^{(i)}_k, \mathbf{x}_p)]^{\mathrm{T}} \cdot \mathbf{F}^{(i)}(\mathbf{x}^{(i)}_k, t_k, \mathbf{p}^{(i)}) > 0; \tag{5.52}$$

(iii) *locally tangential to the equi-measuring function surface in* $\Omega_i \subset \mathscr{R}^n$ *if and only if*

$$\begin{aligned} &G^{(0)}_m(\mathbf{x}^{(i)}_k, \mathbf{x}_p, t) = [\mathbf{n}(\mathbf{x}^{(i)}_k, \mathbf{x}_p)]^{\mathrm{T}} \cdot \mathbf{F}^{(i)}(\mathbf{x}^{(i)}_k, t_k, \mathbf{p}^{(i)}) = 0; \\ &G^{(1)}_m(\mathbf{x}^{(i)}_k, \mathbf{x}_p, t) \neq 0. \end{aligned} \tag{5.53}$$

Proof Using G-functions and Taylor series expansion, this theorem can be proved directly. ■

Definition 5.18 For the ith dynamical subsystem in Eq. (5.1), consider the equi-measuring function $V(\mathbf{x}^{(i)}, \mathbf{x}_p)$ in Eq. (5.32) to be monotonically increased to a metric

function $d(\mathbf{x}, \mathbf{x}_p)$ in Eq. (5.30). A flow $\mathbf{x}^{(i)}(t)$ from $\mathbf{x}_k^{(i)}$ to $\mathbf{x}_{k+1}^{(i)}$ for $t = t_s \in [t_k, t_{k+1}]$ in the domain $\Omega_i \subset \mathscr{R}^n$ is:

(i) uniformly decreasing to the equi-measuring function surface in $\Omega_i \subset \mathscr{R}^n$ if

$$\left.\begin{aligned} V(\mathbf{x}_s^{(i)}, \mathbf{x}_p, t_s) - V(\mathbf{x}_{s-\varepsilon}^{(i)}, \mathbf{x}_p, t_{s-\varepsilon}) < 0, \\ V(\mathbf{x}_{s+\varepsilon}^{(i)}, \mathbf{x}_p, t_{s+\varepsilon}) - V(\mathbf{x}_s^{(i)}, \mathbf{x}_p, t_s) < 0; \end{aligned}\right\} \tag{5.54}$$

(ii) uniformly increasing to the equi-measuring function surface in $\Omega_i \subset \mathscr{R}^n$ if

$$\left.\begin{aligned} V(\mathbf{x}_s^{(i)}, \mathbf{x}_p, t_s) - V(\mathbf{x}_{s-\varepsilon}^{(i)}, \mathbf{x}_p, t_{s-\varepsilon}) > 0, \\ V(\mathbf{x}_{s+\varepsilon}^{(i)}, \mathbf{x}_p, t_{s+\varepsilon}) - V(\mathbf{x}_s^{(i)}, \mathbf{x}_p, t_s) > 0; \end{aligned}\right\} \tag{5.55}$$

(iii) uniformly invariant to the equi-measuring function surface in $\Omega_i \subset \mathscr{R}^n$ if

$$V(\mathbf{x}_{s+\varepsilon}^{(i)}, \mathbf{x}_p, t_{s+\varepsilon}) = V(\mathbf{x}_s^{(i)}, \mathbf{x}_p, t_s) = V(\mathbf{x}_{s-\varepsilon}^{(i)}, \mathbf{x}_p, t_{s-\varepsilon}). \tag{5.56}$$

Theorem 5.2 *For the dynamical subsystem in Eq. (5.1), consider the equi-measuring function $V(\mathbf{x}^{(i)}, \mathbf{x}_p)$ in Eq. (5.32) to be monotonically increased to a metric function $d(\mathbf{x}, \mathbf{x}_p)$ in Eq. (5.30). A flow $\mathbf{x}^{(i)}(t)$ from $\mathbf{x}_k^{(i)}$ to $\mathbf{x}_{k+1}^{(i)}$ for $t \in [t_k, t_{k+1}]$ in the domain $\Omega_i \subset \mathscr{R}^n$ is:*

(i) *uniformly decreasing to the equi-measuring function surface in $\Omega_i \subset \mathscr{R}^n$ if and only if all points $\mathbf{x}^{(i)}(t)$ for $t \in [t_k, t_{k+1}]$ on the flow γ satisfy the following condition*

$$G_m^{(0)}(\mathbf{x}^{(i)}, \mathbf{x}_p, t) = [\mathbf{n}(\mathbf{x}^{(i)}, \mathbf{x}_p)]^{\mathrm{T}} \cdot \mathbf{F}^{(i)}(\mathbf{x}^{(i)}, t, \mathbf{p}^{(i)}) < 0; \tag{5.57}$$

(ii) *uniformly increasing to the equi-measuring function surface in $\Omega_i \subset \mathscr{R}^n$ if and only if all points $\mathbf{x}^{(i)}(t)$ for $t \in [t_k, t_{k+1}]$ on the flow γ satisfy the following condition*

$$G_m^{(0)}(\mathbf{x}^{(i)}, \mathbf{x}_p, t) = [\mathbf{n}(\mathbf{x}^{(i)}, \mathbf{x}_p)]^{\mathrm{T}} \cdot \mathbf{F}^{(i)}(\mathbf{x}^{(i)}, t, \mathbf{p}^{(i)}) > 0; \tag{5.58}$$

(iii) *uniformly invariant to the equi-measuring function surface in $\Omega_i \subset \mathscr{R}^n$ if and only if all points $\mathbf{x}^{(i)}(t)$ for $t \in [t_k, t_{k+1}]$ on the flow γ satisfy the following condition*

$$G_m^{(k)}(\mathbf{x}^{(i)}, \mathbf{x}_p, t) = 0 \; k = 0, 1, 2, \cdots. \tag{5.59}$$

Proof Using G-functions and Taylor series expansion, this theorem can be proved directly. ■

Definition 5.19 For the ith dynamical subsystem in Eq. (5.1), consider the equi-measuring function $V(\mathbf{x}^{(i)}, \mathbf{x}_p)$ in Eq. (5.32) to be monotonically increased to a metric function $d(\mathbf{x}, \mathbf{x}_p)$ in Eq. (5.30). A flow $\mathbf{x}^{(i)}(t)$ at $\mathbf{x}_k^{(i)}$ for $t = t_k$ in the domain $\Omega_i \subset \mathscr{R}^n$ is:

(i) locally decreasing with the $(2s)$th-order to the equi-measuring function surface in $\Omega_i \subset \mathscr{R}^n$ if

$$\begin{aligned} &G_m^{(r)}(\mathbf{x}_k^{(i)}, \mathbf{x}_p, t_k) = 0 \text{ for } r = 0, 1, 2, \cdots, 2s-1; \\ &V(\mathbf{x}_k^{(i)}, \mathbf{x}_p, t_k) - V(\mathbf{x}_{k-\varepsilon}^{(i)}, \mathbf{x}_p, t_{k-\varepsilon}) < 0, \\ &V(\mathbf{x}_{k+\varepsilon}^{(i)}, \mathbf{x}_p, t_{k+\varepsilon}) - V(\mathbf{x}_k^{(i)}, \mathbf{x}_p, t_k) < 0; \end{aligned} \tag{5.60}$$

(ii) locally increasing with the $(2s)$th-order to the equi-measuring function surface in $\Omega_i \subset \mathscr{R}^n$ if

$$\begin{aligned} &G_m^{(r)}(\mathbf{x}_k^{(i)}, \mathbf{x}_p, t_k) = 0 \text{ for } r = 0, 1, 2, \cdots, 2s-1; \\ &V(\mathbf{x}_k^{(i)}, \mathbf{x}_p, t_k) - V(\mathbf{x}_{k-\varepsilon}^{(i)}, \mathbf{x}_p, t_{k-\varepsilon}) > 0, \\ &V(\mathbf{x}_{k+\varepsilon}^{(i)}, \mathbf{x}_p, t_{k+\varepsilon}) - V(\mathbf{x}_k^{(i)}, \mathbf{x}_p, t_k) > 0; \end{aligned} \tag{5.61}$$

(iii) locally tangential with the $(2s-1)$th-order to the equi-measuring function surface in $\Omega_i \subset \mathscr{R}^n$ if

$$\begin{aligned} &G_m^{(r)}(\mathbf{x}_k^{(i)}, \mathbf{x}_p, t_k) = 0 \text{ for } r = 0, 1, 2, \cdots, 2s; \\ &\text{either} \quad \left.\begin{aligned} &V(\mathbf{x}_k^{(i)}, \mathbf{x}_p, t_k) - V(\mathbf{x}_{k-\varepsilon}^{(i)}, \mathbf{x}_p, t_{k-\varepsilon}) < 0, \\ &V(\mathbf{x}_{k+\varepsilon}^{(i)}, \mathbf{x}_p, t_{k+\varepsilon}) - V(\mathbf{x}_k^{(i)}, \mathbf{x}_p, t_k) < 0; \end{aligned}\right\} \\ &\text{or} \quad \left.\begin{aligned} &V(\mathbf{x}_k^{(i)}, \mathbf{x}_p, t_k) - V(\mathbf{x}_{k-\varepsilon}^{(i)}, \mathbf{x}_p, t_{k-\varepsilon}) > 0, \\ &V(\mathbf{x}_{k+\varepsilon}^{(i)}, \mathbf{x}_p, t_{k+\varepsilon}) - V(\mathbf{x}_k^{(i)}, \mathbf{x}_p, t_k) > 0. \end{aligned}\right\} \end{aligned} \tag{5.62}$$

Theorem 5.3 *For the ith dynamical subsystem in Eq.* (5.1), *consider the equi-measuring function* $V(\mathbf{x}^{(i)}, \mathbf{x}_p)$ *in Eq.* (5.32) *to be monotonically increased to a metric function* $d(\mathbf{x}, \mathbf{x}_p)$ *in Eq.* (5.30). *A flow* $\mathbf{x}^{(i)}(t)$ *at* $\mathbf{x}_k^{(i)}$ *for* $t = t_k$ *in the domain* $\Omega_i \subset \mathscr{R}^n$ *is*:

(i) *locally decreasing with the* $(2s)$th-*order to the equi-measuring function surface in* $\Omega_i \subset \mathscr{R}^n$ *if and only if*

$$\begin{aligned} &G_m^{(r)}(\mathbf{x}_k, \mathbf{x}_p, t_k) = 0, \quad \text{for } r = 0, 1, 2, \cdots, 2s-1 \\ &G_m^{(2s)}(\mathbf{x}_k, \mathbf{x}_p, t_k) < 0; \end{aligned} \tag{5.63}$$

(ii) *locally increasing with the* $(2s)$th-*order to the equi-measuring function surface in* $\Omega_i \subset \mathscr{R}^n$ *if and only if*

$$\begin{aligned} &G_m^{(r)}(\mathbf{x}_k, \mathbf{x}_p, t_k) = 0, \quad \text{for } r = 0, 1, 2, \cdots, 2s-1 \\ &G_m^{(2s)}(\mathbf{x}_k, \mathbf{x}_p, t_k) > 0; \end{aligned} \tag{5.64}$$

(iii) *locally tangential with the* $(2s-1)$th*-order to the equi-measuring function surface in* $\Omega_i \subset \mathscr{R}^n$ *if and only if*

$$\begin{aligned} &G_m^{(r)}(\mathbf{x}_k, \mathbf{x}_p, t_k) = 0, \quad \text{for } r = 0, 1, 2, \cdots, 2s \\ &G_m^{(2s+1)}(\mathbf{x}_k, \mathbf{x}_p, t_k) \neq 0. \end{aligned} \tag{5.65}$$

Proof Using G-functions and Taylor series expansion, this theorem can be proved directly. ■

Definition 5.20 For the ith dynamical subsystem in Eq. (5.1), consider the equi-measuring function $V(\mathbf{x}^{(i)}, \mathbf{x}_p)$ in Eq. (5.32) to be monotonically increased to a metric function $d(\mathbf{x}, \mathbf{x}_p)$ in Eq. (5.30). A flow $\mathbf{x}^{(i)}(t)$ from $\mathbf{x}_k^{(i)}$ to $\mathbf{x}_{k+1}^{(i)}$ for $t \in [t_k, t_{k+1}]$ in the domain $\Omega_i \subset \mathscr{R}^n$ is:

(i) globally decreasing to the equi-measuring function surface in $\Omega_i \subset \mathscr{R}^n$ if the equi-measuring function increment for $t \in [t_k, t_{k+1}]$ is less than zero, i.e.,

$$L^{(i)}(\mathbf{x}_p, t_k, t_{k+1}) \equiv \int_{t_k}^{t_{k+1}} [\mathbf{n}(\mathbf{x}^{(i)}, \mathbf{x}_p)]^{\mathrm{T}} \cdot \mathbf{F}^{(i)}(\mathbf{x}^{(i)}, t, \mathbf{p}^{(i)}) dt < 0; \tag{5.66}$$

(ii) globally increasing to the equi-measuring function surface in $\Omega_i \subset \mathscr{R}^n$ if the equi-measuring function increment for $t \in [t_k, t_{k+1}]$ is greater than zero, i.e.,

$$L^{(i)}(\mathbf{x}_p, t_k, t_{k+1}) \equiv \int_{t_k}^{t_{k+1}} [\mathbf{n}(\mathbf{x}^{(i)}, \mathbf{x}_p)]^{\mathrm{T}} \cdot \mathbf{F}^{(i)}(\mathbf{x}^{(i)}, t, \mathbf{p}^{(i)}) dt > 0; \tag{5.67}$$

(iii) globally invariant to the equi-measuring function surface in $\Omega_i \subset \mathscr{R}^n$ if the equi-measuring function increment for $t \in [t_k, t_{k+1}]$ is equal to zero, i.e.,

$$L^{(i)}(\mathbf{x}_p, t_k, t_{k+1}) \equiv \int_{t_k}^{t_{k+1}} [\mathbf{n}(\mathbf{x}^{(i)}, \mathbf{x}_p)]^{\mathrm{T}} \cdot \mathbf{F}^{(i)}(\mathbf{x}^{(i)}, t, \mathbf{p}^{(i)}) dt = 0. \tag{5.68}$$

From the foregoing definition, the global increase, decrease and invariance for a single subsystem are defined. The L-function is pertaining to the averaging of a flow $\mathbf{x}^{(i)}(t)$ to the equi-measuring function surface of $V(\mathbf{x}^{(i)}, \mathbf{x}_p) = C$ for the time period of $[t_k, t_{k+1}]$. To determine the global increase, decrease and invariance for a switching system, the resultant flow of the switching system is the union of all the flows of the subsystems in a certain queue series, and the corresponding L-function can be defined.

Definition 5.21 For a switching system in Eqs. (5.15) and (5.16) on the domain $\mho = \cup_{i=1}^{m_1} \Omega_{l_i} \cup \Omega_0$, there is a resultant flow $\gamma(t_0, t)$, i.e.,

$$\gamma(t_0, t) = \cup_{k=1}^{l-1} \gamma^{(\alpha_k)}(t_{k-1}, t_k) + \gamma^{(\alpha_l)}(t_{l-1}, t), \tag{5.69}$$

where

$$\gamma^{(\alpha_k)}(t_{k-1}, t_k) = \left\{ \mathbf{x}^{(\alpha_k)}(t) \,\middle|\, \begin{array}{l} S_{\alpha_k} : \dot{\mathbf{x}}^{(\alpha_k)} = \mathbf{F}^{(\alpha_k)}(\mathbf{x}^{(\alpha_k)}, t, \mathbf{p}^{(\alpha_k)}) \\ \text{on } \Omega_{\alpha_k} \text{ with } \mathbf{x}^{(i)}(t_{k-1}) = \mathbf{x}_{k-1}^{(i)} \\ \text{for all } t \in [t_{k-1}, t_k] \end{array} \right\}. \tag{5.70}$$

The corresponding L-function along the resultant flow $\gamma(t_0, t)$ is defined as

$$L(\mathbf{x}_p, t_0, t) = \sum_{k=1}^{l-1} \left[L^{(\alpha_k)}(\mathbf{x}_p, t_{k-1}, t_k) + \Delta^{(\alpha_k \alpha_{k+1})}(t_k) \right] + L^{(\alpha_l)}(\mathbf{x}_p, t_{l-1}, t), \tag{5.71}$$

where $\Delta^{(\alpha_k \alpha_{k+1})}(t_k)$ is the quantity increment of the equi-measuring function surface for the switching from dynamical system S_{α_k} to dynamical systems $S_{\alpha_{k+1}}$ through the transport laws in Eq. (5.16), i.e., the quantity increment is equal to

$$\Delta^{(\alpha_k \alpha_{k+1})}(t_k) = V(\mathbf{x}_k^{(\alpha_{k+1})}, \mathbf{x}_p) - V(\mathbf{x}_k^{(\alpha_k)}, \mathbf{x}_p). \tag{5.72}$$

Note that the resultant L-function for the total flow $\gamma(t_0, t)$ is computed by

$$\begin{aligned} L(\mathbf{x}_p, t_0, t) &= \sum_{k=1}^{l-1} \left[L^{(\alpha_k)}(\mathbf{x}_p, t_{k-1}, t_k) + \Delta^{(\alpha_k \alpha_{k+1})} \right] + L^{(\alpha_l)}(\mathbf{x}_p, t_{l-1}, t) \\ &= \sum_{k=1}^{l-1} [\int_{t_{k-1}}^{t_k} G_m^{(0)}(\mathbf{x}^{(\alpha_k)}, \mathbf{x}_p, t) dt + \Delta^{(\alpha_k \alpha_{k+1})}] \\ &\qquad + \int_{t_{l-1}}^{t} G_m^{(0)}(\mathbf{x}^{(\alpha_l)}, \mathbf{x}_p, t) dt \\ &= \sum_{k=1}^{l-1} \left\{ \int_{t_{k-1}}^{t_k} [\mathbf{n}(\mathbf{x}^{(\alpha_k)}, \mathbf{x}_p)]^{\mathrm{T}} \cdot \mathbf{F}^{(\alpha_k)}(\mathbf{x}^{(\alpha_k)}, t, \mathbf{p}^{(\alpha_k)}) dt \right. \\ &\quad \left. + \Delta^{(\alpha_k \alpha_{k+1})} \right\} + \int_{t_{l-1}}^{t} [\mathbf{n}(\mathbf{x}^{(\alpha_l)}, \mathbf{x}_p)]^{\mathrm{T}} \cdot \mathbf{F}^{(\alpha_l)}(\mathbf{x}^{(\alpha_l)}, t, \mathbf{p}^{(\alpha_l)}) dt \\ &= \sum_{k=1}^{l-1} \left[V(\mathbf{x}_k^{(\alpha_k)}, \mathbf{x}_p) - V(\mathbf{x}_{k-1}^{(\alpha_k)}, \mathbf{x}_p) + \Delta^{(\alpha_k \alpha_{k+1})} \right] \\ &\quad + V(\mathbf{x}^{(\alpha_l)}(t), \mathbf{x}_p) - V(\mathbf{x}_{l-1}^{(\alpha_l)}, \mathbf{x}_p). \end{aligned} \tag{5.73}$$

The resultant L-function in Eq. (5.73) can be sketched through the equi-measuring functions, as shown in Fig. 5.6. The measuring functions for each subsystem may not always increase or decrease with increasing time. The total effect of equi-measuring functions to all the queue series subsystems in the switching system should be considered. The solid curves give the equi-measuring-function values of a flow $\gamma^{(\alpha_k)}(t)$ $(k = 1, 2, \cdots, m, \cdots)$. The dashed lines are jumping changes of the equi-measuring function, and the jumping changes are caused by the transport laws between two adjacent queue subsystems. The circular points represent the switching points for two adjacent queue subsystems. The L-function changes for the switching system is clearly presented.

Since any switching system possesses a queue series of subsystems, the total effect of equi-measuring functions to all the queue series subsystems in the switching system should be considered. If each system is uniformly increasing to the equi-measuring function, with a positive impulse, then the switching system is uniformly

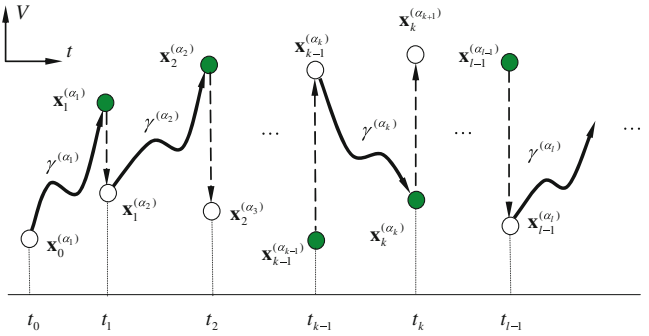

Fig. 5.6 The equi-measuring function varying with flows of sub-systems. The *solid curves* give the equi-measuring function values of a flow $\gamma^{(\alpha_k)}(t)$. The *dashed lines* are jumping changes of the equi-measuring function, and the jumping changes are caused by the transport laws between two adjacent queue subsystems. The circular points represent the switching points for two adjacent queue subsystems

increasing. Otherwise, if each system is uniformly decreasing to the equi-measuring functions, with a negative impulse, then the switching system is uniformly decreasing.

Definition 5.22 For a switching system in Eqs. (5.15) and (5.16) on the domain $\mho = \cup_{i=1}^{m_1}\Omega_{l_i} \cup \Omega_0$, there is an resultant flow $\gamma(t_0, t)$ in Eq. (5.69). For the α_kth dynamical subsystem S_{α_k}, consider the equi-measuring function $V(\mathbf{x}^{(\alpha_k)}, \mathbf{x}_p)$ in Eq. (5.32) to be monotonically increased to a metric function $d(\mathbf{x}, \mathbf{x}_p)$ in Eq. (5.30). A flow $\gamma(t_0, t)$ from $\gamma^{(\alpha_1)}(t_0, t_1)$ to $\gamma^{(\alpha_l)}(t_{l-1}, t)$ for $t \in [t_0, t_l]$ in the domain $\cup_{k=1}^{l}\Omega_{\alpha_k}$ is:

(i) uniformly decreasing to the equi-measuring function surface in $\cup_{k=1}^{l}\Omega_{\alpha_k}$ if

$$\left.\begin{aligned} &V(\mathbf{x}_s^{(\alpha_k)}, \mathbf{x}_p, t_s) - V(\mathbf{x}_{s-\varepsilon}^{(\alpha_k)}, \mathbf{x}_p, t_{s-\varepsilon}) < 0,\\ &V(\mathbf{x}_{s+\varepsilon}^{(\alpha_k)}, \mathbf{x}_p, t_{s+\varepsilon}) - V(\mathbf{x}_s^{(\alpha_k)}, \mathbf{x}_p, t_s) < 0,\\ &\text{for } \mathbf{x}_s^{(\alpha_k)} \in \gamma^{(\alpha_k)}(t_{k-1}, t_k) \text{ with } t_s \in [t_{k-1}, t_k];\\ &\Delta^{(\alpha_k\alpha_{k+1})}(t_k) < 0 \text{ for } k = 1, 2, \cdots, l; \end{aligned}\right\} \tag{5.74}$$

(ii) uniformly increasing to the equi-measuring function surface in $\cup_{k=1}^{l}\Omega_{\alpha_k}$ if

$$\left.\begin{aligned} &V(\mathbf{x}_s^{(\alpha_k)}, \mathbf{x}_p, t_s) - V(\mathbf{x}_{s-\varepsilon}^{(\alpha_k)}, \mathbf{x}_p, t_{s-\varepsilon}) > 0,\\ &V(\mathbf{x}_{s+\varepsilon}^{(\alpha_k)}, \mathbf{x}_p, t_{s+\varepsilon}) - V(\mathbf{x}_s^{(\alpha_k)}, \mathbf{x}_p, t_s) > 0;\\ &\text{for } \mathbf{x}_s^{(\alpha_k)} \in \gamma^{(\alpha_k)}(t_{k-1}, t_k) \text{ with } t_s \in [t_{k-1}, t_k]\\ &\Delta^{(\alpha_k\alpha_{k+1})}(t_k) > 0 \text{ for } k = 1, 2, \cdots, l; \end{aligned}\right\} \tag{5.75}$$

(iii) uniformly and negatively impulsive to the equi-measuring function surface in $\cup_{k=1}^{l}\Omega_{\alpha_k}$ if

$$\left.\begin{array}{l} V(\mathbf{x}_{s+\varepsilon}^{(\alpha_k)}, \mathbf{x}_p, t_{s+\varepsilon}) = V(\mathbf{x}_s^{(\alpha_k)}, \mathbf{x}_p, t_s) = V(\mathbf{x}_{s-\varepsilon}^{(\alpha_k)}, \mathbf{x}_p, t_{s-\varepsilon}) \\ \text{for } \mathbf{x}_s^{(\alpha_k)} \in \gamma^{(\alpha_k)}(t_{k-1}, t_k) \text{ with } t_s \in [t_{k-1}, t_k], \\ \Delta^{(\alpha_k \alpha_{k+1})}(t_k) < 0 \text{ for } k = 1, 2, \cdots, l; \end{array}\right\} \tag{5.76}$$

(iv) uniformly and positively impulsive to the equi-measuring function surface in $\cup_{k=1}^{l} \Omega_{\alpha_k}$ if

$$\left.\begin{array}{l} V(\mathbf{x}_{s+\varepsilon}^{(\alpha_k)}, \mathbf{x}_p, t_{s+\varepsilon}) = V(\mathbf{x}_s^{(\alpha_k)}, \mathbf{x}_p, t_s) = V(\mathbf{x}_{s-\varepsilon}^{(\alpha_k)}, \mathbf{x}_p, t_{s-\varepsilon}) \\ \text{for } \mathbf{x}_s^{(\alpha_k)} \in \gamma^{(\alpha_k)}(t_{k-1}, t_k) \text{ with } t_s \in [t_{k-1}, t_k], \\ \Delta^{(\alpha_k \alpha_{k+1})}(t_k) > 0 \text{ for } k = 1, 2, \cdots, l; \end{array}\right\} \tag{5.77}$$

(v) uniformly invariant to the equi-measuring function surface in $\cup_{k=1}^{l} \Omega_{\alpha_k}$ if

$$\left.\begin{array}{l} V(\mathbf{x}_{s+\varepsilon}^{(\alpha_k)}, \mathbf{x}_p, t_{s+\varepsilon}) = V(\mathbf{x}_s^{(\alpha_k)}, \mathbf{x}_p, t_s) = V(\mathbf{x}_{s-\varepsilon}^{(\alpha_k)}, \mathbf{x}_p, t_{s-\varepsilon}) \\ \text{for } \mathbf{x}_s^{(\alpha_k)} \in \gamma^{(\alpha_k)}(t_{k-1}, t_k) \text{ with } t_s \in [t_{k-1}, t_k], \\ \Delta^{(\alpha_k \alpha_{k+1})}(t_k) = 0 \text{ for } k = 1, 2, \cdots, l. \end{array}\right\} \tag{5.78}$$

From the foregoing definition, the uniformly increasing and decreasing of a resultant flow of the switching system to the equi-measuring surface require that each subsystem should be uniformly increasing with a positive impulse and uniformly decreasing with a negative impulse, respectively. For an intuitive illustration, such uniformly increasing and decreasing of a switching system are presented in Fig. 5.7a and b, respectively. The corresponding trajectories in phase space are presented in Fig. 5.8a and b for uniformly increasing and decreasing.

Consider a dynamical system

$$\dot{x}^{(i)} = y^{(i)} \text{ and } \dot{y}^{(i)} = -c^{(i)} x^{(i)} - 2d^{(i)} y^{(i)} \tag{5.79}$$

with an impulsive function

$$\begin{array}{l} x_{k+}^{(i)} = x_{k-}^{(i)}, y_{k+}^{(i)} = y_{k-}^{(i)} + a^{(i)} \text{sgn}(y_{k-}^{(i)}) (k = 1, 2, \cdots) \\ \text{for } t_k = kT/m \text{ with } T = 2\pi/\sqrt{c}, a^{(i)} > 0. \end{array} \tag{5.80}$$

For the impulsive system in Eq. (5.79), consider a measuring function

$$V^{(i)} = \frac{1}{2}(y^{(i)})^2 + \frac{1}{2} c^{(i)} (x^{(i)})^2. \tag{5.81}$$

The solutions for Eq. (5.79) can be easily obtained. Herein, for $(d^{(i)})^2 < c^{(i)}$, the solution is given for $t \in [t_{k+}, t_{k+1})$

$$\begin{array}{l} x^{(i)} = e^{-d^{(i)}(t-t_{k+})} [C_1^{(i)} \cos \omega_d^{(i)} (t - t_{k+}) + C_2^{(i)} \sin \omega_d^{(i)} (t - t_{k+})], \\ y^{(i)} = e^{-d^{(i)}(t-t_{k+})} [(C_2^{(i)} \omega_d^{(i)} - C_1^{(i)} d^{(i)}) \cos \omega_d^{(i)} (t - t_{k+}) \\ \quad -(C_2^{(i)} d^{(i)} + \omega_d^{(i)} C_1^{(i)}) \sin \omega_d^{(i)} (t - t_{k+})], \end{array} \tag{5.82}$$

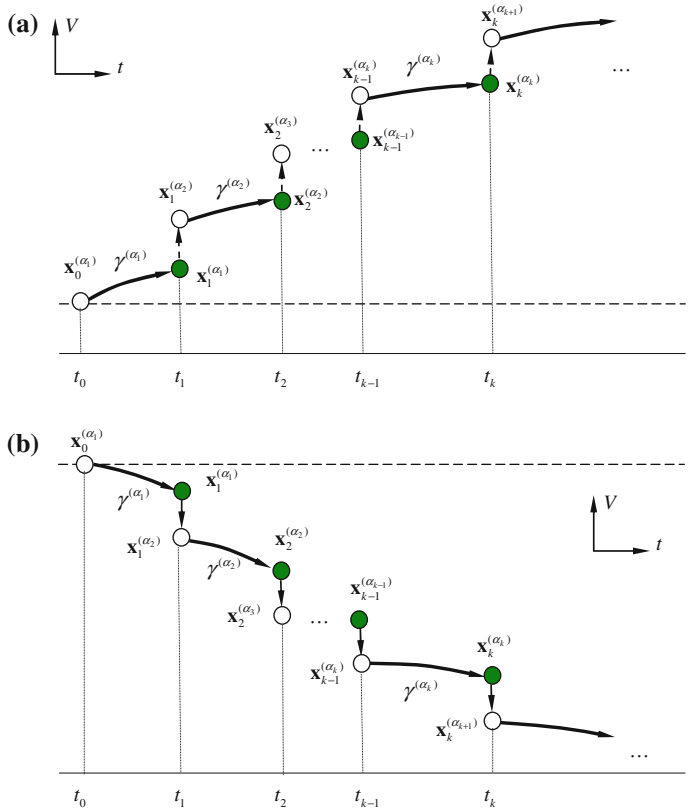

Fig. 5.7 The equi-measuring function varying with time: **a** uniformly increasing, **b** uniformly decreasing. The *solid curves* give the equi-measuring-function values of a flow $\gamma^{(\alpha_k)}(t)$. The *dashed lines* are jumping changes of the equi-measuring function, and the jumping changes are caused by the transport laws between two adjacent queue subsystems. The circular symbols represent the switching points for two adjacent queue subsystems

where

$$C_1^{(i)} = x_{k+}^{(i)}, C_2^{(i)} = (y_{k+}^{(i)} + x_{k+}^{(i)} d^{(i)})/\omega_d^{(i)}; \omega_d^{(i)} = \sqrt{c^{(i)} - (d^{(i)})^2}. \tag{5.83}$$

For simplicity, consider a system with an impulsive function

$$c^{(i)} = c = 1, d^{(i)} = d = -0.005, a^{(i)} = a = 1.0, m = 2; \tag{5.84}$$

and the initial condition is

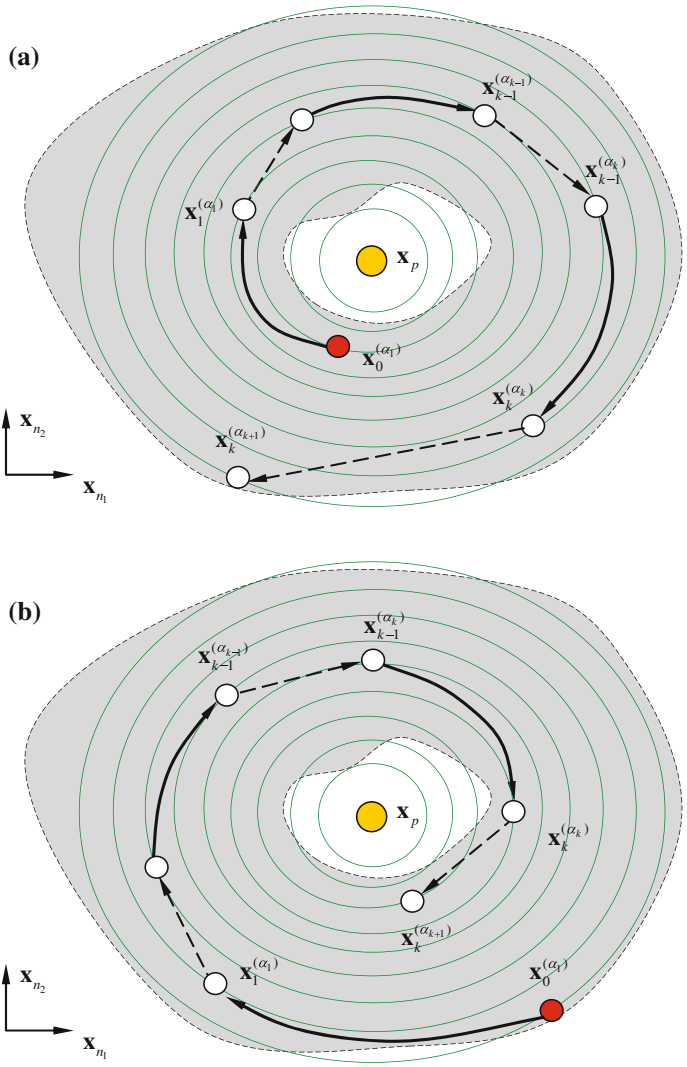

Fig. 5.8 A flow to the equi-measuring function surface in vicinity of point $\mathbf{x}_p$ in phase space: **a** uniform increase, and **b** uniform decrease. The cycles are equi-measuring function surfaces. The *circular symbols* represent the switching points for two adjacent queue subsystems

$$x_0^{(i)} = y_0^{(i)} = 4 \text{ for } t_0 = 0. \tag{5.85}$$

Thus, the dynamical characteristics of the impulsive system are presented in Fig. 5.9. The impulsive system possesses the uniform increases of measuring function with increasing impulses, as presented in Fig. 5.9a. The corresponding trajectory for such an impulsive system is presented in Fig. 5.9b. The time-history of G-function

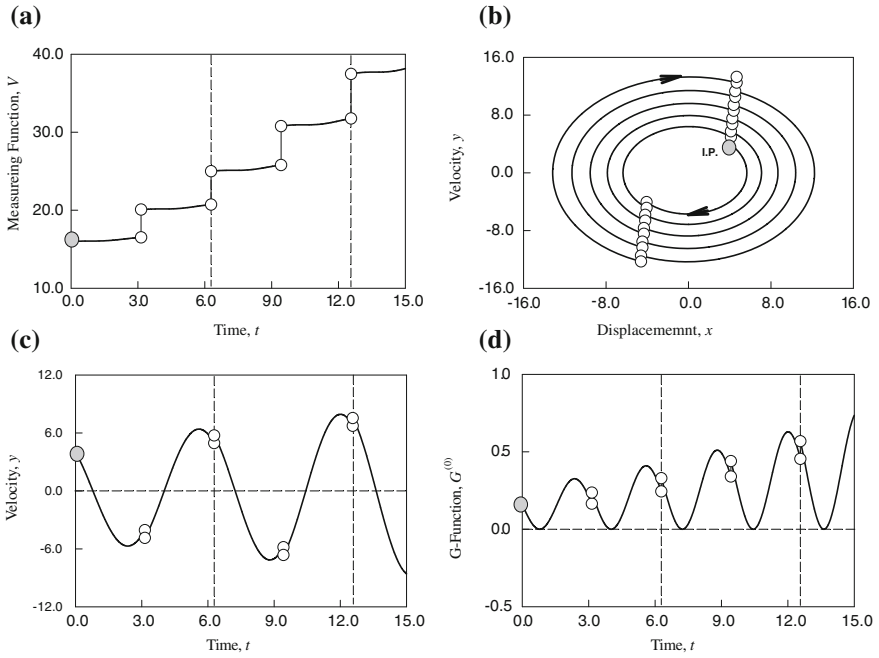

Fig. 5.9 An impulsive system with negative damping: **a** uniformly increasing of measuring function with increasing impulses, **b** trajectory in phase plane, **c** G-function of measuring function, and **d** discontinuous velocity. The *circular symbols* represent the impulsive points for such an impulsive system. Two time impulses for each period are labeled by the *vertical lines*. ($c^{(i)} = c = 1, d^{(i)} = d = -0.01, a^{(i)} = a = 1.0, m = 2$ and $x_0^{(i)} = y_0^{(i)} = 4$ for $t_0 = 0$)

of the equi-measuring function is presented in Fig. 5.9c. It is observed that the G-function is less than zero. Since the impulsive effect is exerted, the velocity is C^0-discontinuous, which is presented in Fig. 5.9d. Thus, the corresponding displacement is C^0-continuous, which will not be presented herein. For uniform deceasing of measuring function, the impulsive rule in Eq. (5.80) can be changed as

$$\begin{aligned} &x_{k+}^{(i)} = x_{k-}^{(i)}, y_{k+}^{(i)} = y_{k-}^{(i)} - a^{(i)}\text{sgn}(y_{k-}^{(i)})(k = 1, 2, \cdots) \\ &\text{for } t_k = kT/m \text{ with } T = 2\pi/\sqrt{c}, a^{(i)} > 0. \end{aligned} \tag{5.86}$$

and the impulsive system with an impulsive function has the following parameters to be considered as

$$c^{(i)} = c = 1, d^{(i)} = d = 0.05, a^{(i)} = a = 1.0, m = 2. \tag{5.87}$$

and the initial condition is

$$x_0^{(i)} = y_0^{(i)} = 4 \text{ for } t_0 = 0. \tag{5.88}$$

Thus, such an impulsive system with uniform decrease of measuring function is in Fig. 5.10. The uniform decrease of measuring function with increasing impulses

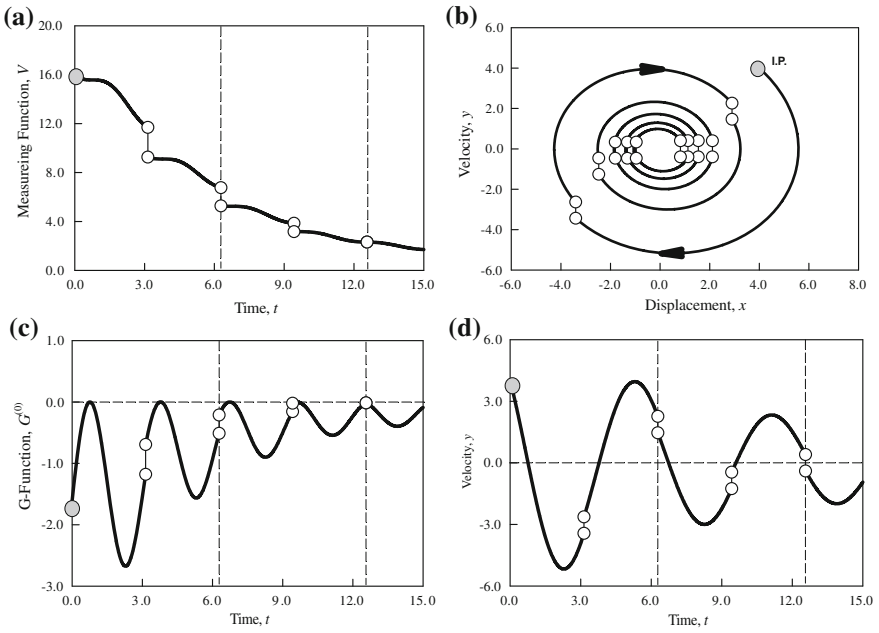

Fig. 5.10 An impulsive system with positive damping: **a** uniformly decreasing of measuring function with decreasing impulses, **b** trajectory in phase plane, **c** G-function of measuring function, and **d** discontinuous velocity. The *circular symbols* represent the impulsive points for such an impulsive system. Two time impulses for each period are labeled by the *vertical lines*. ($c^{(i)} = c = 1, \quad d^{(i)} = d = 0.05, a^{(i)} = a = 1.0, m = 2$ and $x_0^{(i)} = y_0^{(i)} = 4$ for $t_0 = 0$)

for the impulsive system is presented in Fig. 5.10a. The correspond trajectory for such an impulsive system is presented in Fig 5.10b. It is observed that the trajectory will approach the equilibrium point ($x = y = 0$). The time-history of G-function of the equi-measuring function is presented in Fig. 5.10c. It is observed that the G-function is greater than zero. Again, since the impulsive effect are exerted, the C^0-discontinuous velocity is presented in Fig. 5.10d.

For the switching system with uniformly increasing (decreasing) of measuring function at impulses, each subsystem in the switching system is uniformly invariant to the equi-measuring function, and only the uniform, positive (or negative) impulses exist in the switching system, as shown in Fig. 5.11a and b. The corresponding trajectories in phase space are also presented in Fig. 5.12a and b. The dashed lines are jumping changes of the equi-measuring function, and the jumping changes are caused by the transport laws between two adjacent queue subsystems. The circular points represent the switching points for two adjacent queue subsystems.

To illustrate this case, consider the dynamical system in Eq. (5.79) without damping ($d^{(i)} = 0$). The corresponding solution is

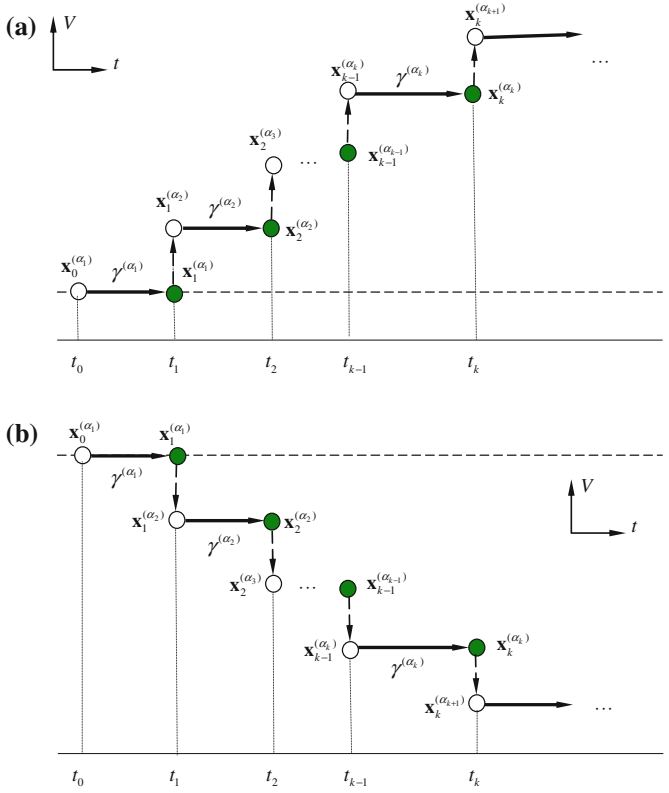

Fig. 5.11 The equi-measuring function varying with time: **a** uniformly positive impulse only, **b** uniformly negative impulse only. The *solid lines* give the invariant equi-measuring-functions of a flow $\gamma^{(\alpha_k)}(t)$. The *dashed lines* are impulsive changes of the equi-measuring function, which are caused by the transport laws between two adjacent queue subsystems. The *circular points* represent the switching points for two adjacent queue subsystems

$$\begin{aligned} x^{(i)} &= [C_1^{(i)} \cos \omega^{(i)}(t - t_{k+}) + C_2^{(i)} \sin \omega^{(i)}(t - t_{k+})], \\ y^{(i)} &= [C_2^{(i)} \omega^{(i)} \cos \omega^{(i)}(t - t_{k+}) - \omega^{(i)} C_1^{(i)} \sin \omega^{(i)}(t - t_{k+})], \end{aligned} \tag{5.89}$$

where

$$C_1^{(i)} = x_{k+}^{(i)}, C_2^{(i)} = y_{k+}^{(i)}/\omega^{(i)}; \omega^{(i)} = \sqrt{c^{(i)}}. \tag{5.90}$$

With the strength of impulsive function ($a = 0.8$) and initial conditions in Eq. (5.87), the corresponding measuring functions and trajectories in phase plane are presented in Figs. 5.13 and 5.14 for the uniformly increasing and decreasing of impulses, respectively.

From the above definition, the corresponding theorem is presented as follows.

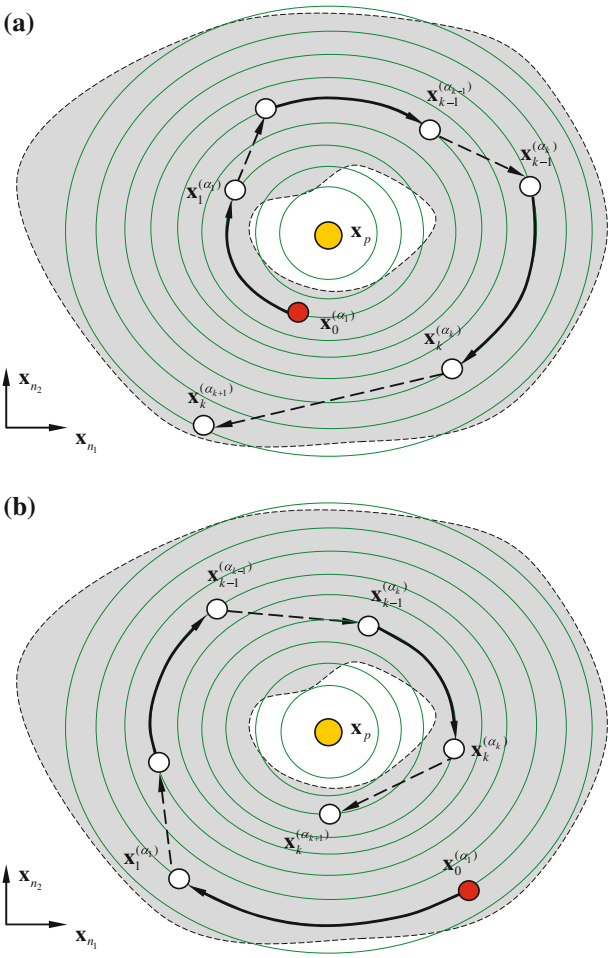

Fig. 5.12 A flow to the equi-measuring function surface in vicinity of point $\mathbf{x}_p$ in phase space: **a** uniformly positive impulse, and **b** uniformly negative impulse. The cycles are equi-measuring function surfaces. The *circular symbols* represent the switching points for two adjacent queue subsystems

Theorem 5.4 *For a switching system in Eqs.* (5.15) *and* (5.16) *on the domain* $\mho = \cup_{i=1}^{m_1} \Omega_{l_i} \cup \Omega_0$, *there is an resultant flow* $\gamma(t_0, t)$ *in Eq.* (5.69). *For the* α_kth *dynamical subsystem* S_{α_k}, consider *the equi-measuring function* $V(\mathbf{x}^{(\alpha_k)}, \mathbf{x}_p)$ *in Eq.* (5.32) *to be monotonically increased to a metric function* $d(\mathbf{x}, \mathbf{x}_p)$ *in Eq.* (5.30). *A flow* $\gamma(t_0, t)$ *from* $\gamma^{(\alpha_1)}(t_0, t_1)$ *to* $\gamma^{(\alpha_l)}(t_{l-1}, t_l)$ *for* $t \in [t_0, t_l]$ *in domain* $\cup_{k=1}^{l} \Omega_{\alpha_k}$ *is*:

(i) *uniformly decreasing to the equi-measuring function surface in* $\cup_{k=1}^{l} \Omega_{\alpha_k}$ *if and only if*

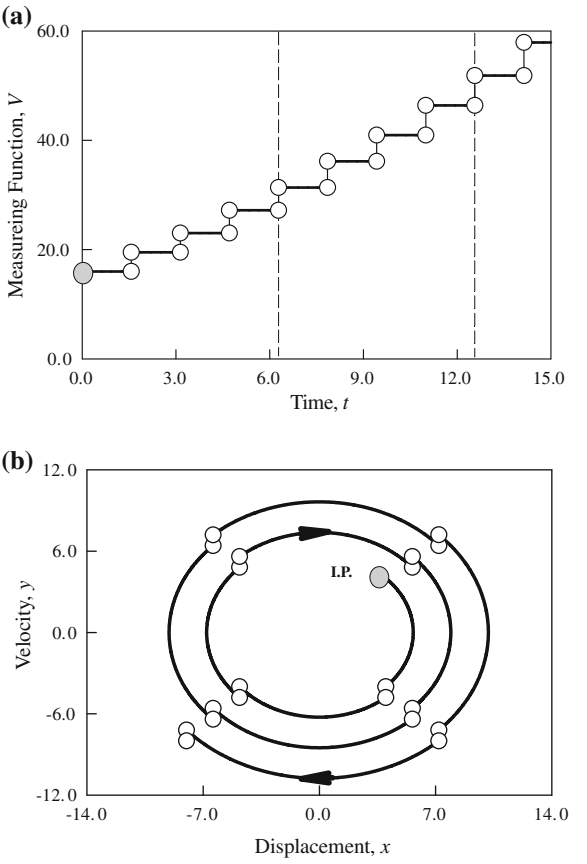

Fig. 5.13 An impulsive system without positive damping: **a** invariant measuring function with increasing impulses, **b** trajectory in phase plane. The *circular symbols* represent the impulsive points for such an impulsive system. Two time impulses for each period are labeled by the *vertical lines*. ($c^{(i)} = c = 1$, $a^{(i)} = a = 0.8$, $m = 4$ and $x_0^{(i)} = y_0^{(i)} = 4$ for $t_0 = 0$)

$$\begin{aligned} &G_m^{(0)}(\mathbf{x}^{(i)}, \mathbf{x}_p, t) = [\mathbf{n}(\mathbf{x}^{(i)}, \mathbf{x}_p)]^{\mathrm{T}} \cdot \mathbf{F}^{(i)}(\mathbf{x}^{(i)}, t, \mathbf{p}^{(i)}) < 0 \\ &\text{for } \mathbf{x}_s^{(\alpha_k)} \in \gamma^{(\alpha_k)}(t_{k-1}, t_k) \text{ with } t_s \in [t_{k-1}, t_k]; \\ &\Delta^{(\alpha_k\alpha_{k+1})}(t_k) < 0 \text{ for } k = 1, 2, \cdots, l; \end{aligned} \tag{5.91}$$

(ii) *uniformly increasing to the equi-measuring function surface in* $\cup_{k=1}^{l} \Omega_{\alpha_k}$ *if and only if*

$$\begin{aligned} &G_m^{(0)}(\mathbf{x}^{(i)}, \mathbf{x}_p, t) = [\mathbf{n}(\mathbf{x}^{(i)}, \mathbf{x}_p)]^{\mathrm{T}} \cdot \mathbf{F}^{(i)}(\mathbf{x}^{(i)}, t, \mathbf{p}^{(i)}) > 0 \\ &\text{for } \mathbf{x}_s^{(\alpha_k)} \in \gamma^{(\alpha_k)}(t_{k-1}, t_k) \text{ with } t_s \in [t_{k-1}, t_k]; \\ &\Delta^{(\alpha_k\alpha_{k+1})}(t_k) > 0 \text{ for } k = 1, 2, \cdots, l; \end{aligned} \tag{5.92}$$

(iii) uniformly and negatively impulsive (or jumping down, or jumping decreasing) to the equi-measuring function surface in $\cup_{k=1}^{l} \Omega_{\alpha_k}$ *if and only if*

$$\begin{aligned} &G_m^{(r)}(\mathbf{x}^{(\alpha_k)}, \mathbf{x}_p, t) = 0 \text{ for } r = 0, 1, 2, \cdots \\ &\text{for } \mathbf{x}_s^{(\alpha_k)} \in \gamma^{(\alpha_k)}(t_{k-1}, t_k) \text{ with } t_s \in [t_{k-1}, t_k], \\ &\Delta^{(\alpha_k\alpha_{k+1})}(t_k) < 0 \text{ for } k = 1, 2, \cdots, l; \end{aligned} \tag{5.93}$$

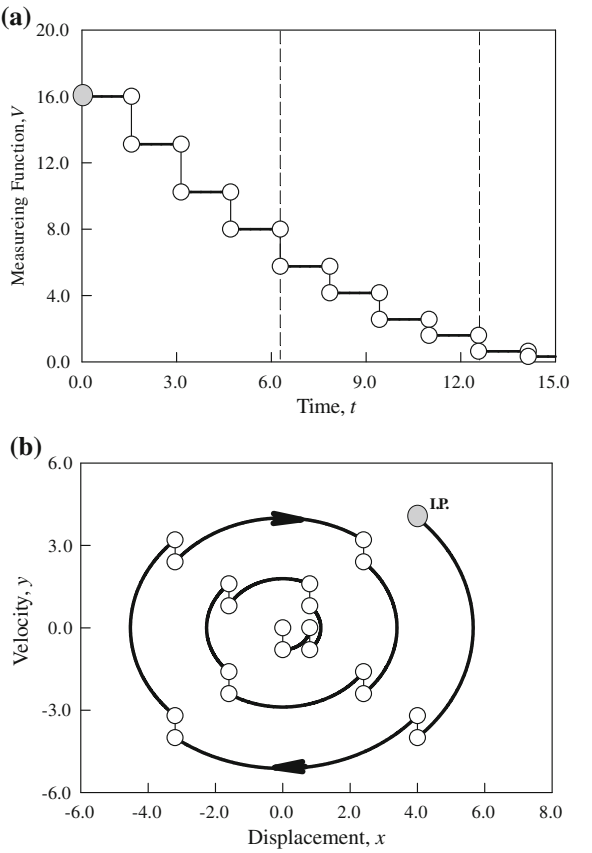

Fig. 5.14 An impulsive system without damping: **a** invariant measuring function with decreasing impulses, **b** trajectory in phase plane. The *circular symbols* represent the impulsive points for such an impulsive system. Two time impulses for each period are labeled by the *vertical lines*. ($c^{(i)} = c = 1, a^{(i)} = a = 0.8, m = 4$ and $x_0^{(i)} = y_0^{(i)} = 4$ for $t_0 = 0$)

(iv) *uniformly and positively impulsive* (*or jumping up*, *or jumping increase*) *to the equi-measuring function surface in* $\cup_{k=1}^{l} \Omega_{\alpha_k}$ *if and only if*

$$\begin{aligned} &G_m^{(r)}(\mathbf{x}^{(\alpha_k)}, \mathbf{x}_p, t) = 0 \ \text{ for } \ r = 0, 1, 2, \cdots \\ &\text{for } \ \mathbf{x}_s^{(\alpha_k)} \in \gamma^{(\alpha_k)}(t_{k-1}, t_k) \ \text{ with } \ t_s \in [t_{k-1}, t_k], \\ &\Delta^{(\alpha_k \alpha_{k+1})}(t_k) > 0 \ \text{ for } \ k = 1, 2, \cdots, l; \end{aligned} \tag{5.94}$$

(v) *uniformly invariant to the equi-measuring function surface in* $\cup_{k=1}^{l} \Omega_{\alpha_k}$ *if and only if*

$$\begin{aligned} &G_m^{(r)}(\mathbf{x}^{(\alpha_k)}, \mathbf{x}_p, t) = 0 \ \text{ for } \ r = 0, 1, 2, \cdots \\ &\text{for } \ \mathbf{x}_s^{(\alpha_k)} \in \gamma^{(\alpha_k)}(t_{k-1}, t_k) \ \text{ with } \ t_s \in [t_{k-1}, t_k], \\ &\Delta^{(\alpha_k \alpha_{k+1})}(t_k) = 0 \ \text{ for } \ k = 1, 2, \cdots, l. \end{aligned} \tag{5.95}$$

Proof Using G-functions and Taylor series expansion, this theorem can be proved directly. ■

For switching dynamical systems, it is very difficult to require all systems are uniformly increasing, or decreasing or invariant. To construct a switching dynamics system, subsystems do not require such strict increase, or decrease and invariance. Thus, as in Definition 5.19, the L-function will be adopted to measure the resultant flow $\gamma(t_0, t)$ with increase, decrease and invariance to the measuring function surface. The increase, decrease and invariance for the entire time interval are called the *global* increase, or decrease, or invariance of the resultant flow to the measuring function surface, which can be used to measure system stability. The corresponding definitions are given as follows.

Definition 5.23 For a switching system in Eqs. (5.15) and (5.16) on the domain $\mho = \cup_{i=1}^{m_1} \Omega_{l_i} \cup \Omega_0$, there is an resultant flow $\gamma(t_0, t)$ in Eq. (5.69). For the α_kth dynamical subsystem S_{α_k}, consider the equi-measuring function $V(\mathbf{x}^{(\alpha_k)}, \mathbf{x}_p)$ in Eq. (5.32) to be monotonically increased to a metric function $d(\mathbf{x}, \mathbf{x}_p)$ in Eq. (5.30). A resultant flow $\gamma(t_0, t_l)$ of the switching system from $\gamma^{(\alpha_1)}(t_0, t_1)$ to $\gamma^{(\alpha_l)}(t_{l-1}, t_l)$ for $t \in [t_0, t_l]$ in the domain $\cup_{k=1}^{l} \Omega_{\alpha_k}$ is:

(i) globally decreasing to the equi-measuring function surface in $\cup_{k=1}^{l} \Omega_{\alpha_k}$ if

$$L(\mathbf{x}_p, t_0, t_l) = \sum_{k=1}^{l} \left[L^{(\alpha_k)}(\mathbf{x}_p, t_{k-1}, t_k) + \Delta^{(\alpha_k \alpha_{k+1})} \right] < 0; \tag{5.96}$$

(ii) globally increasing to the equi-measuring function surface in $\cup_{k=1}^{l} \Omega_{\alpha_k}$ if

$$L(\mathbf{x}_p, t_0, t_l) = \sum_{k=1}^{l} \left[L^{(\alpha_k)}(\mathbf{x}_p, t_{k-1}, t_k) + \Delta^{(\alpha_k \alpha_{k+1})} \right] > 0; \tag{5.97}$$

(iii) globally invariant to the equi-measuring function surface in $\cup_{k=1}^{l} \Omega_{\alpha_k}$ if

$$L(\mathbf{x}_p, t_0, t_l) = \sum_{k=1}^{l} \left[L^{(\alpha_k)}(\mathbf{x}_p, t_{k-1}, t_k) + \Delta^{(\alpha_k \alpha_{k+1})} \right] = 0. \tag{5.98}$$

To illustrate the above definitions, the global increase, global decrease and global invariance of the resultant flow to the equi-measuring function surface can be presented through the equi-measuring function varying with time. The global increase, decrease and invariance of the resultant flow for time interval $t \in [t_0, t_l]$ require the corresponding L-function $L(\mathbf{x}_p, t_0, t_l)$ be *greater than*, *less than* and *equal to* zero. The global increase and decrease are illustrated in Fig. 5.15a and b, respectively. The corresponding trajectories in phase space are presented in Fig. 5.16a and b. The dashed lines are jumping changes of the equi-measuring function, and the jumping changes are caused by the transport laws between two adjacent queue subsystems. The circular points represent the switching points for two adjacent queue subsystems.

Theorem 5.5 *For a switching system on the domain* $\mho = \cup_{i=1}^{m} \Omega_{l_i} \cup \Omega_0$ *in the vicinity of point* $\mathbf{p}_k$ *in Eq.* (5.23), *if there is a periodic flow with periodicity condition in Eq.* (5.24), *then the resultant L-function is zero*, *i.e.*,

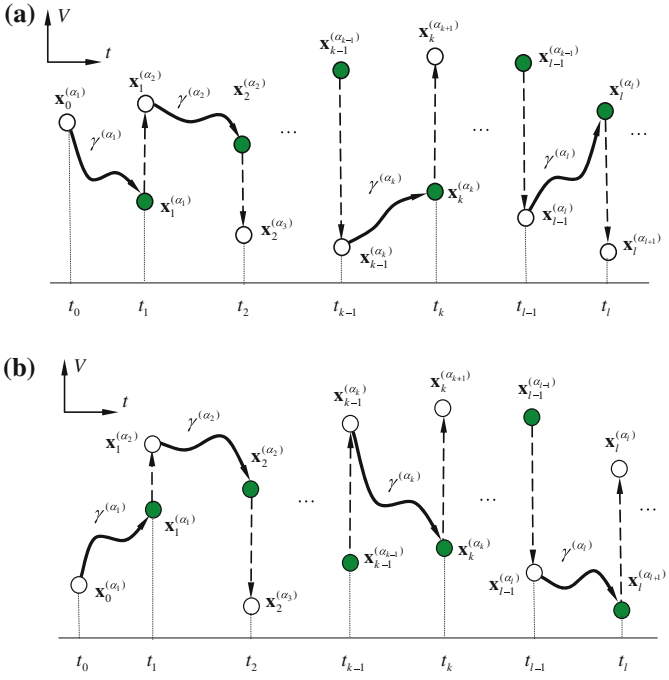

Fig. 5.15 The equi-measuring function varying with time: **a** globally deceasing, **b** globally increasing. The *solid lines* give the invariant equi-measuring-functions of a flow $\gamma^{(\alpha_k)}(t)$. The *dashed lines* are jumping changes of the equi-measuring function, and the jumping changes are caused by the transport laws between two adjacent queue subsystems. The *circular points* represent the switching points for two adjacent queue subsystems

$$\begin{aligned} &L(\mathbf{x}_p, t_0, t_m) = \sum_{k=1}^{m} \left[L^{(\alpha_k)}(\mathbf{x}_p, t_{k-1}, t_k) + \Delta^{(\alpha_k \alpha_{k+1})} \right] = 0 \\ &\mathbf{x}_m^{(\alpha_{m+1})} = \mathbf{x}_0^{(\alpha_1)}, t_m = t_0 + T \ \text{ and } \ \alpha_{m+1} = \alpha_1. \end{aligned} \tag{5.99}$$

Proof From Eq. (5.73) with $\Delta^{(\alpha_k \alpha_{k+1})}(t_k) = V(\mathbf{x}_k^{(\alpha_{k+1})}, \mathbf{x}_p) - V(\mathbf{x}_k^{(\alpha_k)}, \mathbf{x}_p)$, one obtains

$$\begin{aligned} L(\mathbf{x}_p, t_0, t_m) &= \sum_{k=1}^{m} \left[L^{(\alpha_k)}(\mathbf{x}_p, t_{k-1}, t_k) + \Delta^{(\alpha_k \alpha_{k+1})} \right] \\ &= \sum_{k=1}^{m} \left[V(\mathbf{x}_k^{(\alpha_k)}, \mathbf{x}_p) - V(\mathbf{x}_{k-1}^{(\alpha_k)}, \mathbf{x}_p) + \Delta^{(\alpha_k \alpha_{k+1})} \right] \\ &= V(\mathbf{x}_m^{(\alpha_{m+1})}, \mathbf{x}_p) - V(\mathbf{x}_0^{(\alpha_1)}, \mathbf{x}_p). \end{aligned}$$

The periodic flow requires $\mathbf{x}_m^{(\alpha_{m+1})} = \mathbf{x}_0^{(\alpha_1)}, t_m = t_0 + T$ and $\alpha_{m+1} = \alpha_1$, which implies $V(\mathbf{x}_m^{(\alpha_{m+1})}, \mathbf{x}_p) = V(\mathbf{x}_0^{(\alpha_1)}, \mathbf{x}_p)$. Thus, $L(\mathbf{x}_p, t_0, t_m) = 0$. This theorem is proved. ■

Periodic flows in switching systems with impulses are sketched to help one understand the mechanism, characteristics and construction of periodic flow, which are

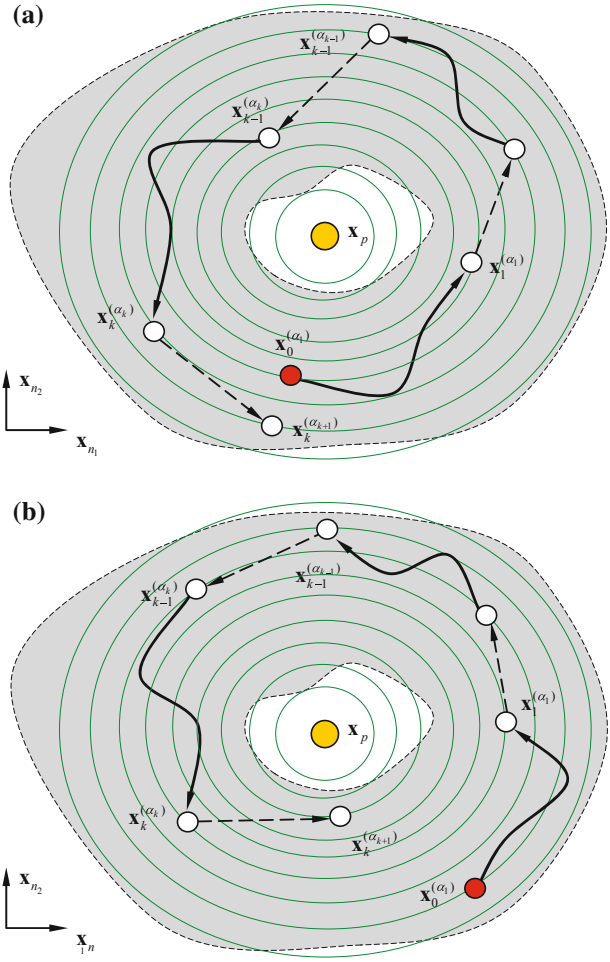

Fig. 5.16 A flow to the equi-measuring function surface in vicinity of point $\mathbf{x}_p$ in phase space: **a** global increase, and **b** global decrease. The cycles are equi-measuring function surfaces. The *circular symbols* represent the switching points for two adjacent queue subsystems

different from the continuous dynamical systems. Herein, the simple cases will be discussed first to build the corresponding concepts. Consider a flow with uniformly invariance to the equi-measuring surface with positive and negative increase with the same amplitude. Such a switching system is a conservative system to the equi-measuring surface for given time intervals with a kind of impulse with a specific transport law at given switching moments. In other words, one has

$$\begin{aligned} &G_m^{(r)}(\mathbf{x}^{(\alpha_k)}, \mathbf{x}_p, t) = 0 \ \text{ for } \ r = 0, 1, 2, \cdots \\ &\text{for } \ \mathbf{x}^{(\alpha_k)}(t) \in \gamma^{(\alpha_k)}(t_{k-1}, t_k) \ \text{ with } \ t \in [t_{k-1}, t_k], \\ &\Delta^{(\alpha_k \alpha_{k+1})}(t_k) = -C \ \text{ or } \ C \ \text{ at switching time } \ t_k; \end{aligned} \tag{5.100}$$

or

$$\begin{aligned}
&V(\mathbf{x}^{(\alpha_k)}(t), \mathbf{x}_p) = V(\mathbf{x}_k^{(\alpha_k)}, \mathbf{x}_p) = V(\mathbf{x}_{k-1}^{(\alpha_k)}, \mathbf{x}_p) \\
&\text{for } \mathbf{x}^{(\alpha_k)}(t) \in \gamma^{(\alpha_k)}(t_{k-1}, t_k) \text{ with } t \in [t_{k-1}, t_k]; \\
&\Delta^{(\alpha_k\alpha_{k+1})}(t_k) = C \text{ for jumping up,} \\
&\Delta^{(\alpha_k\alpha_{k+1})}(t_k) = -C \text{ for jumping down} \\
&\text{with } \Delta^{(\alpha_k\alpha_{k+1})}(t_k) = V(\mathbf{x}_k^{(\alpha_{k+1})}, \mathbf{x}_p) - V(\mathbf{x}_k^{(\alpha_k)}, \mathbf{x}_p).
\end{aligned} \tag{5.101}$$

If the switching systems cannot form a periodic flow, then a chaotic flow can be formed or at least a randomly switching flow can be observed. The stochasticity of such a flow can be determined through a random setting of the switching time. However, for $(2m)$ switching with jumping up and down with constant magnitude, if there is a relation as

$$\begin{aligned}
&\mathbf{x}_0^{(\alpha_1)} = \mathbf{x}_{2m}^{(\alpha_{2m+1})} \text{ and } t_{2m} = t_0 + T \\
&\text{where } T \text{ is period}
\end{aligned} \tag{5.102}$$

then the switching flow can form a periodic flow. In addition, the switching is given by the transport laws

$$\begin{aligned}
&\mathbf{g}^{(\alpha_k\alpha_{k+1})}(\mathbf{x}_k^{(\alpha_k)}, \mathbf{x}_k^{(\alpha_{k+1})}) = 0 \\
&V(\mathbf{x}_k^{(\alpha_{2k+1})}, \mathbf{x}_p) = C_1 \text{ and } V(\mathbf{x}_k^{(\alpha_{2k})}, \mathbf{x}_p) = C_2.
\end{aligned} \tag{5.103}$$

For linear switching systems, such a periodic flow is stable.

For a better understanding of the concepts, the following illustrations are given to form periodic flows. The equi-measuring function varying with time for periodic flows is sketched in Fig. 5.17. In Fig. 5.17a, the periodic motion with positive and negative impulses with the same strength of impulses. In Fig. 5.17b, the periodic flows with positive and negative impulses with different strengths of impulses are presented. The corresponding periodic trajectories for such periodic flows in phase space are presented in Fig. 5.18. For special cases, consider an impulsive system with the measuring functions uniformly increase or decrease with time. However, the impulsive jump can remove such increasing and decreasing of the measuring functions. Thus, the periodic flows can be formed. For intuitive illustration, such periodic flows are presented in Figs. 5.19 and 5.20. The constant increments of measuring function are adopted. In fact, such measuring functions increments are not necessary to be constant. Periodic flows with the uneven increments of measuring functions are sketched in Figs. 5.21 and 5.22. If the total increments of measuring functions can be cancelled by the total increments of impulsive jumps, the periodic flow can formed. In other words, for unstable subsystems in the impulsive system, if impulsive jumps can draw the measuring function to the original level, the resultant impulsive system with unstable subsystems should be stable. For general case, it is not necessary for subsystems to make the measuring function be uniformly increasing or deceasing. The corresponding illustration is given in Fig. 5.23.

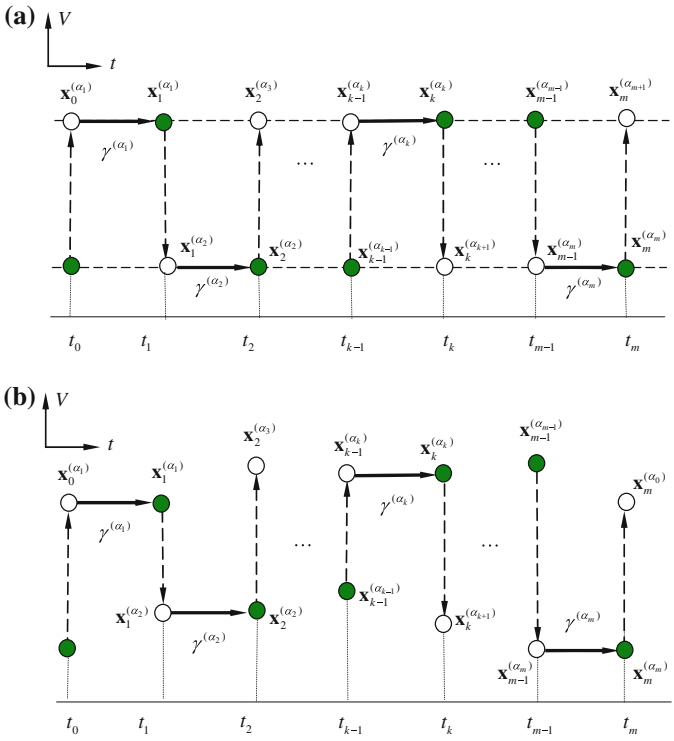

Fig. 5.17 The equi-measuring function varying with time: **a** positive and negative impulses with the same strength, and **b** positive and negative impulses with different strengths. The cycles are equi-measuring function surfaces. The *circular symbols* are for switching points

Consider the dynamical system in Eq. (5.79) without damping ($d^{(i)} = 0$) again. However, the impulsive relation will be changed as

$$\begin{aligned} &x_{k+}^{(i)} = x_{k-}^{(i)}, \, y_{k+}^{(i)} = y_{k-}^{(i)} + a^{(i)} (k = 1, 2, \cdots) \\ &\text{for } \; t_k = kT/m \;\; \text{with } \; T = 2\pi/\sqrt{c}, a^{(i)} > 0. \end{aligned} \tag{5.104}$$

The corresponding solution in Eq. (5.89) and (5.90) will be used for dynamical system in Eq. (5.79). The measuring function in Eq. (5.81) will be used herein.

With the strength of impulsive function ($a = 1.0$) and initial conditions are

$$x_0^{(i)} = 2.0, \, y_0^{(i)} = 2.0 \;\; \text{for } \; t = 0.0. \tag{5.105}$$

The periodic motion for the switching system with impulses ($m = 2$) is presented in Fig. 5.24. The measuring functions are two invariants. The impulses possess "jumping up" and "jumping down" with the same increments, which is clearly presented in Fig. 5.24a. The trajectory of the periodic motion in phase plane is presented in

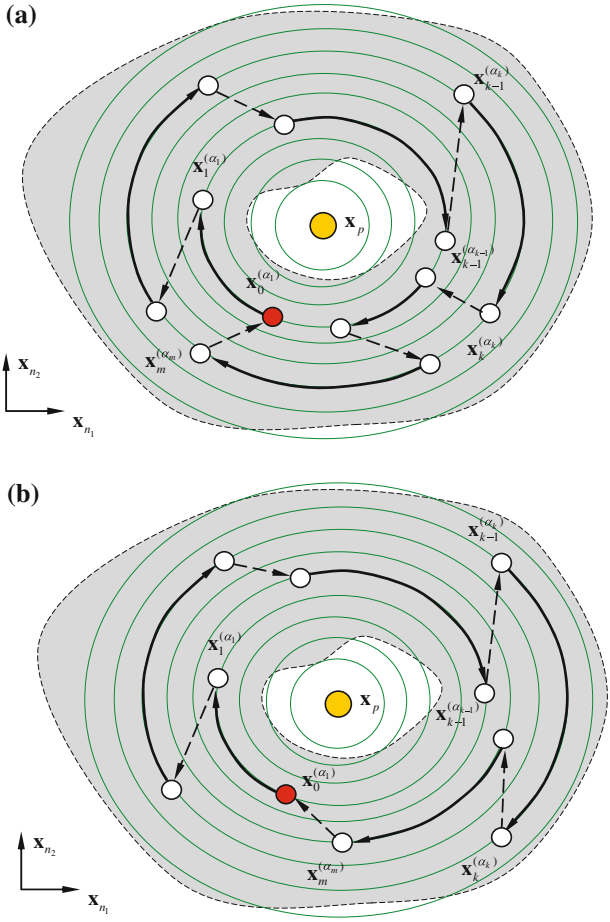

Fig. 5.18 A periodic flow to the equi-measuring function surface in vicinity of point $\mathbf{x}_p$ in phase space: **a** positive and negative impulses with the same strength, and **b** positive and negative impulses with different strengths. The cycles are equi-measuring function surfaces. The *circular symbols* are for switching points

Fig. 5.24b. Since subsystem in Eq. (5.79) with ($d^{(i)} = 0$) is a conservative and the Hamiltonian is selected as a measuring function. Thus, the subsystem possesses the invariant measuring function without impulses. The time-histories of displacement and velocity for such a periodic motion are presented in Fig. 5.24c and d, respectively. Since the impulsive effects are exerted on the velocity. The displacement is C^0-continuous at the impulsive points, but the velocity is C^0-discontinuous. With multiple impulses, the corresponding periodic motions are presented in Fig. 5.25 ($m = 4$). The same initial conditions and system parameters are used. Compared with Fig. 5.24, the impulsive effects on the measuring functions, trajectory in phase plane, displacement and velocity time-histories are observed. If $m \to \infty$, the impul-

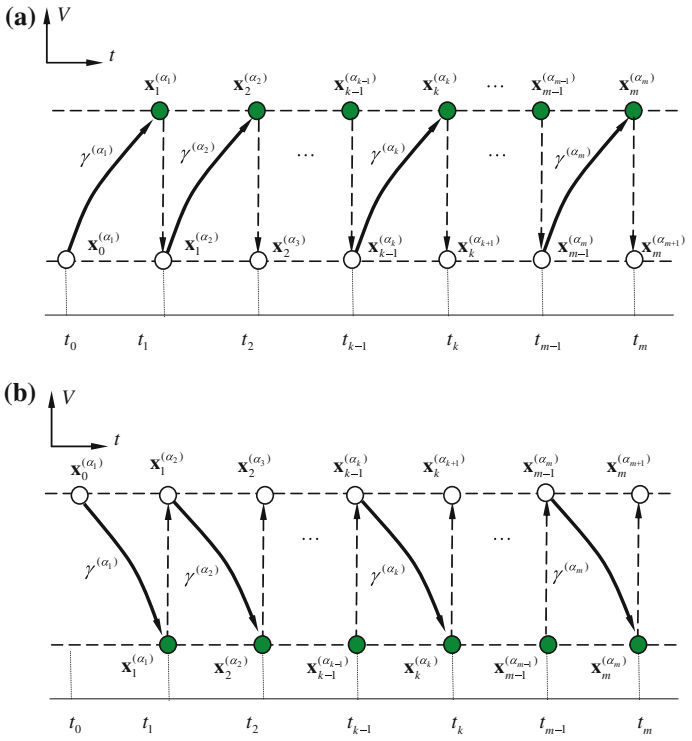

Fig. 5.19 The equi-measuring function varying with time: **a** uniformly increasing with constant jump down only, **b** uniformly increasing with constant jumping up. The *solid lines* give the invariant equi-measuring-functions of a flow $\gamma^{(\alpha_k)}(t)$. The *dashed lines* are jumping changes of the equi-measuring function, and the jumping changes are caused by the transport laws between two adjacent queue subsystems. The *circular points* represent the switching points for two adjacent queue subsystems

sive force will become a constant force exerting on the vibration system. The analytical and numerical solutions can be easily obtained. However, the measuring function is not necessary to be chosen as the Hamiltonian. Consider a measuring function in Eq. (5.81) as

$$V^{(i)} = \frac{1}{2}(y^{(i)})^2 + \frac{1}{4}c^{(i)}(x^{(i)})^2. \tag{5.106}$$

Based on the foregoing measuring functions, the G-function is

$$G^{(0,i)} = y^{(i)}\dot{y}^{(i)} + \frac{1}{2}c^{(i)}x^{(i)}y^{(i)} = -\frac{1}{2}c^{(i)}x^{(i)}y^{(i)}. \tag{5.107}$$

The above measuring function and the corresponding G-functions for the same periodic motion presented in Fig. 5.25 are presented in Fig. 5.26. It is observed that the

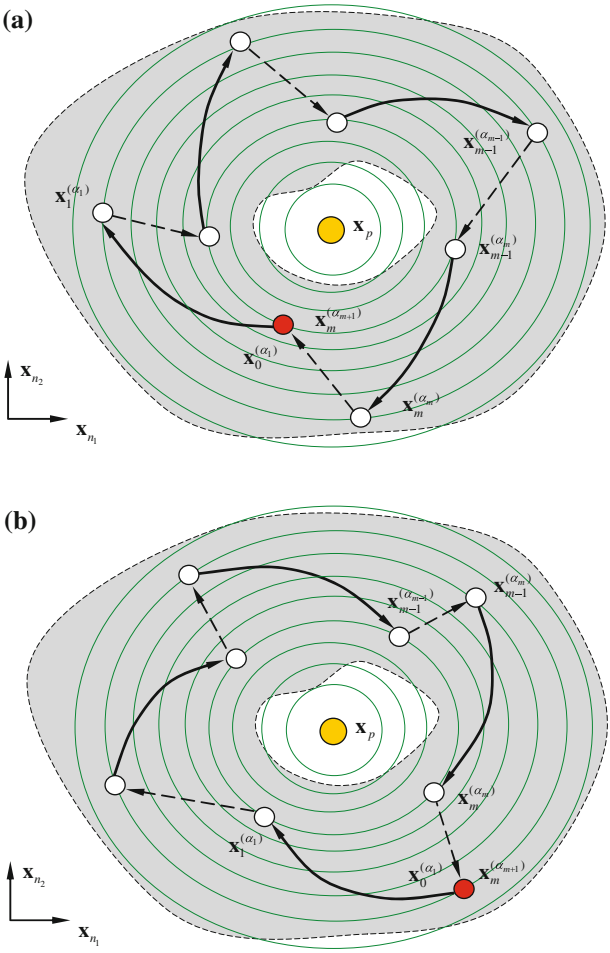

Fig. 5.20 A flow to the equi-measuring function surface in vicinity of point $\mathbf{x}_p$ in phase space: **a** uniform increasing with jump down, and **b** uniform decreasing with jump up. The cycles are equi-measuring function surfaces. The *circular symbols* represent the switching points for two adjacent queue subsystems

measuring function is not uniformly increasing or decreasing. From the traditional Lyapunov method, the stability of this impulsive system cannot be determined. In addition, the switching systems have many subsystems. If one measuring function is used, definitely such a function cannot be the first integral invariant manifolds for all subsystems. Thus, the L-function for measuring function should be adopted.

5.4 Impulsive Systems and Chaotic Diffusions

For further discussion on impulsive systems, consider a dynamical system as

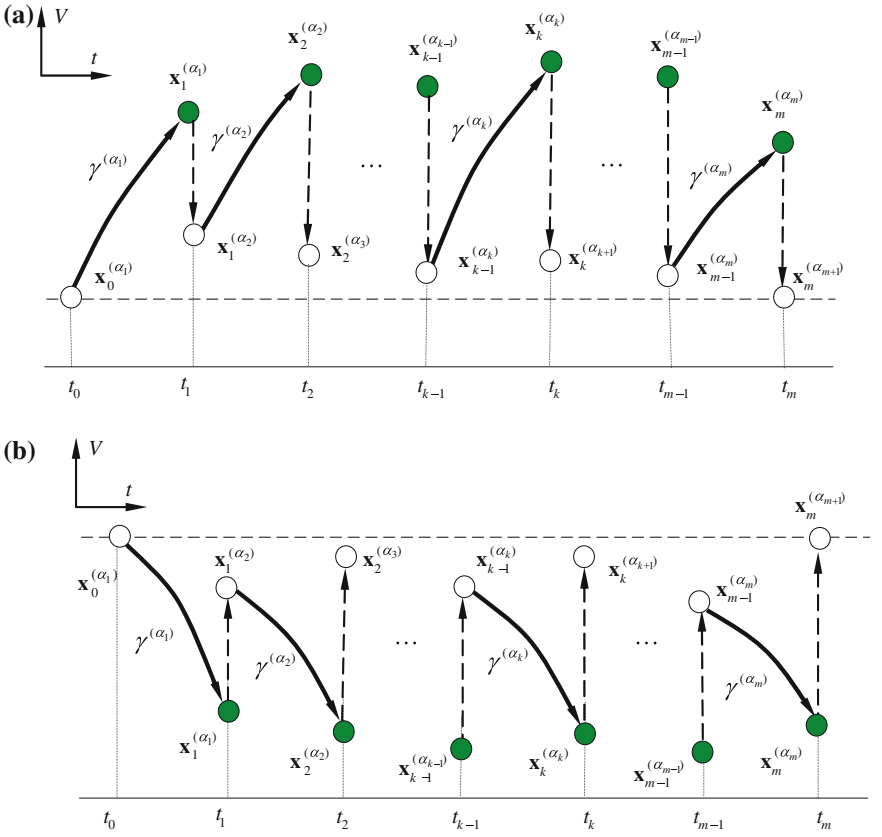

Fig. 5.21 The equi-measuring function varying with time: **a** uniformly invariance with jumps only, **b** uniformly increasing with jumping down. The *solid lines* give the invariant equi-measuring-functions of a flow $\gamma^{(\alpha_k)}(t)$. The *dashed lines* are jumping changes of the equi-measuring function, and the jumping changes are caused by the transport laws between two adjacent queue subsystems. The *circular points* represent the switching points for two adjacent queue subsystems

$$\begin{aligned} &\dot{x}^{(i)} = y^{(i)} \quad \text{and} \quad \dot{y}^{(i)} = -c^{(i)}x^{(i)} + a^{(i)} f(x, y)\delta(t - knT/m) \\ &(k = 1, 2, \cdots; i = 1, 2, \cdots, l). \end{aligned} \tag{5.108}$$

The foregoing equation is equal to subsystems in Eq. (5.79) with $d^{(i)} = 0$ and the impulsive function in Eq. (5.80) becomes

$$\begin{aligned} &x_{k+}^{(i)} = x_{k-}^{(i)}, y_{k+}^{(i)} = y_{k-}^{(i)} + a^{(i)} f^{(i)}(x_{k-}^{(i)}, y_{k-}^{(i)})(k = 1, 2, \cdots) \\ &\text{for } t_k = knT/m \text{ with } T = 2\pi/\Omega, a^{(i)} > 0. \end{aligned} \tag{5.109}$$

The solutions in Eqs. (5.89) and (5.90) are adopted. Thus, for $t = t_{(k+1)-}$, we have

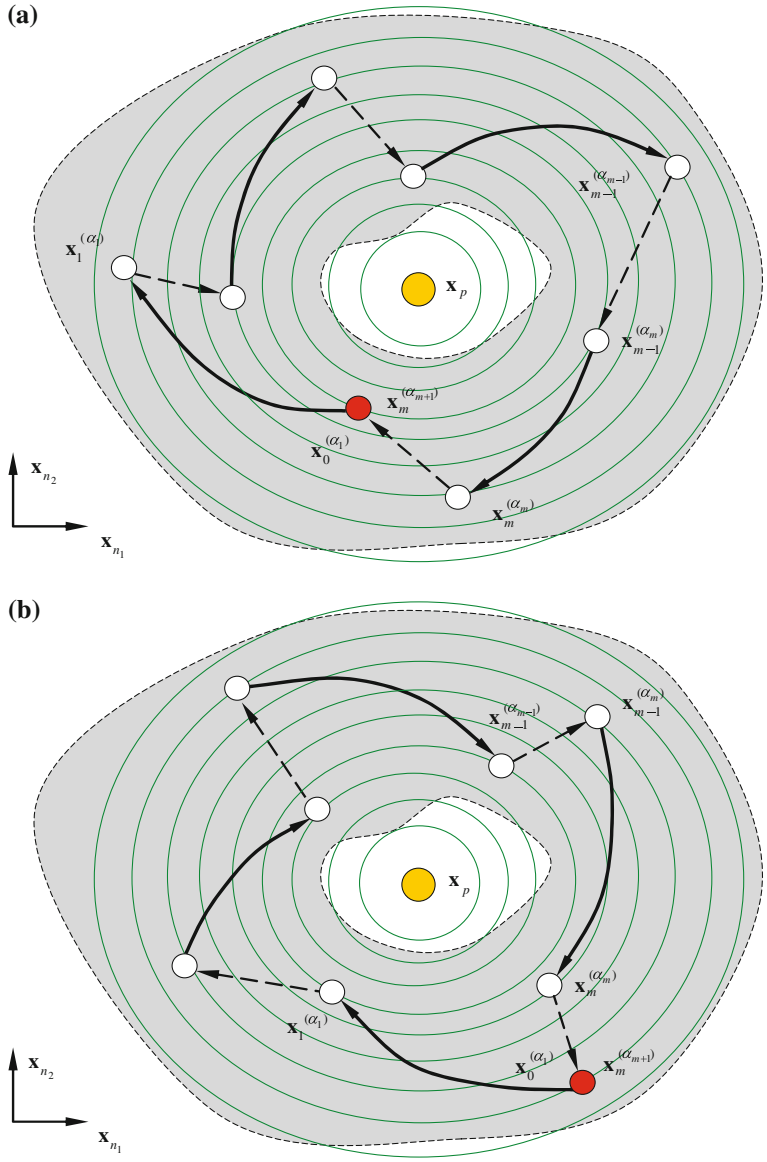

Fig. 5.22 A flow to the equi-measuring function surface in vicinity of point $\mathbf{x}_p$ in phase space: **a** uniform increase, and **b** uniform decrease. The cycles are equi-measuring function surfaces. The *circular symbols* represent the switching points for two adjacent queue subsystems

$$
\begin{aligned}
x_{(k+1)-}^{(i)} &= [x_{k+}^{(i)} \cos \omega^{(i)}(t_{(k+1)-} - t_{k+}) + y_{k+}^{(i)}/\omega^{(i)} \sin \omega^{(i)}(t_{(k+1)-} - t_{k+})], \\
y_{(k+1)-}^{(i)} &= [y_{k+}^{(i)} \cos \omega^{(i)}(t_{(k+1)-} - t_{k+}) - \omega^{(i)} x_{k+}^{(i)} \sin \omega^{(i)}(t_{(k+1)-} - t_{k+})].
\end{aligned}
\tag{5.110}
$$

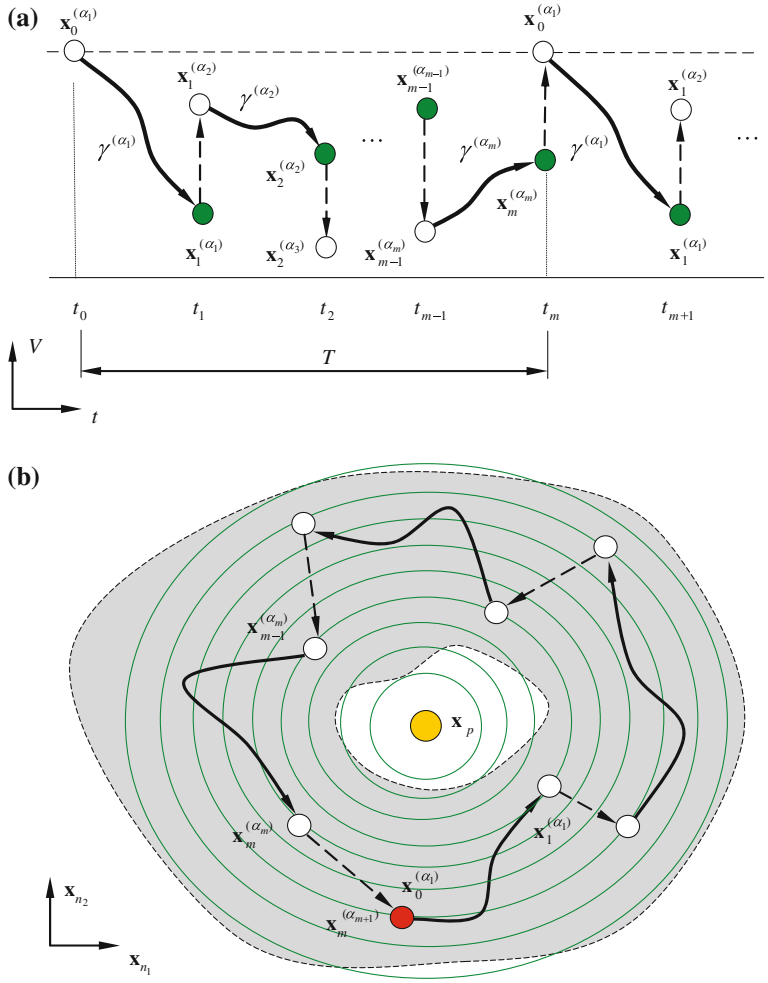

Fig. 5.23 The equi-measuring function varying with time: **a** globally deceasing, **b** globally increasing. The *solid lines* give the invariant equi-measuring-functions of a flow $\gamma^{(\alpha_k)}(t)$. The *dashed lines* are jumping changes of the equi-measuring function, and the jumping changes are caused by the transport laws between two adjacent queue subsystems. The *circular points* represent the switching points for two adjacent queue subsystems

Because

$$\begin{aligned}\cos\omega^{(i)}(t_{(k+1)-}-t_{k+}) &= \cos\frac{2\pi n\omega^{(i)}}{m\Omega} = K_1^{(i)},\\ \sin\omega^{(i)}(t_{(k+1)-}-t_{k+}) &= \sin\frac{2\pi n\omega^{(i)}}{m\Omega} = K_2^{(i)}\end{aligned} \tag{5.111}$$

with Eq. (5.108), Equation (5.111) becomes

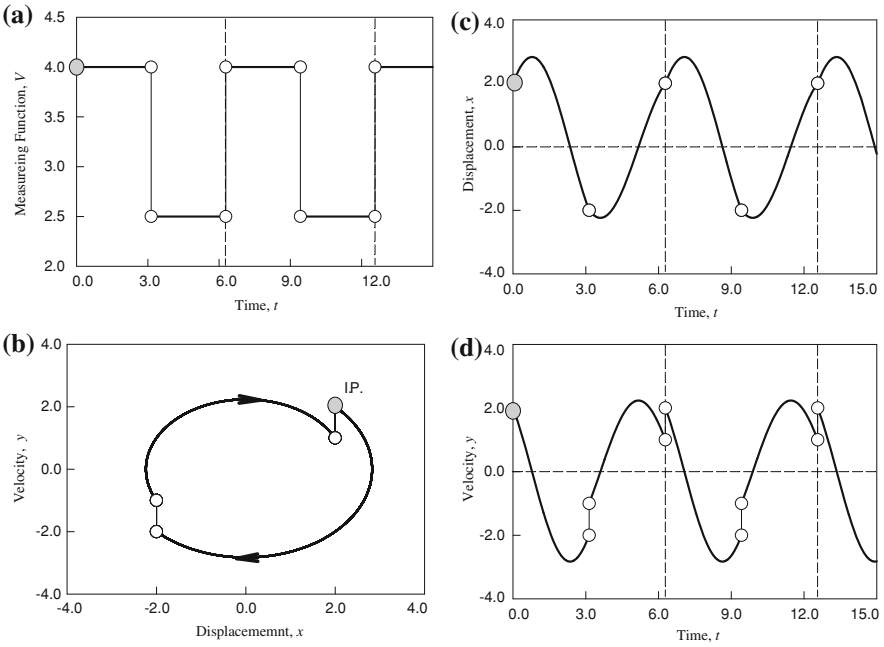

Fig. 5.24 Periodic motions for an impulsive system: **a** Measuring function with impulses, **b** trajectory in phase plane, **c** displacement and **d** discontinuous velocity. The *circular symbols* represent the impulsive points for such an impulsive system. Two time impulses for each period are labeled by the *vertical lines*. ($c^{(i)} = c = 1, a^{(i)} = a = 1.0, m = 2,\ x_0^{(i)} = y_0^{(i)} = 2.0$ for $t_0 = 0$)

$$\begin{aligned} x_{(k+1)-}^{(i)} &= K_1^{(i)} x_{k-}^{(i)} + \frac{K_2^{(i)}}{\omega^{(i)}}[y_{k-}^{(i)} + a^{(i)} f^{(i)}(x_{k-}^{(i)}, y_{k-}^{(i)})], \\ y_{(k+1)-}^{(i)} &= K_1^{(i)}[y_{k-}^{(i)} + a^{(i)} f^{(i)}(x_{k-}^{(i)}, y_{k-}^{(i)})] - K_2^{(i)} \omega^{(i)} x_{k-}^{(i)}. \end{aligned} \tag{5.112}$$

Dropping subscript "-", the foregoing equation becomes

$$\begin{Bmatrix} x_{k+1}^{(i)} \\ y_{k+1}^{(i)} \end{Bmatrix} = \begin{bmatrix} K_1^{(i)} & \dfrac{K_2^{(i)}}{\omega^{(i)}} \\ -K_2^{(i)} \omega^{(i)} & K_1^{(i)} \end{bmatrix} \begin{Bmatrix} x_k^{(i)} \\ y_k^{(i)} \end{Bmatrix} + \begin{Bmatrix} \dfrac{K_2^{(i)}}{\omega^{(i)}} \\ K_1^{(i)} \end{Bmatrix} a^{(i)} f^{(i)}(x_k^{(i)}, y_k^{(i)}). \tag{5.113}$$

The mapping P_i $(i = 1, 2, \cdots, l)$ of Eq. (5.108) for $t \in [t_{k+1}, t_k]$ is developed. Suppose there are m-subsystems during n-periods (nT). The resultant mapping is

$$P = P_{l_m} \circ \cdots \circ P_{l_2} \circ P_{l_1}, l_j \in \{1, 2, \cdots, l\} \text{ and } j \in \{1, 2, \cdots, m\}. \tag{5.114}$$

For $\mathbf{x}_k = (x_k, y_k)^{\mathrm{T}}$, we have

$$\mathbf{x}_{k+m} = P\mathbf{x}_k = P_{l_m} \circ \cdots \circ P_{l_2} \circ P_{l_1} \mathbf{x}_k. \tag{5.115}$$

The corresponding relations are

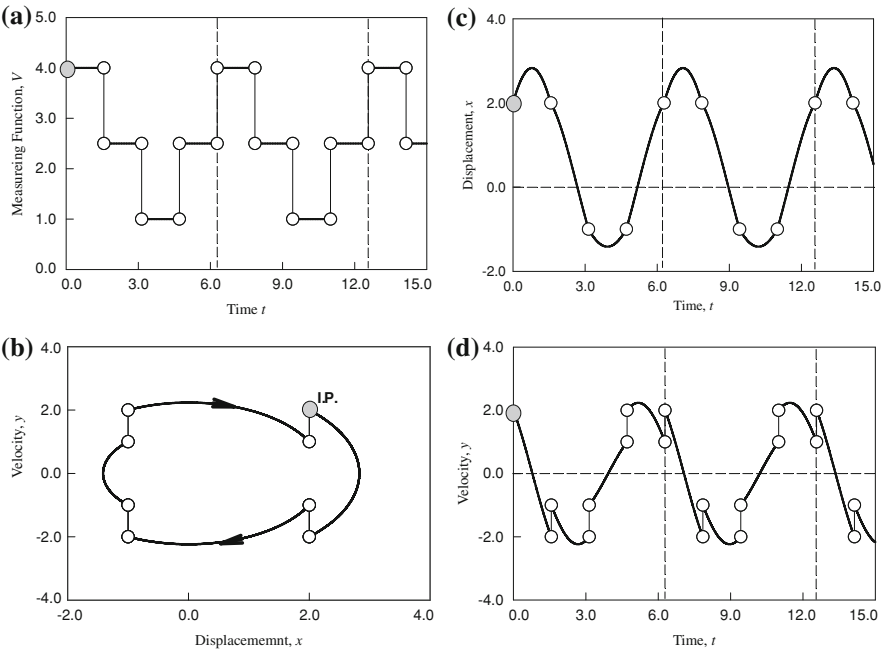

Fig. 5.25 Periodic motions for an impulsive system: **a** Measuring function with impulses, **b** trajectory in phase plane, **c** displacement and **d** discontinuous velocity. The *circular symbols* represent the impulsive points for such an impulsive system. Two time impulses for each period are labeled by the *vertical lines*. ($c^{(i)} = c = 1, a^{(i)} = a = 1.0, m = 4, x_0^{(i)} = y_0^{(i)} = 2.0$ for $t_0 = 0$)

$$\mathbf{x}_{k+j} = \mathbf{g}^{(l_j)}(\mathbf{x}_{k+j-1}) \quad \text{for } j = 1, 2, \cdots, m \tag{5.116}$$

where $\mathbf{g}^{(l_j)}(\mathbf{x}_{k+j-1}) = (g_1^{(l_j)}, g_2^{(l_j)})^{\mathrm{T}}$ with

$$\begin{Bmatrix} g_1^{(l_j)} \\ g_2^{(l_j)} \end{Bmatrix} = \begin{bmatrix} K_1^{(l_j)} & \dfrac{K_2^{(l_j)}}{\omega^{(l_j)}} \\ -K_2^{(l_j)}\omega^{(l_j)} & K_1^{(l_j)} \end{bmatrix} \begin{Bmatrix} x_{k+j-1}^{(l_j)} \\ y_{k+j-1}^{(l_j)} \end{Bmatrix} + \begin{Bmatrix} \dfrac{K_2^{(l_j)}}{\omega^{(l_j)}} \\ K_1^{(l_j)} \end{Bmatrix} a^{(l_j)} f^{(l_j)}(x_{k+j-1}^{(l_j)}, y_{k+j-1}^{(l_j)}). \tag{5.117}$$

For periodic motion during n-periods (nT), the periodicity conditions are

$$\mathbf{x}_{k+m} = \mathbf{x}_k. \tag{5.118}$$

The stability and bifurcation of the periodic solutions can be determined. Herein, it should not be discussed. Similarly problems will be discussed in next section.

To illustrate complex motions in such impulsive system, as in Luo (2011), consider a single system with the following function as example

$$f(x_k, y_k) = \sin x_k. \tag{5.119}$$

Thus, the mapping in Eq. (5.113) becomes

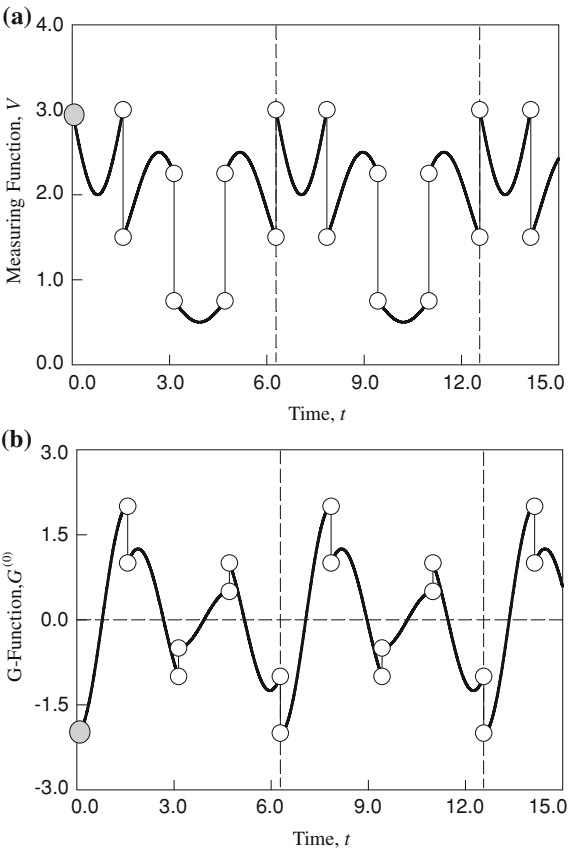

Fig. 5.26 Periodic motions for an impulsive system: **a** Measuring function with impulses, **b** G-functions. The *circular symbols* represent the impulsive points for such an impulsive system. Two time impulses for each period are labeled by the *vertical lines*. ($c^{(i)} = c = 1, a^{(i)} = a = 1.0, m = 4, x_0^{(i)} = y_0^{(i)} = 2.0$ for $t_0 = 0$)

$$\begin{Bmatrix} x_{k+1} \\ y_{k+1} \end{Bmatrix} = \begin{bmatrix} K_1 & \dfrac{K_2}{\omega} \\ -K_2\omega & K_1 \end{bmatrix} \begin{Bmatrix} x_k \\ y_k \end{Bmatrix} + \begin{Bmatrix} \dfrac{K_2}{\omega} \\ K_1 \end{Bmatrix} a \sin x_k. \tag{5.120}$$

During n-periods (nT), the resultant mapping is

$$P^{(m)} = \underbrace{P \circ \cdots \circ P \circ P}_{m}. \tag{5.121}$$

For $\mathbf{x}_k = (x_k, y_k)^{\mathrm{T}}$, we have

$$\mathbf{x}_{k+N} = P^{(N)}\mathbf{x}_k. \tag{5.122}$$

The corresponding relations are

$$\mathbf{x}_{k+j} = \mathbf{g}(\mathbf{x}_{k+j-1}) \quad \text{for } j = 1, 2, \cdots, N \tag{5.123}$$

where $\mathbf{g}(\mathbf{x}_{k+j-1}) = (g_1, g_2)^{\mathrm{T}}$ with

$$\left\{\begin{array}{c} g_1 \\ g_2 \end{array}\right\} = \left[\begin{array}{cc} K_1 & \dfrac{K_2}{\omega} \\ -K_2\omega & K_1 \end{array}\right] \left\{\begin{array}{c} x_{k+j-1} \\ y_{k+j-1} \end{array}\right\} + \left\{\begin{array}{c} \dfrac{K_2}{\omega} \\ K_1 \end{array}\right\} a \sin x_{k+j-1}. \tag{5.124}$$

From the mapping in Eq. (5.123), the quasi-periodic motions and chaos can be obtained via the impulsive points. The impulsive switching scenario with impulsive strength is presented in Fig. 5.27 for $c^{(i)} = c = 1,\ \Omega = 1.0,\ n = 1,\ m = 3, x_0^{(i)} = y_0^{(i)} = 4.0$ and $a^{(i)} = a$ for $t_0 = 0$. The critical value of impulsive strength $a_{cr} \approx 1.2974$ is for the motion from the quasi-periodic motion to the chaotic motion. If $a > a_{cr}$, the chaotic diffusion will be observed. With such chaotic diffusion, long-range interactions can exist via such an impulsive action. The quasi-periodic motion and chaotic diffusion for $\mathrm{mod}(n\omega, m\Omega) = l$ with $l = 1, 2, \cdots, m-1$ are same. Without loss of generality, we can set $\omega = \Omega$. All possible quasi-periodic motions and chaotic diffusion can be obtained by $\mathrm{mod}(n, m) = l$. The switching sections are same for any specific l with all numbers of n with $\mathrm{mod}(n, m) = l$. For $n > m$, the trajectories in phase plane are same, which are different from the trajectory for $n = l$. However, the time responses are different for different n.

Consider $a = 1.0$ with $n = l = 1$ and $m=3$ for illustration in Fig. 5.28 with same parameters and same initial conditions. The trajectory in phase plane and impulsive switching sections are presented in Fig. 5.28a and b, respectively. The impulsive switching points before impulse jumps are labeled by circular symbols. To show switching pattern, the impulsive switching points after impulse jumps are not labeled. The impulsive jumps are connected by vertical lines. The switching sections is based on the impulsive switching points before impulsive jumps. The trajectory in phase plane is for $n = l = 1$ and $m = 3$ only. However, the switching section is for the quasi-periodic motion relative to all integers of n with mod $(n, 3) = 1$ for a specific $l=1$. In other words, for $n = km+1$ $(k = 0, 1, 2, \cdots)$, the switching section are same. For this problem in Eq. (5.108), the trajectories for $k \neq 0$ and $k=0$ are different. However, all trajectories for $k \neq 0$ are identical but the corresponding time-histories of responses (e.g., displacement and velocity) are different. In Fig. 5.29a and b, the trajectories in phase plane for $n=1,4$ are presented, respectively. It is observed that the switching points are same but the trajectories are different. Thus, the time-histories of velocity for $n=1,4$ are presented in Fig. 5.29c and d, respectively.

As $a > a_{cr}$, the chaotic diffusion generates the chaotic impulsive motion pattern with long-range interactions. The switching sections of chaotic impulsive motion for $(n = 1, m = 3, a = 1.4$ and $a_{cr} \approx 1.2974)$ and $(n = 2, m = 3, a = 1.89$ and $a_{cr} \approx 1.8855)$ are presented in Fig. 5.30a and b. The 20,000 impulsive switching points are used to generate the switching sections. The chaotic diffusion patterns are very clearly observed for two types of chaotic diffusion. They have three branches for diffusion. The chaotic diffusion patterns for (1:3) and (2:3) resonant impulses are different. For a further view of the chaotic diffusion patterns, the chaotic diffusion patterns for (1:3), (1:4), (1:5) and (1:6) resonant impulses are presented in

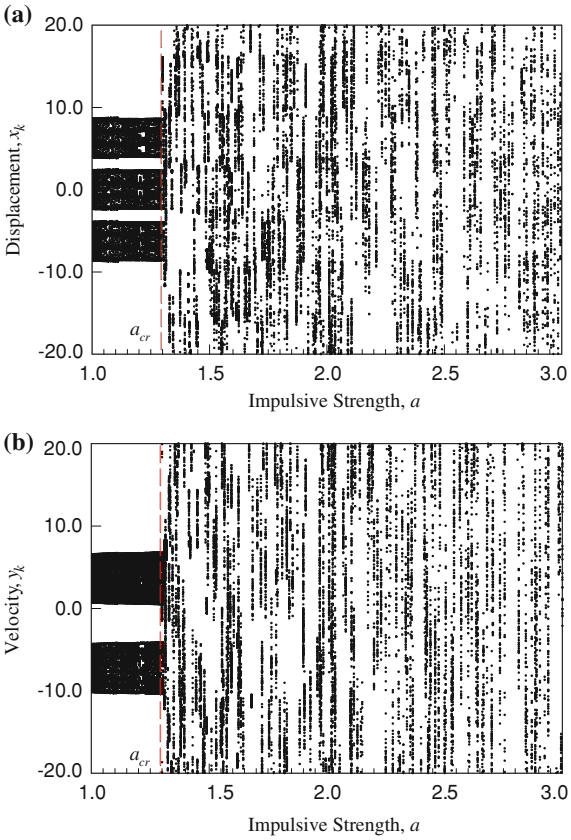

Fig. 5.27 Impulsive switching scenario with impulsive strength: **a** switching displacement, **b** switching velocity. ($c^{(i)} = c = 1, a^{(i)} = a, \quad \Omega = 1., n = 1, m = 3, n = 1, m = 3, a = 1.89$). ($c^{(i)} = c = 1, a^{(i)} = a, \quad \Omega = 1,$ $x_0^{(i)} = y_0^{(i)} = 4.0$ for $t_0 = 0$)

Fig. 5.31a–d, respectively. Each branch of the chaotic diffusion is colored by a different color for a better view of chaotic diffusion pattern. This deterministic system shows random walks properties. The complexity and randomness needs to be further investigated.

5.5 Mappings and Periodic Flows

To describe the switching of sub-systems, consider a switching set for the ith subsystem to be

$$\Sigma^{(i)} = \left\{ \mathbf{x}_k^{(i)} \middle| \mathbf{x}_k^{(i)} = \mathbf{x}^{(i)}(t_k), k \in \{0, 1, 2, \cdots\} \right\}. \tag{5.125}$$

From the solution of the ith subsystem, a mapping P_i for a time interval $[t_{k-1}, t_k]$ is defined as

$$P_i : \Sigma^{(i)} \to \Sigma^{(i)} \quad \text{for } i = 1, 2, \cdots, m \tag{5.126}$$

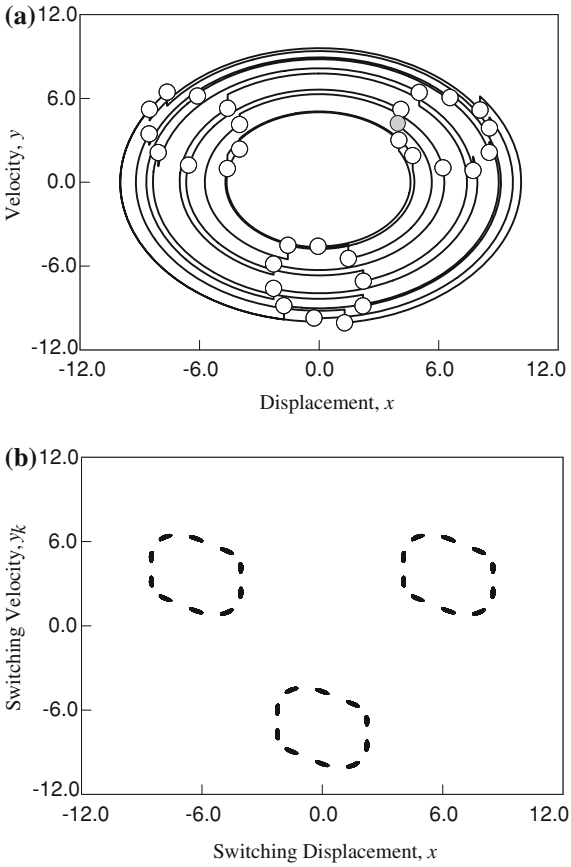

Fig. 5.28 A quasi-periodic impulsive motions: **a** trajectory in phase plane, **b** switching sec-tions. ($c^{(i)} = c = 1, a^{(i)} = a = 1.0, \Omega = 1.n = 1, m = 3,\ x_0^{(i)} = y_0^{(i)} = 4.0$ for $t_0 = 0$)

or

$$P_i : \mathbf{x}_{k-1}^{(i)} \to \mathbf{x}_k^{(i)} \quad \text{for } i = 1, 2, \cdots, m. \tag{5.127}$$

Define a time difference parameter for the ith subsystem for a time interval $[t_{k-1}, t_k]$ which can be set arbitrarily.

$$\alpha_k^{(i)} = t_k - t_{k-1}. \tag{5.128}$$

For simplicity, introduce two vectors herein

$$\mathbf{f}^{(i)} = (f_1^{(i)}, f_2^{(i)}, \cdots f_n^{(i)})^{\mathrm{T}} \text{ and } \mathbf{x}^{(i)} = (x_1^{(i)}, x_2^{(i)}, \cdots x_n^{(i)})^{\mathrm{T}}. \tag{5.129}$$

From the solution in Eq. (5.9) for the ith subsystem, the foregoing equation gives for $(i = 1, 2, \cdots, m)$

$$\mathbf{f}^{(i)}(\mathbf{x}_k^{(i)}, \mathbf{x}_{k-1}^{(i)}) = \mathbf{x}_k^{(i)} - \mathbf{\Phi}^{(i)}(\mathbf{x}_{k-1}^{(i)}, t_k, t_{k-1}, \mathbf{p}^{(i)}) = \mathbf{0}. \tag{5.130}$$

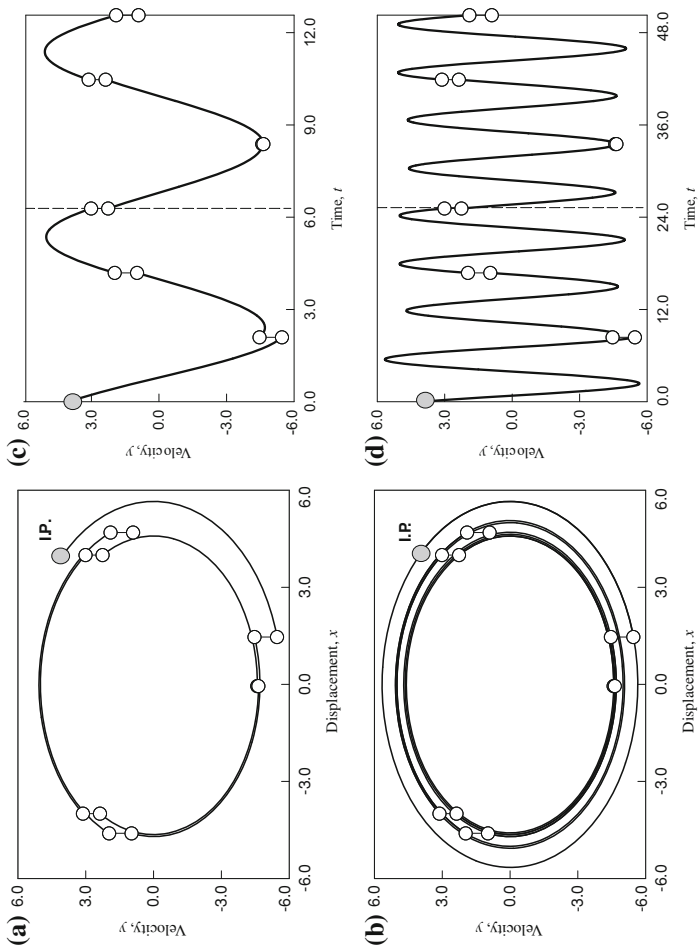

Fig. 5.29 Quasi-periodic impulsive motions ($m = 3$) : **a** trajectory ($n = 1$), **b** trajectory ($n = 4$), **c** velocity ($n = 1$) and **d** velocity ($n = 4$). ($c^{(i)} = c = 1, a^{(i)} = a = 1.0,\ \Omega = 1,\ x_0^{(i)} = y_0^{(i)} = 4.0$ for $t_0 = 0$)

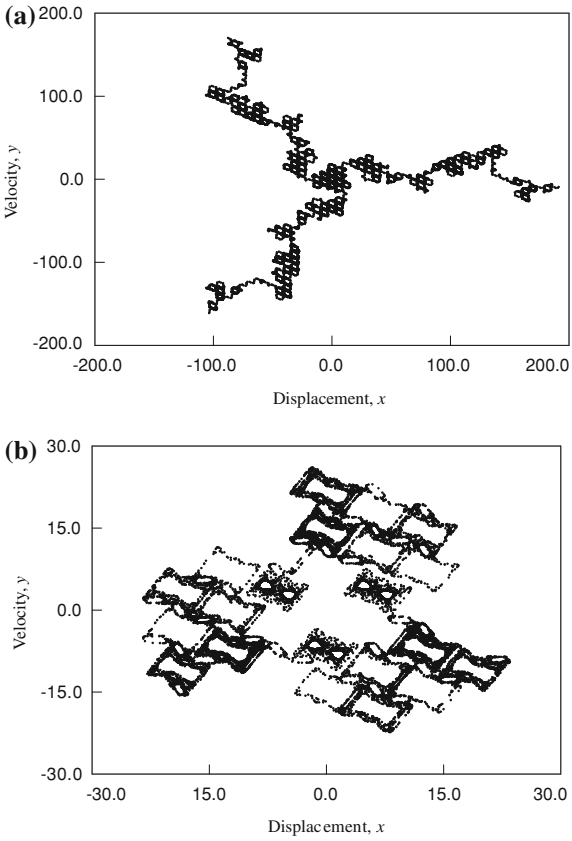

Fig. 5.30 Switching sections for chaotic impulsive motions: **a** ($n = 1,\ m = 3,\ a = 1.4$) and **b** ($n = 2,\ m = 3,\ a = 1.89$).($c^{(i)} = c = 1, a^{(i)} = a, \Omega = 1, x_0^{(i)} = y_0^{(i)} = 4.0$ for $t_0 = 0$)

Suppose the two trajectories of the ith and jth systems in phase space at the switching time t_k is continuous, i.e.,

$$\mathbf{x}_k^{(j)} = \mathbf{x}_k^{(i)} \quad \text{at time} \quad t_k \tag{5.131}$$

or

$$(x_{1(k)}^{(j)}, \cdots, x_{n(k)}^{(j)}) = (x_{1(k)}^{(i)}, \cdots, x_{n(k)}^{(i)}) \quad \text{for} \quad i, j \in \{1, 2, \cdots, m\}. \tag{5.132}$$

If the two solutions of the ith and jth subsystems at the switching time t_k are discontinuous, for instance, an impulsive switching system needs transport laws. From Luo (2006), a vector for the transport law from the ith to jth systems is introduced as

$$\mathbf{g}^{(ij)} = (g_1^{(ij)}, g_2^{(ij)}, \cdots g_m^{(ij)})^{\mathrm{T}}. \tag{5.133}$$

So the transport law between the ith and jth subsystems can be written as

$$\mathbf{g}^{(ij)}(\mathbf{x}_k^{(i)}, \mathbf{x}_k^{(j)}) = \mathbf{0} \text{ at time } t_k. \tag{5.134}$$

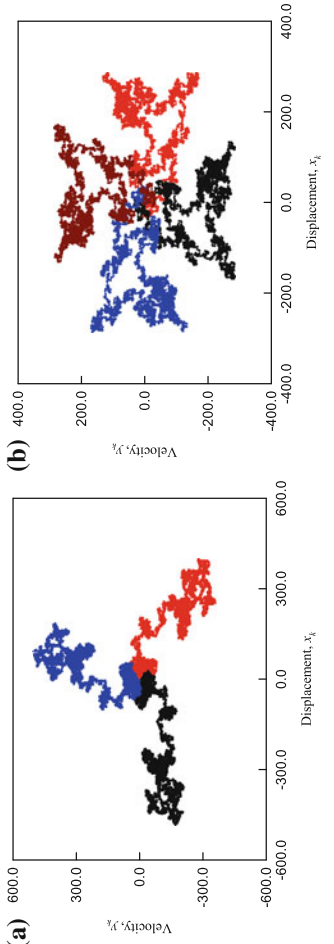

Fig. 5.31 Switching sections for chaotic impulsive motions: **a** $(n = 1, m = 3, a = 3.0)$, **b** $(n = 1, m = 4, a = 3.0)$, **c** $(n = 1, m = 5, a = 4.0)$, **d** $(n = 1, m = 4, a = 4.0)$. $(c^{(i)} = c = 1, \quad a^{(i)} = a, \quad \Omega = 1, x_0^{(i)} = y_0^{(i)} = 4.0$ for $t_0 = 0)$

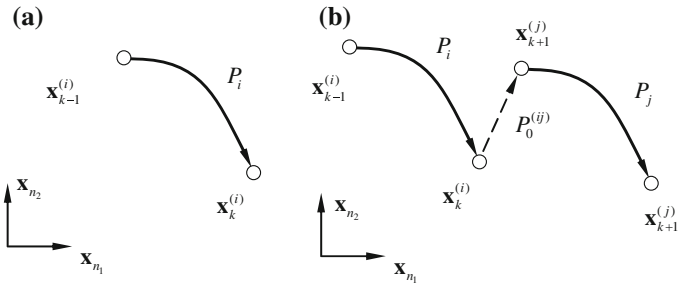

Fig. 5.32 **a** Mapping P_i and **b** transport mapping $P_0^{(ij)}$ in phase plane $(n_1 + n_2 = n)$

In other words, one obtains

$$\left.\begin{aligned} x_{1(k)}^{(j)} &= g_1^{(ij)}(x_{1(k)}^{(i)}, \cdots, x_{n(k)}^{(i)}) \\ x_{2(k)}^{(j)} &= g_2^{(ij)}(x_{1(k)}^{(i)}, \cdots, x_{n(k)}^{(i)}) \\ &\vdots \\ x_{n(k)}^{(j)} &= g_n^{(ij)}(x_{1(k)}^{(i)}, \cdots, x_{n(k)}^{(i)}) \end{aligned}\right\} \quad \text{for } i, j \in \{1, 2, \cdots, m\}. \tag{5.135}$$

From the transport law, a transport mapping is introduced as for $i, j \in \{1, 2, \cdots, m\}$

$$P_0^{(ij)} : \Sigma^{(i)} \to \Sigma^{(j)}, \tag{5.136}$$

i.e.,

$$P_0^{(ij)} : \mathbf{x}_k^{(i)} \to \mathbf{x}_k^{(j)} \quad \text{or} \quad P_0^{(ij)} : (x_{1(k)}^{(i)}, \cdots, x_{n(k)}^{(i)}) \to (x_{1(k)}^{(j)}, \cdots, x_{n(k)}^{(j)}). \tag{5.137}$$

The algebraic equations for the transport mapping are given in Eq. (5.135).

The mapping P_i for the ith subsystem for time $t \in [t_{k-1}, t_k]$ and the transport mapping at time $t = t_k$ are sketched in Figs. 5.32 and 5.33. The initial and final points of mapping P_i are $\mathbf{x}_{k-1}^{(i)}$ and $\mathbf{x}_k^{(i)}$. Similarly, the initial and final points of mapping P_j are $\mathbf{x}_k^{(j)}$ and $\mathbf{x}_{k+1}^{(j)}$. The mappings relative to subsystems are sketched by solid curves. The two mappings are connected by a transport mapping at $t = t_k$, which is depicted by the dashed line. In phase space, there is a non-negative distance governed by Eq. (5.134). However, the time-history of flows for the switching system experiences a jump at time $t = t_k$. If the transport law gives a special case to satisfy Eq. (5.131), the solutions of two sub-systems are C^0-continuous at the switching time $t = t_k$. The jump phenomenon will disappear.

Consider a flow of the switching system with a mapping structure for $t \in \cup_{j=1}^{N}[t_{k+j-1}, t_{k+j}]$ as

$$P = P_0^{(l_N l_{N+1})} \circ P_{l_N} \circ \cdots \circ P_{l_2} \circ P_0^{(l_1 l_2)} \circ P_{l_1} \equiv P_{l_N \cdots l_2 l_1}, \tag{5.138}$$

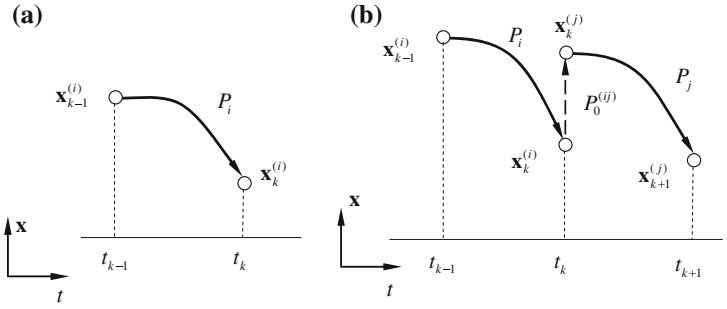

Fig. 5.33 **a** Mapping P_i and **b** transport mapping $P_0^{(ij)}$ in the time-history

where

$$P_{l_j} \in \{ P_i \,|\, i = 1, 2, \cdots, m \} \quad \text{for} \quad j = 1, 2, \cdots, m. \tag{5.139}$$

Consider the initial and final states $\mathbf{x}_k^{(l_1)} = (x_{1(k)}^{(l_1)}, \cdots, x_{n(k)}^{(l_1)})^{\mathrm{T}}$ at $t = t_k$ and $\mathbf{x}_{k+N}^{(l_{N+1})} = (x_{1(k+N)}^{(l_{N+1})}, \cdots, x_{n(k+N)}^{(l_{N+1})})^{\mathrm{T}}$ at $t = t_{k+N}$, respectively.

$$\mathbf{x}_{k+N}^{(l_{N+1})} = P\mathbf{x}_k^{(l_1)} = P_0^{(l_N l_{N+1})} \circ P_{l_N} \circ \cdots \circ P_{l_2} \circ P_0^{(l_1 l_2)} \circ P_{l_1} \mathbf{x}_k^{(l_1)}. \tag{5.140}$$

With each time difference, the total time difference is

$$t_{k+N} - t_k = \sum_{j=1}^{N} \alpha_{k+j}^{(l_j)}. \tag{5.141}$$

In addition, equation (5.140) gives the following mapping relations

$$\begin{aligned}
\mathbf{x}_{k+1}^{(l_1)} &= P_{l_1} \mathbf{x}_k^{(l_1)} \Rightarrow P_{l_1} : \mathbf{x}_k^{(l_1)} \to \mathbf{x}_{k+1}^{(l_1)}, \\
\mathbf{x}_{k+1}^{(l_2)} &= P_0^{(l_1 l_2)} \mathbf{x}_{k+1}^{(l_1)} \Rightarrow P_0^{(l_1 l_2)} : \mathbf{x}_{k+1}^{(l_1)} \to \mathbf{x}_{k+1}^{(l_2)}, \\
\mathbf{x}_{k+2}^{(l_2)} &= P_{l_2} \mathbf{x}_{k+1}^{(l_2)} \Rightarrow P_{l_2} : \mathbf{x}_{k+1}^{(l_2)} \to \mathbf{x}_{k+2}^{(l_2)}, \\
\mathbf{x}_{k+1}^{(l_3)} &= P_0^{(l_2 l_3)} \mathbf{x}_{k+2}^{(l_2)} \Rightarrow P_0^{(l_1 l_3)} : \mathbf{x}_{k+2}^{(l_2)} \to \mathbf{x}_{k+2}^{(l_3)}, \\
&\vdots \\
\mathbf{x}_{k+n}^{(l_N)} &= P_{l_N} \mathbf{x}_{k+N-1}^{(l_N)} \Rightarrow P_{l_N} : \mathbf{x}_{k+N-1}^{(l_N)} \to \mathbf{x}_{k+N}^{(l_N)}, \\
\mathbf{x}_{k+N}^{(l_{N+1})} &= P_0^{(l_N l_{N+1})} \mathbf{x}_{k+N}^{(l_N)} \Rightarrow P_0^{(l_N l_{N+1})} : \mathbf{x}_{k+N}^{(l_N)} \to \mathbf{x}_{k+N}^{(l_{N+1})}.
\end{aligned} \tag{5.142}$$

Mapping relations in Eq. (5.137) yields a set of algebraic equations as

$$\left.\begin{aligned}
&\mathbf{f}^{(l_1)}(\mathbf{x}_{k+1}^{(l_1)}, \mathbf{x}_k^{(l_1)}, \alpha_k^{(l_1)}) = \mathbf{0},\\
&\mathbf{g}^{(l_1 l_2)}(\mathbf{x}_{k+1}^{(l_1)}, \mathbf{x}_{k+1}^{(l_2)}) = \mathbf{0},\\
&\vdots\\
&\mathbf{f}^{(l_N)}(\mathbf{x}_{k+N}^{(l_N)}, \mathbf{x}_{k+N-1}^{(l_N)}, \alpha_{k+N}^{(l_N)}) = \mathbf{0},\\
&\mathbf{g}^{(l_N l_{N+1})}(\mathbf{x}_{k+N}^{(l_N)}, \mathbf{x}_{k+N}^{(l_{N+1})}) = \mathbf{0}.
\end{aligned}\right\} \tag{5.143}$$

If there is a periodic motion, the periodicity for $t_{k+N} = T + t_k$ is

$$\left.\begin{aligned}
&\mathbf{x}_{k+N}^{(l_{N+1})} = \mathbf{x}_k^{(l_1)} \ \text{ for } \ l_{N+1} = l_1 \ \text{ or}\\
&x_{1(k+N)}^{(l_{N+1})} = x_{1(k)}^{(l_1)}, \cdots, x_{m(k+N)}^{(l_{N+1})} = \dot{x}_{m(k)}^{(l_1)}
\end{aligned}\right\} \tag{5.144}$$

where T is time period. The resultant periodic solution of the switching system is for $i = 1, 2, \cdots, m$

$$\left.\begin{aligned}
&\mathbf{x}^{(l_i)}(t) = \left\{\mathbf{x}^{(l_i)}(t) \middle| \, t \in [t_{k+Ns+i-1}, t_{k+Ns+i}] \ \text{ for } \ s = 0, 1, 2 \cdots\right\},\\
&\mathbf{x}_{k+Ns+i}^{(l_i)} = \mathbf{x}_{k+Ns+i}^{(l \bmod (i,N)+1)} \ \text{ for } \ s = 0, 1, 2, \cdots.
\end{aligned}\right\} \tag{5.145}$$

From Eqs. (5.138) and (5.139), the corresponding switching points for the periodic motion can be determined. From the time difference, the time interval parameter is defined as

$$q_{k+j}^{(l_j)} = \frac{\alpha_{k+j}^{(l_j)}}{T}. \tag{5.146}$$

Thus, one obtains

$$\sum_{j=1}^{N} q_{k+j}^{(l_j)} = 1. \tag{5.147}$$

If a set of the time interval parameters for switching subsystems during the next period is the same as during the current period, the periodic flow is called *the equi-time-interval periodic flow*. The pattern of the resultant flow for the switching system during the next period will repeat the pattern of the flow during the current period. If a set of the time interval parameters for the second period is different from the first period, the periodic motion is called the *non-equi-time-interval periodic motion*. For such a flow, the switching pattern during the next period is different from the current one. For a general case, during two periods, only one pattern makes Eq. (5.147) be satisfied. Hence, this switching pattern can be treated as a periodic flow with two periods. To determine the stability of such a periodic motion, the Jacobian matrix can be computed, for $j = 1, 2, \cdots, n$ i.e.,

$$DP = DP_0^{(l_N l_1)} \cdot DP_{l_N} \cdot \ldots \cdot DP_{l_2} \cdot DP_0^{(l_1 l_2)} \cdot DP_{l_1} \tag{5.148}$$

with

$$DP_{l_j} = \left[\frac{\partial \mathbf{x}_{k+j}^{(l_j)})}{\partial \mathbf{x}_{k+j-1}^{(l_j)}}\right]_{m\times m} = \left[\frac{\partial(x_{1(k+j)}^{(l_j)}, x_{2(k+j)}^{(l_j)}, \cdots x_{m(k+j)}^{(l_j)})}{\partial(x_{1(k+j-1)}^{(l_j)}, x_{2(k+j-1)}^{(l_j)}, \cdots x_{m(k+j-1)}^{(l_j)})}\right]_{m\times m}$$
$$= -\left[\frac{\partial \mathbf{f}^{(l_j)}}{\partial \mathbf{x}_{k+j}^{(l_j)}}\right]_{m\times m}^{-1}\left[\frac{\partial \mathbf{f}^{(l_j)}}{\partial \mathbf{x}_{k+j-1}^{(l_j)}}\right]_{m\times m}. \tag{5.149}$$

Due to Eq. (5.130), one obtains

$$\left[\frac{\partial \mathbf{f}^{(l_j)}}{\partial \mathbf{x}_{k+j-1}^{(l_j)}}\right]_{m\times m} + \left[\frac{\partial \mathbf{f}^{(l_j)}}{\partial \mathbf{x}_{k+j-1}^{(l_j)}}\right]_{m\times m}\left[\frac{\partial \mathbf{x}_{k+j}^{(l_j)}}{\partial \mathbf{x}_{k+j-1}^{(l_j)}}\right]_{m\times m} = \mathbf{0}. \tag{5.150}$$

Similarly, from the transport law, one obtains

$$\left[\frac{\partial \mathbf{g}^{(l_j l_{j+1})}}{\partial \mathbf{x}_{k+j}^{(l_j)}}\right]_{m\times m} + \left[\frac{\partial \mathbf{g}^{(l_j l_{j+1})}}{\partial \mathbf{x}_{k+j}^{(l_{j+1})}}\right]_{m\times m}\left[\frac{\partial \mathbf{x}_{k+j}^{(l_{j+1})}}{\partial \mathbf{x}_{k+j}^{(l_j)}}\right]_{m\times m} = \mathbf{0}, \tag{5.151}$$

$$DP_0^{(l_j l_{j+1})} = \left[\frac{\partial \mathbf{x}_{k+j}^{(l_{j+1})})}{\partial \mathbf{x}_{k+j}^{(l_j)}}\right]_{m\times m} = \left[\frac{\partial(x_{1(k+j)}^{(l_{j+1})}, x_{2(k+j)}^{(l_{j+1})}, \cdots x_{m(k+j)}^{(l_{j+1})})}{\partial(x_{1(k+j)}^{(l_j)}, x_{2(k+j)}^{(l_j)}, \cdots x_{m(k+j)}^{(l_j)})}\right]_{m\times m}$$
$$= -\left[\frac{\partial \mathbf{g}^{(l_j l_{j+1})}}{\partial \mathbf{x}_{k+j}^{(l_{j+1})}}\right]_{m\times m}^{-1}\left[\frac{\partial \mathbf{g}^{(l_j l_{j+1})}}{\partial \mathbf{x}_{k+j}^{(l_j)}}\right]_{m\times m}. \tag{5.152}$$

If the magnitudes of two eigenvalues of the total Jacobian matrix DP are less than 1 (i.e., $|\lambda_\alpha| < 1,\ \alpha = 1, 2, \cdots, m$), the periodic motion is stable. If the magnitude of one of two eigenvalues is greater than 1 ($|\lambda_\alpha| > 1,\ \alpha \in \{1, 2, \cdots, m\}$), the periodic motion is unstable. If one of eigenvalues is a positive one (+1) and the rest of eigenvalues are in the unit cycle, the periodic flow experiences a saddle-node bifurcation. If one of eigenvalues is a negative one (−1) and the rest of eigenvalues are in the unit cycle, the periodic flow possesses a period-doubling bifurcation. If a pair of complex eigenvalues is on the unit cycle and the rest of eigenvalues are in the unit cycle, the Neimark bifurcation of the periodic flow occurs.

Consider a switching system as a combination of two subsystems (i.e., l_1th and l_2th subsystems). A point $\mathbf{x}_k^{(l_1)}$ at $t = t_k$ is selected as the initial point for the l_1th-subsystem. A mapping P_{l_1} maps the initial state to the final state $\mathbf{x}_{k+1}^{(l_1)}$ at $t = t_{k+1}$. For the l_1th subsystem switching to the l_2th subsystem, the transport mapping $P_0^{(l_1 l_2)}$ will be adopted at time $t = t_{k+1}$ and the initial condition of the l_2th subsystem will be obtained (i.e.,$\mathbf{x}_{k+1}^{(l_2)}$). Through the mapping P_{l_2} of the l_2th subsystem, the

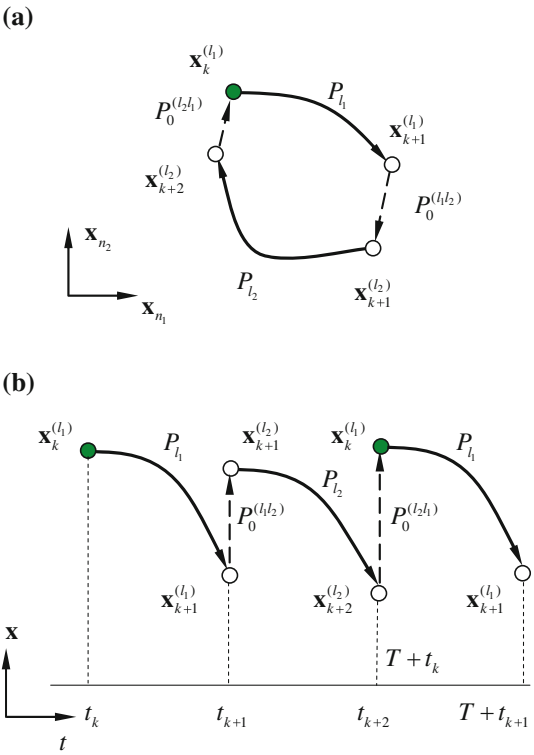

Fig. 5.34 A periodic motion of mapping structure $P_{l_2 l_1}$: **a** phase space and **b** time-history ($n_1 + n_2 = n$)

final state $\mathbf{x}_{k+2}^{(l_2)}$ is obtained at time $t = t_{k+2}$. To form a periodic flow, the transport mapping $P_0^{(l_2 l_1)}$ will map the point $\mathbf{x}_{k+2}^{(l_2)}$ to the starting point $\mathbf{x}_k^{(l_1)}$ with $t_{k+2} = t_k + T$. This process of flow formation is sketched in Fig. 5.34. The solid curves give the mappings for the l_1th and l_2th subsystems, and the dashed lines represent the transport mappings.

5.6 Linear Switching Systems

As in Luo and Wang (2009a, b) consider the ith subsystem in a resultant switching system for a time interval $t \in [t_{k-1}, t_k]$ in a form of

$$\dot{\mathbf{x}} = \mathbf{A}^{(i)}\mathbf{x} + \mathbf{Q}^{(i)}(t) \quad \text{for } i = 1, 2, \cdots, m, \tag{5.153}$$

where $\mathbf{A}^{(i)}$ is a matrix for the ith system matrix in the time interval $t \in [t_{k-1}, t_k]$. $\mathbf{Q}^{(i)}$ is a time-dependent vector function for the ith subsystem.

$$\mathbf{A}^{(i)} = \left(a_{kl}^{(i)}\right)_{n\times n} \text{ and } \mathbf{Q}^{(i)} = \left(Q_{kl}^{(i)}(t)\right)_{n\times 1}. \tag{5.154}$$

Eigenvalues of $\mathbf{A}^{(i)}$, given by $|\lambda^{(i)} I - \mathbf{A}^{(i)}| = 0$, possess p pairs of conjugated complex eigenvalues ($\lambda_{1,2} = u_1 \pm v_1\mathbf{i}, \lambda_{3,4} = u_2 \pm v_2\mathbf{i}, \cdots, \quad \lambda_{2p-1,2p} = u_p \pm v_p\mathbf{i}$)

with $\mathbf{i} = \sqrt{-1}$ and $(n-2p)$ real eigenvalues of $\lambda_{2p+1}, \lambda_{2p+2}, \cdots, \lambda_n$. The closed-form solution of the ith subsystem in Eq. (5.153) will be given herein to demonstrate the methodology, i.e.,

$$\begin{aligned}\mathbf{x}^{(i)} = &\sum_{r=2p+1}^{n} L_r^{(k)} \mathbf{B}_r^{(i)} \exp\left[\lambda_r^{(i)}(t-t_{k-1})\right] + \sum_{r=1}^{p} \exp\left[u_r^{(i)}(t-t_{k-1})\right] \\ &\times \left\{\mathbf{S}_r^{(i)} \cos v_r^{(i)}(t-t_{k-1}) - \mathbf{T}_r^{(i)} \sin v_r^{(i)}(t-t_{k-1})\right\} + \mathbf{x}_p^{(i)}(t).\end{aligned} \tag{5.155}$$

where

$$\begin{aligned}\mathbf{B}_r^{(i)} &= (1, c_{2(r)}^{(i)}, \cdots, c_{n(r)}^{(i)})^{\mathrm{T}}, \\ \mathbf{S}_j^{(i)} &= (M_j^{(k)}, U_{2(j)}^{(i)} M_j^{(k)} - V_{2(j)}^{(i)} N_j^{(k)}, \cdots, U_{n(j)}^{(i)} M_j^{(k)} - V_{n(j)}^{(i)} N_j^{(k)})^{\mathrm{T}}, \\ \mathbf{T}_j^{(i)} &= (N_j^{(k)}, U_{2(j)}^{(i)} N_j^{(k)} + V_{2(j)}^{(i)} M_j^{(k)}, \cdots, U_{n(j)}^{(i)} N_j^{(k)} + V_{n(j)}^{(i)} M_j^{(k)})^{\mathrm{T}}.\end{aligned} \tag{5.156}$$

and the coefficients can be obtained by

$$\left.\begin{aligned}\mathbf{c}^{(i)} &= \left[\mathbf{C}_{11}^{(i)} - \mathbf{I}\lambda_r^{(i)}\right]^{-1}\left[-\mathbf{a}^{(i)}\right], \\ \begin{bmatrix}\mathbf{U}^{(i)} \\ \mathbf{V}^{(i)}\end{bmatrix} &= \begin{bmatrix}\mathbf{C}_{11}^{(i)} - \mathbf{I}a_k^{(i)} & \mathbf{I}b_k^{(i)} \\ -\mathbf{I}b_k^{(i)} & \mathbf{C}_{11}^{(i)} - \mathbf{I}a_k^{(i)}\end{bmatrix}^{-1}\begin{bmatrix}-\mathbf{a}^{(i)} \\ \mathbf{0}\end{bmatrix},\end{aligned}\right\} \tag{5.157}$$

where

$$\begin{aligned}&\mathbf{c}^{(i)} = (c_{2(r)}^{(i)}, c_{3(r)}^{(i)}, \cdots, c_{m(r)}^{(i)})^{\mathrm{T}}, \mathbf{U}^{(i)} = (U_{2(k)}^{(i)}, U_{3(k)}^{(i)}, \cdots, U_{n(k)}^{(i)})^{\mathrm{T}}, \\ &\mathbf{V}^{(i)} = (V_{2(k)}^{(i)}, V_{3(k)}^{(i)}, \cdots, V_{n(k)}^{(i)})^{\mathrm{T}}, \mathbf{a}^{(i)} = [a_{21}^{(i)}, a_{31}^{(i)}, \cdots, a_{n1}^{(i)}]^{\mathrm{T}},\end{aligned} \tag{5.158}$$

and $\mathbf{C}_{11}^{(i)}$ is a matrix relative to the minor of $a_{11}^{(i)}$ in matrix $\mathbf{A}^{(i)}$,

$$\mathbf{C}_{11}^{(i)} = \begin{bmatrix} a_{22}^{(i)} & a_{23}^{(i)} & \cdots & a_{2n}^{(i)} \\ a_{32}^{(i)} & a_{33}^{(i)} & \cdots & a_{3n}^{(i)} \\ \vdots & \vdots & \vdots & \vdots \\ a_{n2}^{(i)} & a_{n3}^{(i)} & \cdots & a_{nn}^{(i)} \end{bmatrix}. \tag{5.159}$$

The corresponding coefficients are

$$\begin{aligned}\mathbf{M}^{(k)} &= [M_1^{(k)}, M_2^{(k)}, \cdots, M_p^{(k)}]^{\mathrm{T}}, \\ \mathbf{N}^{(k)} &= [N_1^{(k)}, N_2^{(k)}, \cdots, N_p^{(k)}]^{\mathrm{T}}, \\ \mathbf{L}^{(k)} &= [L_{2p+1}^{(k)}, L_{2p+2}^{(k)}, \cdots, L_m^{(k)}]^{\mathrm{T}};\end{aligned} \tag{5.160}$$

$$\begin{bmatrix}\mathbf{M}^{(k)}\\ \mathbf{N}^{(k)}\\ \mathbf{L}^{(k)}\end{bmatrix}=\begin{bmatrix}1 & 0 & \cdots & 1 & 0 & 1 & \cdots & 1\\ U_{2(1)}^{(i)} & -V_{2(1)}^{(i)} & \cdots & U_{2(p)}^{(i)} & -V_{2(p)}^{(i)} & c_{2(2p+1)}^{(i)} & \cdots & c_{2(n)}^{(i)}\\ \vdots & \vdots & \vdots & \vdots & \vdots & \vdots & \vdots & \vdots\\ U_{n(1)}^{(i)} & -V_{n(1)}^{(i)} & \cdots & U_{n(p)}^{(i)} & -V_{n(p)}^{(i)} & c_{n(2p+1)}^{(i)} & \cdots & c_{n(n)}^{(i)}\end{bmatrix}^{-1}\times\left[\mathbf{x}^{(i)}(t_{k-1})-\mathbf{x}_p^{(i)}(t_{k-1})\right];\tag{5.161}$$

where $\mathbf{x}_p^{(i)}(t_{k-1})$ is $\mathbf{x}_p^{(i)}(t)$ at time t_{k-1} and $\mathbf{x}_{k-1}^{(i)}=\mathbf{x}^{(i)}(t_{k-1})$.

Consider three simple external forcing as examples herein

$$\begin{aligned}\mathbf{Q}^{(1)}(t)&=\sum\nolimits_{s=0}^{J_1}\mathbf{a}_s^{(1)}(t-t_{k-1})^s,\\ \mathbf{Q}^{(2)}(t)&=\sum\nolimits_{s=0}^{J_2}\mathbf{a}_s^{(2)}\cos\left[\Omega_s^{(2)}(t-t_{k-1})\right]+\mathbf{b}_s^{(2)}\sin\left[\Omega_s^{(2)}(t-t_{k-1})\right],\\ \mathbf{Q}^{(3)}(t)&=\sum\nolimits_{s=0}^{J_3}\mathbf{a}_s^{(3)}\exp\left[\lambda_s^{(3)}(t-t_{k-1})\right]\end{aligned}\tag{5.162}$$

with

$$\begin{aligned}\mathbf{a}_s^{(i)}&=\left[a_{1(s)}^{(i)}\ a_{2(s)}^{(i)}\ \cdots\ a_{n(s)}^{(i)}\right]^{\mathrm{T}},\\ \mathbf{b}_s^{(2)}&=\left[b_{1(s)}^{(2)}\ b_{2(s)}^{(2)}\ \cdots\ b_{n(s)}^{(2)}\right]^{\mathrm{T}}\end{aligned}\tag{5.163}$$

where $a_{l(s)}^{(i)}(i=1,2,3;\,l=1,\cdots,n)$ and $\Omega_j^{(2)}$, $\varphi_j^{(2)}$ and $\lambda_j^{(3)}$ are coefficients. The corresponding particular solutions are

$$\begin{aligned}\mathbf{x}_p^{(1)}(t)&=\sum\nolimits_{j=0}^{J_1}\mathbf{A}_j^{(1)}(t-t_{k-1})^j,\\ \mathbf{x}_p^{(2)}(t)&=\sum\nolimits_{j=0}^{J_2}\mathbf{A}_j^{(2)}\cos\left[\Omega_j^{(2)}(t-t_{k-1})\right]+\mathbf{B}_j^{(2)}\sin\left[\Omega_j^{(2)}(t-t_{k-1})\right],\\ \mathbf{x}_p^{(3)}(t)&=\sum\nolimits_{j=0}^{J_3}\mathbf{A}_j^{(3)}\exp\left[\lambda_j^{(3)}(t-t_{k-1})\right]\end{aligned}\tag{5.164}$$

where

$$\begin{aligned}&\left.\begin{aligned}\mathbf{A}_s^{(1)}&=\mathbf{A}^{-1}[\mathbf{A}_{s+1}^{(1)}(s+1)-\mathbf{a}_s^{(1)}],\\ \mathbf{A}_{J_1}^{(1)}&=-\mathbf{A}^{-1}\mathbf{a}_{J_1}^{(1)}\end{aligned}\right\}(s=0,1,2,\cdots,J_1-1);\\ &\begin{bmatrix}\mathbf{A}_s^{(2)}\\ \mathbf{B}_s^{(2)}\end{bmatrix}=-\begin{bmatrix}\mathbf{A}^{(i)} & -\mathbf{I}\Omega_s^{(2)}\\ \mathbf{I}\Omega_s^{(2)} & \mathbf{A}^{(i)}\end{bmatrix}^{-1}\begin{bmatrix}\mathbf{a}_s^{(2)}\\ \mathbf{b}_s^{(2)}\end{bmatrix},(s=0,1,2,\cdots,J_2);\\ &\mathbf{A}_s^{(3)}=-\left[\mathbf{A}-I\lambda_s^{(3)}\right]^{-1}\mathbf{a}_s^{(3)},(s=0,1,2,\cdots,J_3).\end{aligned}\tag{5.165}$$

Consider a periodic flow as in Eq. (5.140). The vector function for mapping P_{l_j} of the l_jth system is

$$\begin{aligned}\mathbf{f}^{(l_j)}(\mathbf{x}_{k+j}^{(l_j)}, \mathbf{x}_{k+j-1}^{(l_j)}) &= \mathbf{x}_{k+j}^{(l_j)} - \mathbf{g}^{(l_j)}(\mathbf{x}_{k+j-1}^{(l_j)}) - \mathbf{d}^{(l_j)}(t_{k+j}) \\ &= \mathbf{x}_{k+j}^{(l_j)} - \sum\nolimits_{r=2p+1}^{n} L_r^{(k)} \mathbf{B}_r^{(l_j)}(\mathbf{x}_{k+j-1}^{(l_j)}) \exp[\lambda_r^{(l_j)}(t_{k+j} - t_{k+j-1})] \\ &\quad - \sum\nolimits_{r=1}^{p} \exp\,[u_r^{(l_j)}(t_{k+j} - t_{k+j-1})] \\ &\quad \times \left\{ \mathbf{S}_r^{(l_j)}(\mathbf{x}_{k+j-1}^{(l_j)}) \cos v_r^{(l_j)}(t_{k+j} - t_{k+j-1}) - \mathbf{T}_r^{(l_j)}(\mathbf{x}_{k+j-1}^{(l_j)}) \right. \\ &\quad \left. \times \sin v_r^{(l_j)}(t_{k+j} - t_{k+j-1}) \right\} - \mathbf{x}_p^{(l_j)}(t_{k+j}).\end{aligned} \tag{5.166}$$

From $\mathbf{f}^{(l_j)}(\mathbf{x}_{k+j}^{(l_j)}, \mathbf{x}_{k+j-1}^{(l_j)}) = 0$, one obtains

$$\mathbf{x}_{k+j}^{(l_j)} = \mathbf{G}^{(l_j)} \mathbf{x}_{k+j-1}^{(l_j)} + \mathbf{d}^{(l_j)} \tag{5.167}$$

where the corresponding mapping and constant vector are given by

$$\mathbf{G}^{(l_j)} = \frac{\partial \mathbf{g}^{(l_j)}(\mathbf{x}_{k+j-1}^{(l_j)})}{\partial \mathbf{x}_{k+j-1}^{(l_j)}} \text{ and } \mathbf{d}^{(l_j)} = \mathbf{x}_p^{(l_j)}. \tag{5.168}$$

Consider the transport law to be an affine transformation

$$\mathbf{g}^{(l_{j+1}l_j)}(\mathbf{x}_{k+j}^{(l_{j+1})}, \mathbf{x}_{k+j}^{(l_j)}) = 0 \Rightarrow \mathbf{x}_{k+j}^{(l_{j+1})} = \mathbf{E}^{(l_{j+1}l_j)} \mathbf{x}_{k+j-1}^{(l_j)} + \mathbf{e}^{(l_{j+1}l_j)}. \tag{5.169}$$

For the mapping structure in Eq. (5.140), one obtains

$$\mathbf{x}_{k+j}^{(l_{j+1})} - \mathbf{C}^{(l_{j+1})} \mathbf{x}_k^{(l_1)} = \mathbf{D}^{(l_{j+1})} \tag{5.170}$$

where for $j = 0, 1, 2, \cdots, N$

$$\mathbf{C}^{(l_{j+1})} = \mathbf{E}^{(l_{j+1}l_j)} \mathbf{G}^{(l_{j+1})} \cdots \mathbf{G}^{(l_{j+1})} \mathbf{E}^{(l_{j+1}l_j)} \mathbf{G}^{(l_j)} \cdots \mathbf{E}^{(l_2 l_1)} \mathbf{G}^{(l_1)}, \tag{5.171}$$

$$\begin{aligned}\mathbf{D}^{(l_{N+1})} &= (\mathbf{E}^{(l_{N+1}l_N)} \mathbf{G}^{(l_N)}) \mathbf{D}^{(l_N)} + \mathbf{e}^{(l_{N+1}l_N)}, \cdots, \\ \mathbf{D}^{(l_{j+1})} &= (\mathbf{E}^{(l_{j+1}l_j)} \mathbf{G}^{(l_j)}) \mathbf{D}^{(l_j)} + \mathbf{e}^{(l_{j+1}l_j)}, \cdots, \\ \mathbf{D}^{(l_2)} &= (\mathbf{E}^{(l_2 l_1)} \mathbf{G}^{(l_1)}) \mathbf{d}^{(l_1)} + \mathbf{e}^{(l_2 l_1)}, \mathbf{D}^{(l_1)} = \mathbf{d}^{(l_1)}.\end{aligned} \tag{5.172}$$

The periodic motion requires

$$\mathbf{x}_{k+N}^{(l_{N+1})} = \mathbf{x}_k^{(l_1)}. \tag{5.173}$$

If $\mathbf{D}^{(l_{N+1})} \neq 0$, the existence condition for periodic motion is

$$|\mathbf{I} - \mathbf{C}^{(l_{N+1})}| \neq 0. \tag{5.174}$$

In other words, the solution for the periodic flow does not exist if

$$|\mathbf{I} - \mathbf{C}^{(l_{N+1})}| = 0. \tag{5.175}$$

That is, the existence condition for periodic flow with mapping in Eq. (5.140) is that the eigenvalue of matrix is not one (+1). On the other hand, for the stability of the linear switching system, equation (5.170) for $j = N$ gives

$$\Delta\mathbf{x}_{k+N}^{(l_{N+1})} = DP\,\Delta\mathbf{x}_k^{(l_1)} = \mathbf{C}^{(l_{N+1})}\Delta\mathbf{x}_k^{(l_1)}. \tag{5.176}$$

Let $\Delta\mathbf{x}_{k+N}^{(l_{N+1})} = \lambda\Delta\mathbf{x}_k^{(l_1)}$, and the foregoing equation gives

$$|DP - \lambda\mathbf{I}| = |\mathbf{C}^{(l_{N+1})} - \lambda\mathbf{I}| = 0. \tag{5.177}$$

If the magnitudes of all eigenvalues λ_j $(j = 1, 2, \cdots, n)$ are less than one (i.e., $|\lambda_j| < 1$), the periodic flow in the switching system is stable. If the magnitude of one of eigenvalues λ_j $(j = 1, 2, \cdots, n)$ is greater than one, the periodic flow in the switching system is unstable. However, the saddle-node bifurcation of such periodic flow occurs if one of eigenvalues λ_j $(j \in \{1, 2, \cdots, n\})$ is one. Meanwhile, the periodic flow with such a mapping structure will disappear.

5.6.1 Vibrations with Piecewise Forces

As in Luo and Wang (2009a), consider the ith oscillator in a resultant switching system for a time interval $t \in [t_{k-1}, t_k]$ as

$$\ddot{x} + 2\delta^{(i)}\dot{x} + (\omega^{(i)})^2 x = Q^{(i)}(t) \quad \text{for} \quad i = 1, 2, \cdots, m, \tag{5.178}$$

where $\delta^{(i)}$ and $\omega^{(i)}$ are damping coefficient and natural frequency in the ith oscillator in the time interval $t \in [t_{k-1}, t_k]$, respectively. $Q^{(i)}(t)$ is the ith external forcing. For a case $(\delta^{(i)} < |\omega^{(i)}|)$, the closed-form solution of the ith oscillator in Eq. (5.178) will be given herein.

$$\begin{aligned}
x^{(i)}(t) =& e^{-\delta^{(i)}(t-t_{k-1})}\left[c_1^{(k)}\cos\omega_d^{(i)}(t-t_{k-1}) + c_2^{(k)}\sin\omega_d^{(i)}(t-t_{k-1})\right] + x_p^{(i)}(t),\\
\dot{x}^{(i)}(t) =& e^{-\delta^{(i)}(t-t_{k-1})}\left[(-\delta^{(i)}c_1^{(k)} + \omega_d^{(i)}c_2^{(k)})\cos\omega_d^{(i)}(t-t_{k-1})\right.\\
&\left. - (\delta^{(i)}c_2^{(k)} + \omega_d^{(i)}c_1^{(k)})\sin\omega_d^{(i)}(t-t_{k-1})\right] + \dot{x}_p^{(i)}(t);
\end{aligned} \tag{5.179}$$

with $\omega_d^{(i)} = \sqrt{(\omega^{(i)})^2 - (\delta^{(i)})^2}$ and the two coefficients $c_1^{(k)}$ and $c_2^{(k)}$ are given by

$$
\begin{aligned}
c_1^{(k)} &= x_{k-1}^{(i)} - x_p^{(i)}(t_{k-1}),\\
c_2^{(k)} &= \frac{1}{\omega_d^{(i)}}[\dot{x}_{k-1}^{(i)} - \dot{x}_p^{(i)}(t_{k-1}) + \delta^{(i)} c_1^{(k)}],
\end{aligned}
\tag{5.180}
$$

where $x_p^{(i)}(t_{k-1})$ and $\dot{x}_p^{(i)}(t_{k-1})$ are $x_p^{(i)}(t)$ and $\dot{x}_p^{(i)}(t)$ at time t_{k-1}, $x_{k-1}^{(i)} = x^{(i)}(t_{k-1})$ and $\dot{x}_{k-1}^{(i)} = \dot{x}^{(i)}(t_{k-1})$. Consider three simple external forcing as

$$
\begin{aligned}
Q^{(1)}(t) &= \sum\nolimits_{j=0}^{J_1} a_j^{(1)}(t - t_{k-1})^j,\\
Q^{(2)}(t) &= \sum\nolimits_{j=0}^{J_2} a_j^{(2)} \cos[\Omega_j^{(2)}(t - t_{k-1}) + \varphi_j^{(2)}],\\
Q^{(3)}(t) &= \sum\nolimits_{j=0}^{J_3} a_j^{(3)} \exp\,[\lambda_j^{(3)}(t - t_{k-1})]
\end{aligned}
\tag{5.181}
$$

where $a_j^{(l)}(l = 1, 2, 3)$ and $\Omega_j^{(2)}, \varphi_j^{(2)}$ and $\lambda_j^{(3)}$ are coefficients. The corresponding particular solutions are

$$
\begin{aligned}
x_p^{(1)}(t) &= \sum\nolimits_{j=0}^{J_1} A_j^{(1)}(t - t_{k-1})^j,\\
x_p^{(2)}(t) &= \sum\nolimits_{j=1}^{J_2} A_j^{(2)} \cos[\Omega_j^{(2)}(t - t_{k-1}) + \Phi_j^{(2)}],\\
x_p^{(3)}(t) &= \sum\nolimits_{j=0}^{J_3} \frac{a_j^{(3)}}{(\lambda_j^{(3)})^2 + 2\delta^{(i)}\lambda_j^{(3)} + (\omega^{(i)})^2} \exp\,[\lambda_j^{(3)}(t - t_{k-1})]
\end{aligned}
\tag{5.182}
$$

where

$$
\begin{aligned}
&A_{J_1}^{(1)} = \frac{a_{J_1}^{(1)}}{(\omega^{(i)})^2}, A_{J_1-1}^{(1)} = \frac{a_{J_1-1}^{(1)} - 2\delta^{(i)} J_1 A_{J_1}^{(1)}}{(\omega^{(i)})^2},\\
&A_J^{(1)} = \frac{1}{(\omega^{(i)})^2}[a_J^{(1)} - (J+2)(J+1)A_{J+2}^{(1)} - 2\delta^{(i)}(J+1)A_{J+1}^{(1)}]\\
&\quad (J = 0, 1, 2, \cdots, J_1 - 1),
\end{aligned}
\tag{5.183}
$$

$$
\begin{aligned}
A_j^{(2)} &= \frac{a_j^{(2)}}{\sqrt{[(\omega^{(i)})^2 - (\Omega_j^{(2)})^2]^2 + (2\delta^{(i)}\Omega_j^{(2)})^2}},\\
\Phi_j^{(2)} &= \varphi_j^{(2)} - \arctan\frac{2\delta^{(i)}\Omega_j^{(2)}}{(\omega^{(i)})^2 - (\Omega_j^{(2)})^2}.
\end{aligned}
\tag{5.184}
$$

Consider a switching set for the ith oscillator to be

$$
\Sigma^{(i)} = \left\{ (x_k^{(i)}, \dot{x}_k^{(i)}) \,\middle|\, x_k^{(i)} = x^{(i)}(t_k), \dot{x}_k^{(i)} = \dot{x}^{(i)}(t_k), k \in \{0, 1, 2, \cdots\} \right\}. \tag{5.185}
$$

From the solution of the ith oscillator, a mapping P_i for a time interval $t \in [t_{k-1}, t_k]$ is defined as

$$P_i : \Sigma^{(i)} \to \Sigma^{(i)} \quad \text{for } i = 1, 2, \cdots, m \tag{5.186}$$

or

$$P_i : (x_{k-1}^{(i)}, \dot{x}_{k-1}^{(i)}) \to (x_k^{(i)}, \dot{x}_k^{(i)}) \quad \text{for } i = 1, 2, \cdots, m. \tag{5.187}$$

For simplicity, introduce two vectors for mapping P_i herein

$$\mathbf{f}^{(i)} = (f_1^{(i)}, f_2^{(i)})^{\mathrm{T}} \text{ and } \mathbf{x}^{(i)} = (x^{(i)}, \dot{x}^{(i)})^{\mathrm{T}}. \tag{5.188}$$

From the displacement and velocity solutions of the ith oscillator for the starting and ending points, the two component functions of the vector function $\mathbf{f}^{(i)}$ can be determined. For instance, from the starting point $(x_{k-1}^{(i)}, \dot{x}_{k-1}^{(i)})$ at time t_{k-1} and the ending points $(x_k^{(i)}, \dot{x}_k^{(i)})$ at time t_k, the two components of the vector function $\mathbf{f}^{(i)}$ can be written for $i = 1, 2, \cdots, m$ by two algebraic equations, i.e.,

$$\left.\begin{aligned} f_1^{(i)}(\mathbf{x}_k^{(i)}, \mathbf{x}_{k-1}^{(i)}) &\equiv f_1^{(i)}(x_k^{(i)}, \dot{x}_k^{(i)}, x_{k-1}^{(i)}, \dot{x}_{k-1}^{(i)},) = 0, \\ f_2^{(i)}(\mathbf{x}_k^{(i)}, \mathbf{x}_{k-1}^{(i)}) &\equiv f_2^{(i)}(x_k^{(i)}, \dot{x}_k^{(i)}, x_{k-1}^{(i)}, \dot{x}_{k-1}^{(i)}) = 0. \end{aligned}\right\} \tag{5.189}$$

Using Eq. (5.179), the algebraic equations of mapping P_i for $t \in [t_{k-1}, t_k]$ are

$$\begin{aligned} f_1^{(i)}(\mathbf{x}_k^{(i)}, \mathbf{x}_{k-1}^{(i)}) =& x_k^{(i)} - e^{-\delta^{(i)}(t_k - t_{k-1})}[c_1^{(k-1)} \cos \omega_d^{(i)}(t_k - t_{k-1}) \\ &+ c_2^{(k-1)} \sin \omega_d^{(i)}(t_k - t_{k-1})] + x_p^{(i)}(t_k) = 0, \\ f_2^{(i)}(\mathbf{x}_k^{(i)}, \mathbf{x}_{k-1}^{(i)}) =& \dot{x}_k^{(i)} - e^{-\delta^{(i)}(t_k - t_{k-1})}[(-\delta^{(i)} c_1^{(k)} + \omega_d^{(i)} c_2^{(k)}) \cos \omega_d^{(i)}(t_k - t_{k-1}) \\ &- (\delta^{(i)} c_2^{(k)} + \omega_d^{(i)} c_1^{(k)}) \sin \omega_d^{(i)}(t_k - t_{k-1})] + \dot{x}_p^{(i)}(t_k) = 0. \end{aligned} \tag{5.190}$$

Suppose the two trajectories of the ith and jth oscillators in phase space at the switching time t_k is continuous, i.e.,

$$(x_k^{(i)}, \dot{x}_k^{(i)}) = (x_k^{(j)}, \dot{x}_k^{(j)}) \quad \text{for } i, j \in \{1, 2, \cdots, m\}. \tag{5.191}$$

If the two responses of the ith and jth oscillators at the switching time t_k are discontinuous, a transport law is needed. The transport law is assumed as

$$\mathbf{x}_k^{(j)} = \mathbf{g}^{(ij)}(\mathbf{x}_k^{(i)}) \text{ where } \mathbf{g}^{(ij)} = (g_1^{(ij)}, g_2^{(ij)})^{\mathrm{T}}. \tag{5.192}$$

In other words, the transport law can be written as

$$\left.\begin{aligned} x_k^{(j)} &= g_1^{(ij)}(x_k^{(i)}, \dot{x}_k^{(i)}) \\ \dot{x}_k^{(j)} &= g_2^{(ij)}(x_k^{(i)}, \dot{x}_k^{(i)}) \end{aligned}\right\} \quad \text{for } i, j \in \{1, 2, \cdots, m\}. \tag{5.193}$$

The ith and jth dynamical systems are evolving in the time intervals $[t_{k-1}, t_k]$ and $[t_k, t_{k+1}]$, respectively. The switching point for the two dynamical systems is at time t_k. The transport law between the ith and jth dynamical systems is to transport the final state of the ith dynamical system to the initial state of the jth dynamical system. This process makes the responses of the two systems to be continued at time t_k. This phenomenon described by the transport law or the transport mapping extensively exists, such as impact, control logic laws, impulse and other physical laws to make the discontinuity. To describe the entire responses of the resultant systems, the mapping structures are adopted as a kind of symbolic description. Thus, the transport mapping relative to the transport law is used to possess the same function as the transport law. From the transport law, a transport mapping is introduced as

$$P_0^{(ij)} : \Sigma^{(i)} \to \Sigma^{(j)} \text{ for } i, j \in \{1, 2, \cdots, m\}, \tag{5.194}$$

or

$$P_0^{(ij)} : (x_k^{(i)}, \dot{x}_k^{(i)}) \to (x_k^{(j)}, \dot{x}_k^{(j)}) \quad \text{for } i, j \in \{1, 2, \cdots, m\}. \tag{5.195}$$

The algebraic equations for the transport mapping are given by Eq. (5.193). The transport mapping $P_0^{(ij)}$ is to make the final point of the trajectory of the ith system jump to the starting point of the trajectory of the jth system at time t_k.

If the system parameters of the oscillators in Eq. (5.178) will be invariant, consider a switching system governed by a rectangular wave forcing as an example, i.e.,

$$Q^{(i)}(t) = (-1)^{i+1} C^{(i)} \quad \text{for } t \in [t_{k-1}, t_k] \text{ and } i \in \{1, 2\}. \tag{5.196}$$

The corresponding exact solution for each piece of the rectangular wave force is

$$\begin{aligned} x^{(i)}(t) &= e^{-\delta^{(i)}(t-t_{k-1})} \left[c_1^{(k)} \cos \omega_d^{(i)}(t - t_{k-1}) + c_2^{(k)} \sin \omega_d^{(i)}(t - t_{k-1}) \right] \\ &\quad + (-1)^{i+1} \frac{C^{(i)}}{(\omega^{(i)})^2} \\ \dot{x}^{(i)}(t) &= e^{-\delta^{(i)}(t-t_{k-1})} \left[(-\delta^{(i)} c_1^{(k)} + \omega_d^{(i)} c_2^{(k)}) \cos \omega_d^{(i)}(t - t_{k-1}) \right. \\ &\quad \left. - (\delta^{(i)} c_2^{(k)} + \omega_d^{(i)} c_1^{(k)}) \sin \omega_d^{(i)}(t - t_{k-1}) \right] \end{aligned} \tag{5.197}$$

where

$$c_1^{(k)} = x_{k-1}^{(i)} - (-1)^{i+1} \frac{C^{(i)}}{(\omega^{(i)})^2} \text{ and } c_2^{(k)} = \frac{1}{\omega_d^{(i)}} (\dot{x}_{k-1}^{(i)} + \delta^{(i)} c_1^{(k)}). \tag{5.198}$$

For this switching system, the two subsystems switch with the transport law as

$$(x_{k+j}^{(l_1)}, \dot{x}_{k+j}^{(l_1)}) = (x_{k+j}^{(l_2)}, \dot{x}_{k+j}^{(l_2)}) \text{ for } l_1, l_2 \in \{1, 2\} \text{ and } j = 1, 2, \cdots. \tag{5.199}$$

Consider $Q^{(1)}(t) = C^{(1)}$ and $Q^{(2)}(t) = -C^{(2)}$. The total solution of the resultant system is for $i = 1, 2$

$$\left.\begin{aligned}
&\mathbf{x}(t) = \left\{ (x^{(i)}(t), \dot{x}^{(i)}(t)) \middle| \, t \in [t_{k+2j+i-1}, t_{k+2j+i}] \text{ and } j = 0, 1, \cdots \right\} \\
&(x^{(1)}_{k+j+1}, \dot{x}^{(1)}_{k+j+1}) = (x^{(2)}_{k+j+1}, \dot{x}^{(2)}_{k+j+1}) \text{ for } j = 0, 1, 2, \cdots .
\end{aligned}\right\} \quad (5.200)$$

If the piecewise discontinuous forcing in switching systems is periodic, one often uses the Fourier series expansion method to obtain the corresponding responses of the switching systems. However, the Fourier series expansion method has smoothened the discontinuity of piecewise discontinuous forcing. Suppose the infinite-term summation of the Fourier series can approach such piecewise discontinuous forcing. In fact, once the discontinuity of the piecewise forcing is smoothened, the non-smooth responses of the dynamical system cannot be accurately described. For the jump or impulsive discontinuity of the forcing, the Gibbs phenomenon can never be avoided. The method presented herein can treat the switching system through subsystems with switching connections, and the entire exact solutions can be obtained through subsystems in the switching system. Such a method does not use the Dirichlet conditions. If a piecewise forcing in subsystems is non-periodic, one cannot find a traditional method to obtain any approximate solution to approach the exact solution. From the method presented herein, the exact solutions of the switching systems consisting of a group of linear systems can be obtained for any randomly selected piecewise forcing, as well as randomly impulsive forcing (see Luo and Wang, 2009a). One cannot find any Fourier series to model such a random piecewise forcing. The traditional methods based on the Lipschitz condition (e.g., Fourier series and Taylor series expansions) cannot provide adequate solutions for the oscillator with the random piecewise forcing. The method presented herein can easily achieve the exact solution for such a switching linear system. In vibration testing, only random, piecewise, sinusoidal waves can be used in shaking tables. Thus, this method can provide a reasonable wave for actuators to drive the shaking table in random vibration testing.

Consider an excitation of a two-uneven rectangular wave with the time interval spans of $T_1 = 0.75T$ and $T_2 = 0.25T$ (e.g.,$T = 2$) and $C^{(i)} = 1$. The two pieces of the excitation are considered as two different forcing, and the oscillator can be treated as two switching systems to switch at given times. Therefore, from the presented method in the previous section, the responses of the oscillator under such rectangular wave forcing are presented in Fig. 5.35. Such a rectangular excitation forcing is illustrated in Fig. 5.35a. The two pieces of the rectangular uneven wave is illustrated. The time-histories of displacement, velocity and acceleration for such oscillator are presented in Fig. 5.35b–d. It is observed that the exact solution of displacement is smooth. However, the exact velocity response is non-smooth because the rectangular wave forcing is discontinuous. Such a discontinuity causes the acceleration of the oscillator to be discontinuous. However, for the Fourier series solution of this system, the responses of velocity and acceleration are continuous. For a further look at the dynamical behaviors of the oscillator, the trajectory for periodic response is presented in Fig. 5.35e, and the corresponding forcing distribution along the displacement is presented in Fig. 5.35f.

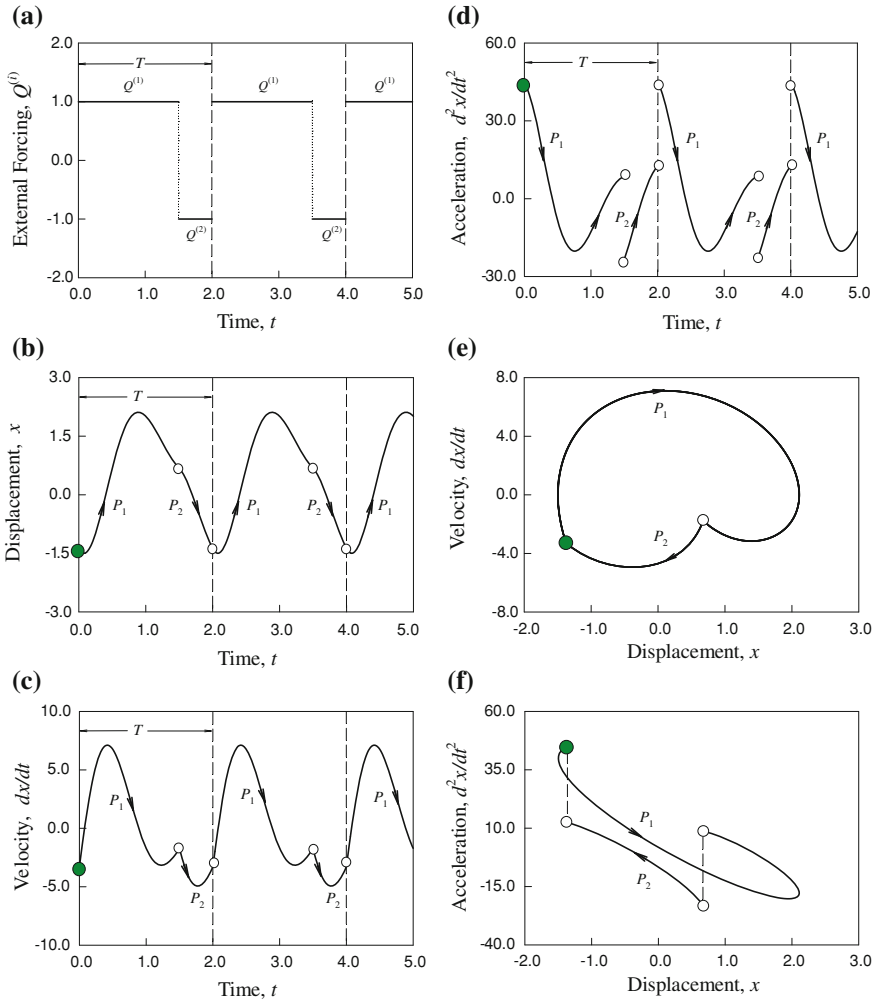

Fig. 5.35 Periodic motion under two pieces of *rectangular waves*: **a** forcing, **b** displacement **c** velocity, **d** acceleration, **e** phase plane and **f** acceleration versus displacement ($\omega^{(i)} = 4.0$, $\delta^{(i)} = 1.0$, $C^{(i)} = 1$, $T_1 = 1.5$, $T_2 = 0.5$, $x(0) = -1.3728$, and $\dot{x}(0) = -3.2947$)

5.6.2 Switching Systems with Impulses

As in Luo and Wang (2009b), consider a switching system with two 2-D subsystems with two matrices for $j = 0, 1, 2, \cdots$

$$\begin{aligned}
\mathbf{A}^{(1)} &= \begin{bmatrix} a_1 & b_1 \\ c_1 & d_1 \end{bmatrix} \quad \text{for } t \in [t_{k+2j}, t_{k+2j+1}], \\
\mathbf{A}^{(2)} &= \begin{bmatrix} a & b \\ c & d \end{bmatrix} \quad \text{for } t \in [t_{k+2j+1}, t_{k+2j+2}], \\
\mathbf{Q}^{(i)} &= (Q_1, Q_2)^{\mathrm{T}} \cos \Omega t \quad \text{for } i = 1, 2.
\end{aligned} \tag{5.201}$$

The corresponding switching points are continuous but non-smooth, i.e.,

$$x_1^{(1)}(t_{k+j}) = x_1^{(2)}(t_{k+j}) \text{ and } x_2^{(1)}(t_{k+j}) = x_2^{(2)}(t_{k+j}). \tag{5.202}$$

Without losing generality, the parameters for a dynamical system are fixed and the parameters for another subsystem are varied. Select parameters as

$$a = a_1 = d_1 = -1, b_1 = 1, c_1 = -2. \tag{5.203}$$

From Eqs. (5.146) and (5.147), the time-interval parameters can be expressed as

$$\begin{aligned}
q_{2k+i-1}^{(i)} &= \frac{t_{2k+i} - t_{2k+i-1}}{T} \quad \text{for } i = 1, 2 \text{ and} \\
1 &= \sum\nolimits_{i=1}^{2} \sum\nolimits_{k=1}^{N} q_{2k+i-1}^{(i)} \quad \text{for } k = 1, 2, \cdots.
\end{aligned} \tag{5.204}$$

If $q_{2k+i-1}^{(i)} = q^{(i)}$, the ith subsystem possesses the equi-time interval. Otherwise, the ith subsystem possesses the non-equi-time interval. Consider a simple periodic motion with a mapping structure of P_{21}, and the corresponding time interval parameter can be set as $q^{(1)}$ and $q^{(2)}$. For $q^{(1)} = 0$ ($q^{(2)} = 1$), the switching system is formed by the second subsystem only. For $q^{(1)} = 1$ ($q^{(2)} = 0$), the switching system is formed by the first subsystem only. For a periodic flow with $P = P_{21}$, consider an initial state $\mathbf{x}_k^{(1)}$ and the final state $\mathbf{x}_{k+1}^{(1)}$ for the first subsystem in the resultant, switching system, and an initial state $\mathbf{x}_{k+1}^{(2)}$ and the final state $\mathbf{x}_{k+2}^{(2)}$ for the second subsystem. The analytical prediction of a periodic flow for such a mapping structure is given in Fig. 5.36 for parameters ($b = -5.0, d = 1.6, q^{(1)} = 0.25$ and $q^{(2)} = 0.75$, $Q_1 = 1.0$, $Q_2 = 1.5$, $\Omega = 1.5$) with other parameters in Eq. (5.202) (i.e., $a = a_1 = d_1 = -1, b_1 = 1, c_1 = -2$). With varying parameter c, the switching points of the periodic flow with P_{21} for the two subsystems are obtained, and the corresponding stability is presented in Fig. 5.37 through the eigenvalue analysis. The stable and unstable ranges of periodic flows of P_{21} for parameter c are clearly observed. With increasing parameter c, the stable range for such a simple periodic flow becomes large. If $c > 10$, all the periodic flow is always stable. The infinity solutions for the switching points are observed when the eigenvalue is equal to positive one (+1), which agreed very well with the afore-mentioned discussion. To further look into the stability of such a periodic flow, the parameter map between the parameters d and c are developed, as shown in Fig. 5.36 for parameters ($b = -5.0$, $q^{(1)} = 0.25$ and $q^{(2)} = 0.75$ $a = a_1 = d_1 = -1$, $b_1 = 1$,

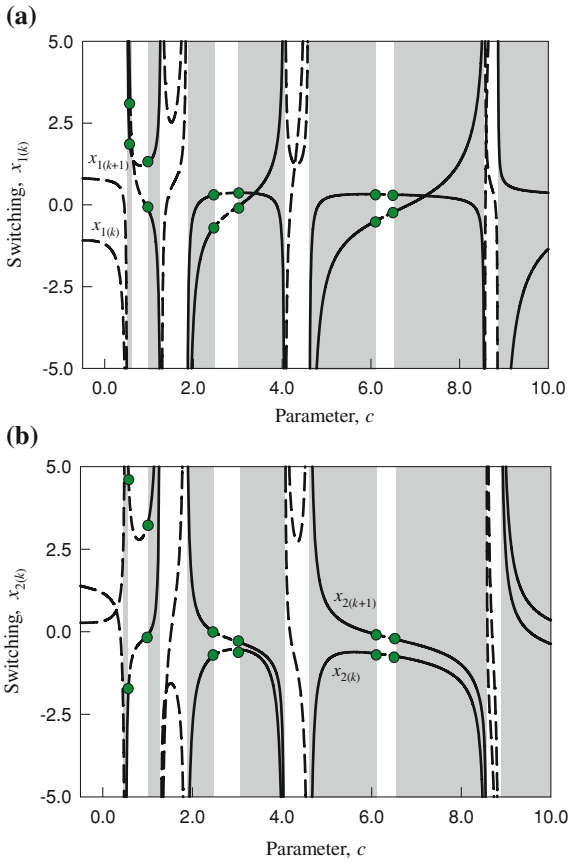

Fig. 5.36 Periodic motion scenario with P_{21} : **a** switching $x_1(k)$ and **b** switching $x_{2(k)}$. ($b = -5.0, d = 1.6,\ q^{(1)} = 0.25$ and $q^{(2)} = 0.75, a = a_1 = d_1 = -1, b_1 = 1, c_1 = -2, Q_1 = 1.0, Q_2 = 1.5,\ \omega = 1.5$). The *solid* and *dashed curves* represent stable and unstable periodic flows with P_{21}, respectively

$c_1 = -2,\quad Q_1 = 1.0,\ Q_2 = 1.5,\ \Omega = 1.5$). In Fig. 5.38, the stable and unstable periodic flows lie in the shaded and non-shaded areas, respectively. For the switching system, the time-interval of each sub-system is significant to influence the stability characteristics of the resultant system. The parameter maps between the parameter d and the time interval parameter $q^{(1)}$ for a periodic flow of P_{21} are presented with ($c = -0.5, 0.5, 1.0$ and 2.0) in Fig. 5.39a–d, respectively. For $c = -0.5$, the minimum value of d for the unstable periodic motion is $d \approx -0.271$ with $q^{(1)} \approx 0.09$. The cusp point exists for this parameter map. Only two dents in parameter map exist for the unstable periodic flow. For $c = 0.5$, the minimum value of d for the unstable periodic motion is $d \approx 0.557$ with $q^{(1)} \approx 0.2$. The three dents in parameter map exist for the unstable periodic flow, but the cusp points do not exist. For $c = 1.0$ and 2.0, the number of dents in the parameter maps becomes four and five accordingly. The dents in the stability maps are not uniform.

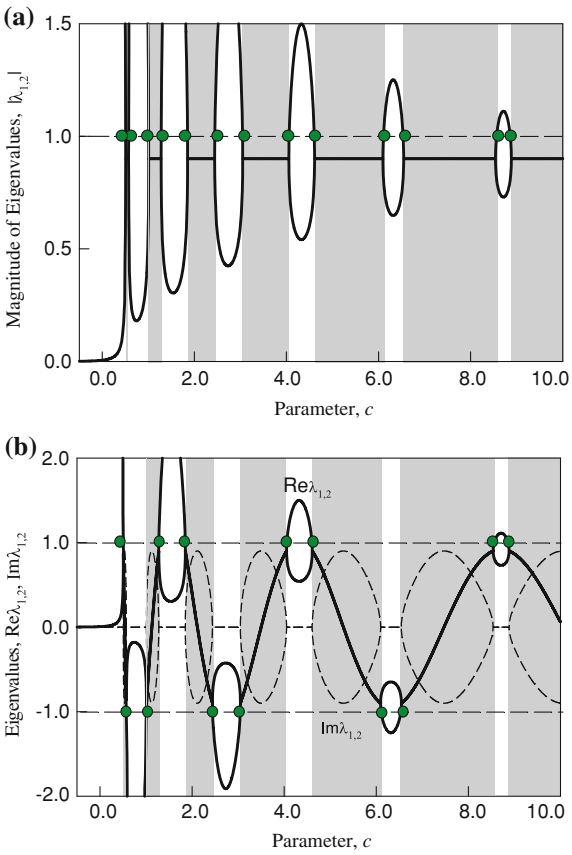

Fig. 5.37 Eigenvalue analysis for periodic motions with P_{21} : **a** magnitudes and **b** real and imaginary parts of eigenvalues ($b = -5.0,\ \ d = 1.6,\ \ q^{(1)} = 0.25,\ \ q^{(2)} = 0.75,\ \ a = a_1 = d_1 = -1,\ \ b_1 = 1,\ \ c_1 = -2,\ Q_1 = 1.0,\ \ Q_2 = 1.5,\ \Omega = 1.5$)

Table 5.1 Input data for numerical simulations of stable and unstable periodic flows of P_{21} ($b = -5.0, d = 1.6, q^{(1)} = 0.25, q^{(2)} = 0.75,\ \ a = a_1 = d_1 = -1, b_1 = 1, c_1 = -2, Q_1 = 1.0,\ \ Q_2 = 1.5,\ \Omega = 1.5,\ t_0 = 0.0$)

	Parameter c	Initial condition	Stability
Figure 5.41a	$c = 0.45$	$x_1^{(1)} \approx -5.4975, x_2^{(1)} \approx -2.0072$	Unstable
Figure 5.41b	$c = 0.55$	$x_1^{(1)} \approx 5.1645, x_2^{(1)} \approx 6.2506$	stable
Figure 5.41c	$c = 0.80$	$x_1^{(1)} \approx 0.2707, x_2^{(1)} \approx 2.7373$	Unstable
Figure 5.41d	$c = 1.10$	$x_1^{(1)} \approx -0.6420, x_2^{(1)} \approx 4.1622$	Stable

5.6.3 Numerical Illustrations

(A) *A 2-D Switching System*: The matrices and vectors for the 2-dimensional system in Eq. (5.201) will be considered again, and the parameters in Eq. (5.203) will be used. From the analytical prediction, the time histories for state variables for a stable periodic flow of $P_{21}(c = 0.55)$ are plotted in Fig. 5.40 for parameters ($b = -5.0$,

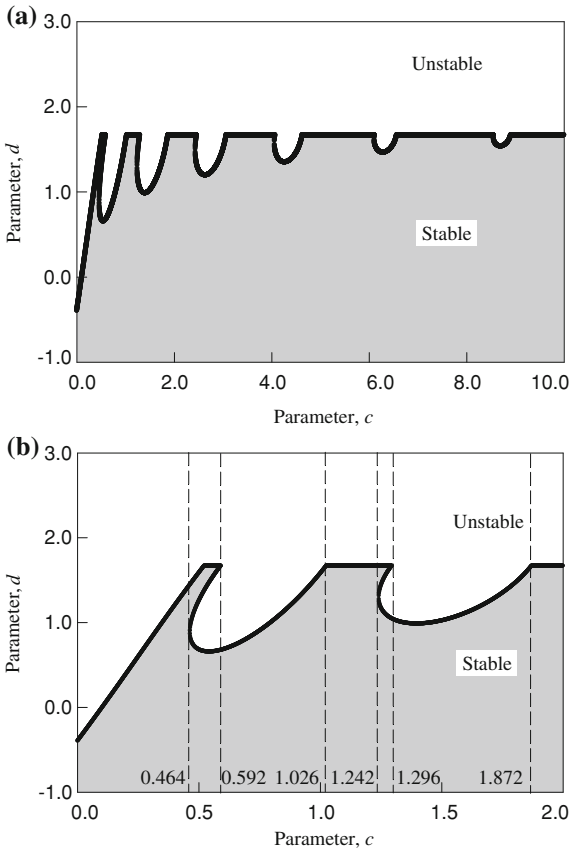

Fig. 5.38 Parameter maps of (d, c): **a** stable and unstable motion regions, **b** zoomed view ($b = -5.0,\ q^{(1)} = 0.25$ and $q^{(2)} = 0.75,\ a = a_1 = d_1 = -1, b_1 = 1, c_1 = -2,\ Q_1 = 1.0,\ Q_2 = 1.5,\ \Omega = 1.5$)

$d = 1.6,\quad q^{(1)} = 0.25,\quad q^{(2)} = 0.75,\quad a = a_1 = d_1 = -1,\quad b_1 = 1, c_1 = -2,\ Q_1 = 1.0,\quad Q_2 = 1.5,\quad \Omega = 1.5$) and the initial conditions ($t_0 = 0.0,\quad x_1^{(1)} \approx 5.1645,\quad x_2^{(1)} \approx 6.2506$). The non-smooth behavior of the periodic flow for state variables (x_1 and x_2) are observed. For a further observation of non-smooth characteristics of the switching system, the trajectories of stable and unstable periodic flows in phase plane for P_{21} is presented in Fig. 5.41a–d for $d = 1.6$, and the corresponding input data is listed in Table 5.1. The initial conditions are obtained from the analytical prediction. In Fig. 5.41a, the periodic flow for $c = -0.5$ is unstable. The asymptotic instability of the periodic flow in phase plane is observed. With increasing parameter c, a stable periodic flow with $c = 0.5$ is presented in Fig. 5.41b. For $c = 0.8$, another unstable periodic flow can be observed, as plotted in Fig. 5.41c. Compared to the trajectory in Fig. 5.41a, the configuration of trajectory is different. For $c = 1.1$, the stable periodic flow is observed, and the profile of the trajectory in phase plane is changed. The stability of the periodic flows can be obtained through the parameter map in Fig. 5.38.

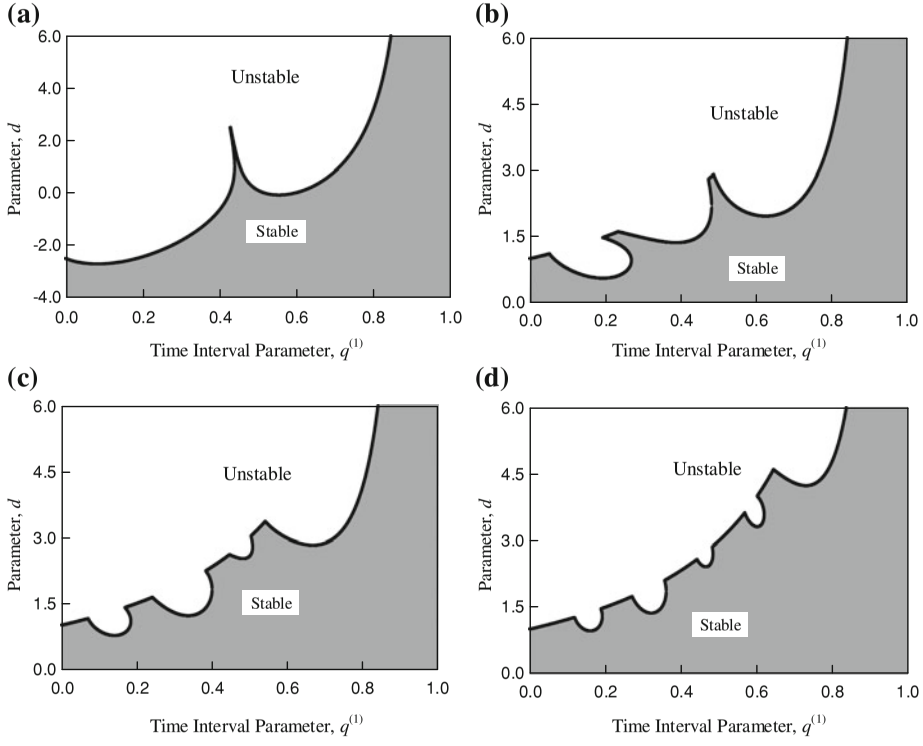

Fig. 5.39 Parameter maps of $(q^{(1)}, d)$: **a** $c = -0.5$, **b** $c = 0.5$, **c** $c = 1.0$ and **d** $c = 2.0$. ($b = -5.0, \quad a = a_1 = d_1 = -1, \quad b_1 = 1, c_1 = -2, \quad Q_1 = 1.0, \quad Q_2 = 1.5, \quad \Omega = 1.5$)

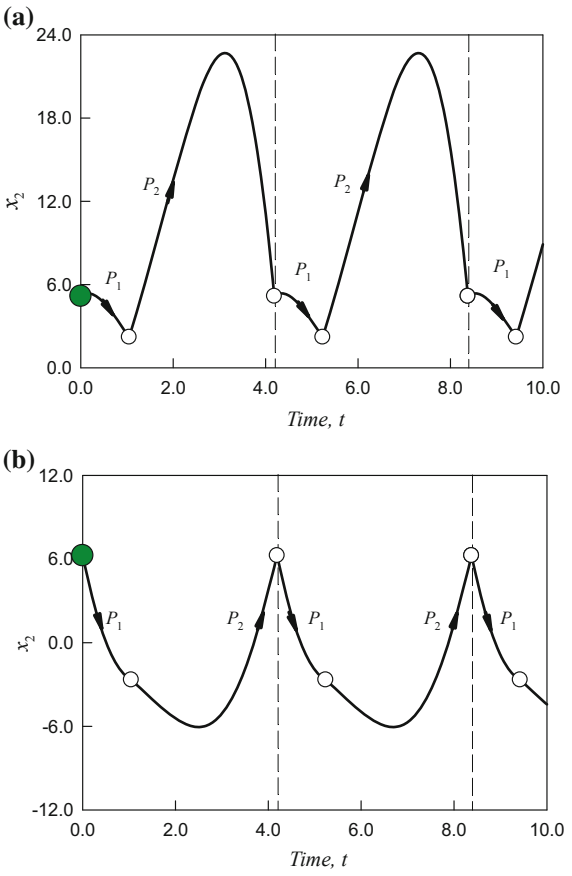

Fig. 5.40 A stable periodic flow of P_{21} ($c = 0.55$) for a 2-D switching system: **a** time-history of x_1 and **b** time-history of x_2 ($b = -5.0, d = 1.6, \quad q^{(1)} = 0.25, q^{(2)} = 0.75, a = a_1 = d_1 = -1, \quad b_1 = 1, c_1 = -2, \quad Q_1 = 1.0, Q_2 = 1.5, \ \Omega = 1.5$) ($t_0$=0.0, $x_1^{(1)} \approx 5.1645$, $x_2^{(1)} \approx 6.2506$)

In the foregoing illustrations, the switching between two subsystems is continuous but non-smooth. In fact, the switching between two systems can be completed through a transport law. To discuss effects of the transport law on periodic motion, the transport law in Eq. (5.169) for the 2-D switching system will be used. Four cases of the linear transformation are:

(i) continuous switching for two sub-systems

$$\mathbf{x}_k^{(1)} = \mathbf{x}_k^{(2)} \quad \text{for} \ \ k = 1, 2, \cdots ; \tag{5.205}$$

(ii) translation switching as a switching transport law

$$\left.\begin{array}{l} \mathbf{x}^{(1)}(t_{k+}) = \mathbf{x}^{(2)}(\mathrm{t}_{k-}) + \mathbf{e}^{12)} \\ \mathbf{x}^{(2)}(t_{k+}) = \mathbf{x}^{(1)}(\mathrm{t}_{k-}) + \mathbf{e}^{(21)} \\ \mathbf{e}^{(12)}, \mathbf{e}^{(21)} = \text{const} \end{array}\right\} \quad \text{for} \ \ k = 1, 2, \cdots ; \tag{5.206}$$

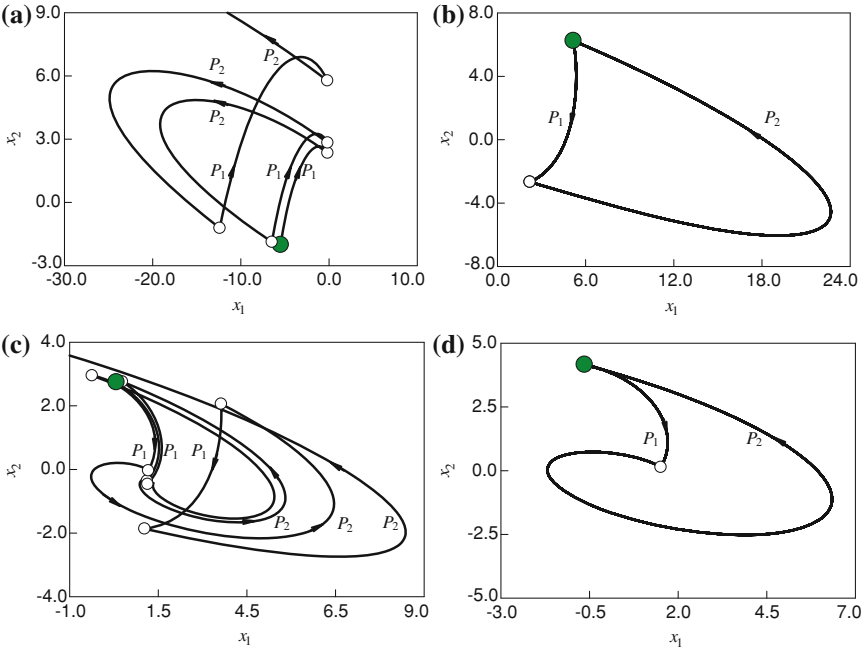

Fig. 5.41 Trajectories of stable and unstable periodic flows in phase plane with P_{21} for a 2-D switching system ($t_0 = 0.0$) : **a** ($c = 0.45, x_1^{(1)} \approx -5.4975, x_2^{(1)} \approx -2.0072$), **b** ($c = 0.55$, $x_1^{(1)} \approx 5.1645$, $x_2^{(1)} \approx 6.2506$), **c** ($c = 0.80$, $x_1^{(1)} \approx 0.2707$, $x_2^{(1)} \approx 2.7373$) and **d** ($c = 1.10$, $x_1^{(1)} \approx -0.6420$, $x_2^{(1)} \approx 4.1622$). ($b = -5.0, d = 1.6$, $q^{(1)} = 0.25, q^{(2)} = 0.75$, $a = a_1 = d_1 = -1$, $b_1 = 1, c_1 = -2$, $Q_1 = 1.0$, $Q_2 = 1.5$, $\Omega = 1.5$)

(iii) scaling switching as a switching transport law

$$\left.\begin{array}{l} \mathbf{x}^{(2)}(t_{k+}) = \mathbf{E}^{(12)} \cdot \mathbf{x}^{(1)}(t_{k-}) \\ \mathbf{x}^{(1)}(t_{k+}) = \mathbf{E}^{(21)} \cdot \mathbf{x}^{(2)}(t_{k-}) \\ \mathbf{E}^{(12)}, \mathbf{E}^{(21)} \text{ is diaginal matrix} \end{array}\right\} \quad \text{for } k = 1, 2, \cdots; \tag{5.207}$$

(iv) affine switching as a switching transport law

$$\left.\begin{array}{l} \mathbf{x}^{(2)}(t_{k+}) = \mathbf{E}^{(12)} \cdot \mathbf{x}^{(1)}(t_{k-}) + \mathbf{e}^{(12)} \\ \mathbf{x}^{(1)}(t_{k+}) = \mathbf{E}^{(21)} \cdot \mathbf{x}^{(2)}(t_{k-}) + \mathbf{e}^{(21)} \\ \mathbf{E}^{(12)}, \mathbf{E}^{(21)} \text{ are const matrices} \\ \mathbf{e}^{(12)}, \mathbf{e}^{(21)} \text{ are const vectors} \end{array}\right\} \quad \text{for } k = 1, 2, \cdots. \tag{5.208}$$

Consider the effects of the transport laws to the dynamical behaviors of the resultant system. The same system parameters are used but the switching laws are different. The corresponding input data for numerical simulation is tabulated in Table 5.2 for stable and unstable periodic flows of P_{21} with the transport laws.The trajectories

Table 5.2 Input data for numerical simulations of stable and unstable periodic flows of P_{21} with transportation laws ($a = -1, b = -5,\ c = 1.5,\ d = 0.5,\ q^{(1)} = 0.25$ and $q^{(2)} = 0.75$, $a_1 = d_1 = -1, b_1 = 1, c_1 = -2,\ Q_1 = 1.0,\ Q_2 = 1.5,\ \Omega = 1.5$)

	Parameter c		Initial condition (x_{10}, x_{20})	Transport law
Figure 5.42a	$\mathbf{E}^{12} = \begin{bmatrix} 1 & 0 \\ 0 & 1 \end{bmatrix}$	$\mathbf{e}^{12} = \begin{bmatrix} 0 \\ 1 \end{bmatrix}$	$(-8.7597, 8.8674)$	Translation
	$\mathbf{E}^{21} = \begin{bmatrix} 1 & 0 \\ 0 & 1 \end{bmatrix}$	$\mathbf{e}^{21} = \begin{bmatrix} 0 \\ 2 \end{bmatrix}$		
Figure 5.42b	$\mathbf{E}^{12} = \begin{bmatrix} 0.5 & 0 \\ 0 & 0.6 \end{bmatrix}$	$\mathbf{e}^{12} = \begin{bmatrix} 0 \\ 0 \end{bmatrix}$	$(-14.7546, 2.6000)$	Scaling
	$\mathbf{E}^{21} = \begin{bmatrix} 3 & 0 \\ 0 & 4 \end{bmatrix}$	$\mathbf{e}^{21} = \begin{bmatrix} 0 \\ 0 \end{bmatrix}$		
Figure 5.42c	$\mathbf{E}^{12} = \begin{bmatrix} 0.8 & 0.3 \\ 0.2 & 0.6 \end{bmatrix}$	$\mathbf{e}^{12} = \begin{bmatrix} 0 \\ 0 \end{bmatrix}$	$(7.3426, 4.3876)$	Linear transformation
	$\mathbf{E}^{21} = \begin{bmatrix} 8 & 5 \\ 3 & 4 \end{bmatrix}$	$\mathbf{e}^{21} = \begin{bmatrix} 0 \\ 0 \end{bmatrix}$		
Figure 5.42d	$\mathbf{E}^{12} = \begin{bmatrix} 0.5 & 0 \\ 0 & 0.6 \end{bmatrix}$	$\mathbf{e}^{12} = \begin{bmatrix} 0 \\ -1 \end{bmatrix}$	$(3.6392, 3.1714)$	Affine transformation
	$\mathbf{E}^{21} = \begin{bmatrix} 2 & 3 \\ 1.5 & 1 \end{bmatrix}$	$\mathbf{e}^{21} = \begin{bmatrix} 0 \\ 2 \end{bmatrix}$		

of periodic flows with mapping structure P_{21} are plotted in Fig. 5.42. In Fig. 5.42a, the translation switching for the variable x_2 is considered. The jump of variable x_2 is observed in phase plane. For this translation switching, the stability condition is the same as in the continuous switching. Only the switching points are different. In Fig. 5.42b, the scaling transport law is considered. From the first subsystem to the second subsystem, the shrinking transport law is used, but the stretching transport law is adopted from the second subsystem to the first subsystem. Such a stretching and shrinking can be observed very clearly. The scaling transport law will change the stability for the switching of two subsystems. In Fig. 5.42c, a linear transformation is used as a transport law, and the linear transformations with the shrinking and stretching are for the first to second subsystem and for the second to first subsystem, respectively. This linear transformation transport law will also change the stability for the two system switching. Finally, the affine transformations as transport laws are used for the switching of the two sub-systems in Fig. 5.42d. This affine transformation includes the rotation, scaling and translation transformation.

(B) *A 3-D Switching System*: Consider three linear subsystems with matrices as

$$\mathbf{A}^{(1)} = \begin{bmatrix} -1 & 2 & -1 \\ -2 & 1 & -1 \\ 1 & 3 & -3 \end{bmatrix}, \mathbf{A}^{(2)} = \begin{bmatrix} -1 & 0.5 & 2 \\ -1.5 & 1 & -1 \\ -1 & 2 & -1 \end{bmatrix}, \mathbf{A}^{(3)} = \begin{bmatrix} -1 & -1 & 2 \\ 2 & -3 & -1 \\ 1 & -2 & -2 \end{bmatrix} \quad (5.209)$$

and from eigenvalue analysis of the three matrices, $\lambda_1^{(1)} = -1.4735$, $\lambda_{2,3}^{(1)} = -0.7633 \pm 2.0416\mathbf{i}$, $\lambda_1^{(2)} = -3.3672$, $\lambda_{2,3}^{(2)} = 0.1836 \pm 2.4906\mathbf{i}$, and $\lambda_1^{(3)} = -4.4260$, $\lambda_{2,3}^{(3)} = -0.787 \pm 1.1891\mathbf{i}$ where $\mathbf{i} = \sqrt{-1}$. Because the time for

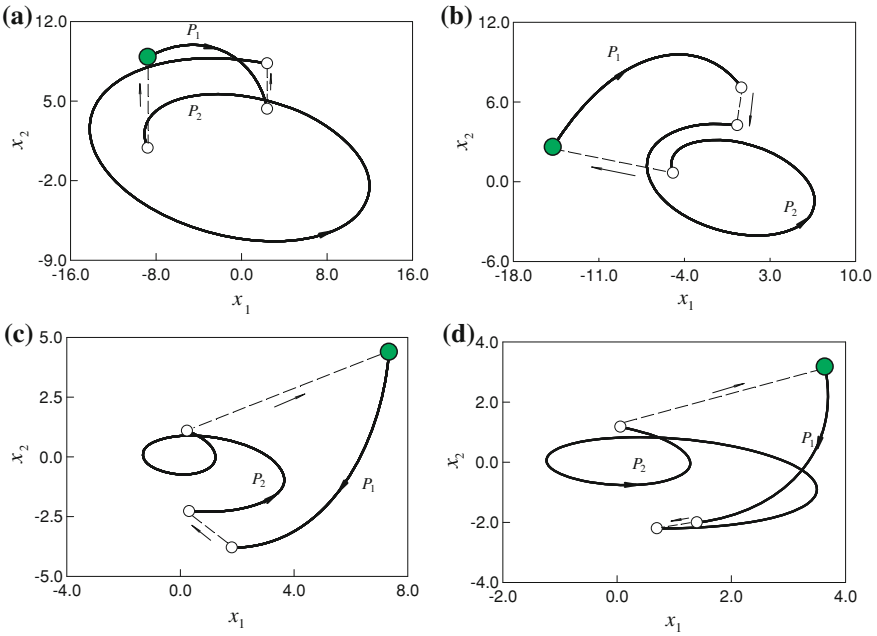

Fig. 5.42 Trajectories of stable periodic flows in phase plane with P_{21} for a 2-D switching system ($t_0 = 0.0$): **a** ($x_1^{(1)} \approx -8.7597, x_2^{(1)} \approx 8.8674$), **b** ($x_1^{(1)} \approx -14.7546, x_2^{(1)} \approx 2.6000$), **c** ($x_1^{(1)} \approx 7.3426, x_2^{(1)} \approx 4.3876$) and **d** ($x_1^{(1)} \approx 3.6392, x_2^{(1)} \approx 3.1714$). ($a = -1, b = -5,\ c = 1.5,\ d = 0.5,\ q^{(1)} = 0.25$ and $q^{(2)} = 0.75,\ a_1 = d_1 = -1, b_1 = 1, c_1 = -2,\ Q_1 = 1.0,\ Q_2 = 1.5,\ \Omega = 1.5$)

subsystems in switching systems is finite, it is not very significant that subsystems are stable or unstable. It is sufficient that the solutions of subsystems exist during the given time interval. The important issue is whether the flow of the resultant switching system is stable or unstable. The time interval for each system in the switching system is a key issue to control the stability of the resultant flow of the switching system. The external excitations for three subsystems in the 3-D switching system are

$$\mathbf{Q}^{(i)} = (A_1^{(i)} e^{t-t_0}, A_2^{(i)} \times (t - t_0), A_3^{(i)})^{\mathrm{T}} \tag{5.210}$$

where $A_1^{(1)} = A_2^{(1)} = A_3^{(1)} = 1, A_1^{(2)} = A_2^{(2)} = A_3^{(3)} = 1, A_3^{(2)} = A_1^{(3)} = A_2^{(3)} = -1$. Select the period of $T = 4.5$ arbitrarily, and consider the time interval parameters as $q^{(1)} = \frac{2}{9},\ \ q^{(2)} = \frac{4}{9}$ and $q^{(3)} = \frac{1}{9}$ for a periodic flow with a mapping structure P_{321} for the 3-D switching system. The continuous and impulsive switching with the same subsystems is considered for illustrations.

For the continuous switching, the analytical prediction gives the initial condition $x_1(0) \approx -2.7348,\ x_2(0) \approx -1.2346$ and $x_3(0) \approx -1.7856$ for the periodic flow

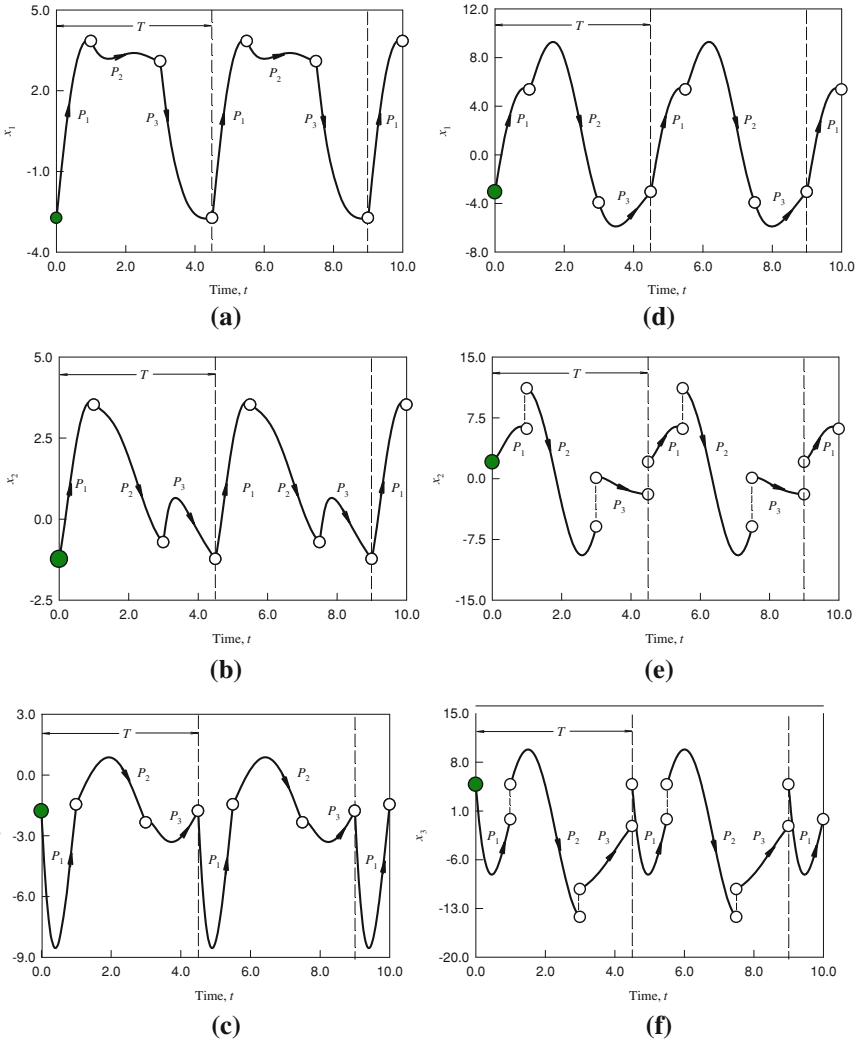

Fig. 5.43 Time-histories of variables $(x_i, i = 1, 2, 3)$ for two 3-D switching systems: **a–c** continuous switching $(x_1(0) \approx -3.0672,\ x_2(0) \approx 2.0328,\ x_3(0) \approx 4.7815)$ and **d–f** impulsive switching $(x_1(0) \approx -2.7348;\ \ x_2(0) \approx -1.2346,\ \ x_3(0) \approx -1.7856)$. $(A_1^{(1)} = A_2^{(1)} = A_3^{(1)} = 1,\ \ A_1^{(2)} = A_2^{(2)} = 1,\ A_3^{(2)} = -1,\ A_1^{(3)} = A_2^{(3)} = -1,\ A_3^{(3)} = 1, T = 4.5;\ \ q^{(1)} = \frac{2}{9};\ \ q^{(2)} = \frac{4}{9}; q^{(3)} = \frac{1}{3})$

of P_{321}. For the impulsive switching, the impulsive vectors between the two subsystems are $\mathbf{e}^{(12)} = (0, 5, 5)^{\mathrm{T}}$, $\mathbf{e}^{(23)} = (0, 6, 4)^{\mathrm{T}}$ and $\mathbf{e}^{(31)} = (0, 4, 6)^{\mathrm{T}}$. The state variable x_1 is continuous, but the stable variables x_2 and x_3 are discontinuous at switching points. The initial condition for the 3-D, impulsive switching system is

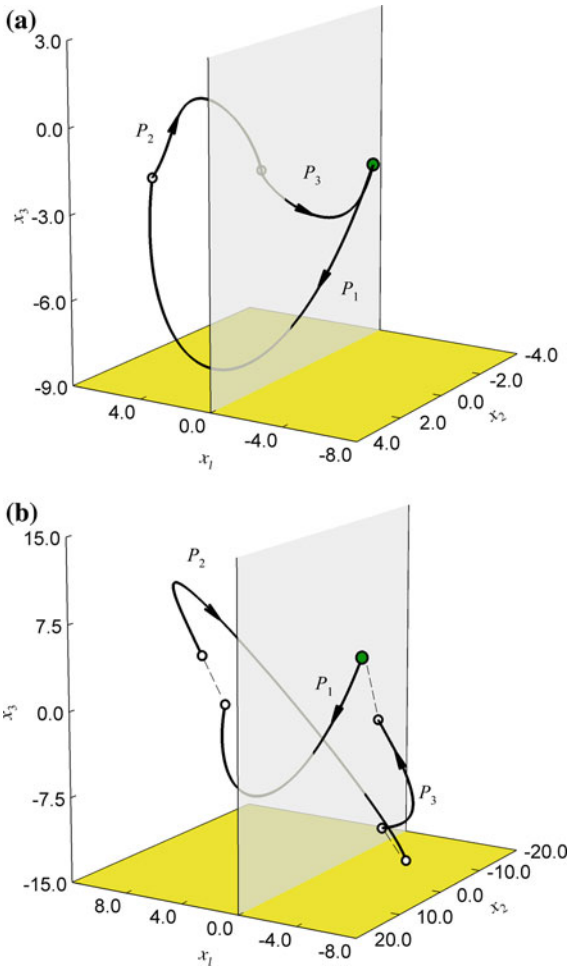

Fig. 5.44 Trajectories in phase space $(x_i, i = 1, 2, 3)$ for two 3-D switching systems: **a–c** continuous switching $(x_1(0) \approx -3.0672,\ x_2(0) \approx 2.0328,\ x_3(0) \approx 4.7815)$ and **d–f** impulsive switching $x_1(0) \approx -2.7348;\ x_2(0) \approx -1.2346,\ x_3(0) \approx -1.7856.$ $(A_1^{(1)} = A_2^{(1)} = A_3^{(1)} = 1,\ A_1^{(2)} = A_2^{(2)} = 1,\ A_3^{(2)} = -1,\ A_1^{(3)} = A_2^{(3)} = -1,\ A_3^{(3)} = 1.T = 4.5;\quad q^{(1)} = \frac{2}{9};\quad q^{(2)} = \frac{4}{9}; q^{(3)} = \frac{1}{3})$

$x_1(0) \approx -3.0672,\ x_2(0) \approx 2.0328,\ x_3(0) \approx 4.7815$. The time-histories of three state variables $(x_i,\ i = 1, 2, 3)$ for the periodic flow of the 3-D linear switching system are presented in Fig. 5.43. In Fig. 5.43a–c, the periodic flows for the continuous switching system are presented. It is observed that the periodic flow at all the switching points is continuous but non-smooth. In Fig. 5.43d–f, the periodic flow for the 3-D, impulsive switching system switching are presented. The time-history of the state variable x_1 is continuous, while the time-history of the state variables x_2 and x_3 are discontinuous due to impulsive at switching points. The trajectories in phase space for the continuous and impulsive switching are presented in Fig. 5.44a and b, respectively.

References

Luo, A.C.J., 2005, A theory for non-smooth dynamical systems on connectable domains, *Communication in Nonlinear Science and Numerical Simulation*, **10**, pp. 1–55.

Luo, A.C.J., 2006, *Singularity and Dynamics on Discontinuous Vector Fields*, Amsterdam: Elsevier.

Luo, A.C.J., 2008a, A theory for flow switchability in discontinuous dynamical systems, *Nonlinear Analysis*: *Hybrid Systems*, **2**(4), pp. 1030–1061.

Luo, A.C.J., 2008b, *Global Transversality*, *Resonance and Chaotic Dynamics*, Singapore: World Scientific.

Luo, A.C.J., 2011, Chaos and diffusion in dynamical systems with periodic impulses, *Proceedings of the ASME 2011 International Design Engineering Technical Conferences & Computers and Information in Engineering Conference*, IDETC/CIE2011, August 28–31, 2011, Washington, DC, USA, DETC2011-47387.

Luo, A.C.J., Wang, Y., 2009a, Switching dynamics of Multiple oscillators, *Communications in Nonlinear Science and Numerical Simulation*, **44**, pp. 3472–3485.

Luo, A.C.J., Wang, Y., 2009b, Periodic flows and stability of a switching system with multiple subsystems, *Dynamics of Continuous Discrete and Impulsive Systems*, **16**, pp. 825–848.